Characterization of Associating Polymer (AP) Solutions

- Influences on flow behavior by the degree of hydrophobicity and salinity

Master`s thesis
Petroleum Technology – Reservoir Chemistry

Elise Kvåle Perttamo

Department of Physics and Technology

uniCIPR

Centre for Integrated Petroleum Research

University of Bergen

May 2013

Acknowledgement

I would like to express my gratitude to Dr. Tormod Skauge for his guidance and support during the work of this thesis. This thesis would not have been possible without him.

I would also like to thank PhD student Abduljelil Kedir for experimental training and taking so much interest in my work. A great appreciation goes to Dr. Ketil Djuurhus for always being available for discussions and counseling.

Special thanks to my supervisor Professor Harald Høiland and co- supervisor Professor Arne Skauge for counseling. Thanks to CIPR for lending of laboratories and equipment, and for providing me with an office during my two years as a master student.

Furthermore, I am so grateful for all my fellow students for social discussions and activities, especially Ragnhild Østensen, Jeelaja Kaliyugarasan, Daniel Sævland, Olav Lindgren Østensen, Artur Burdek, Kristine Bø and Solveig Riisøen.

Finally, I would like to thank the rest of my friends and family for their support, especially Mathias Dahle Bryde- Erichsen for always believing in me.

Elise Kvåle Perttamo

Bergen, May 2013

Summary

The most applied polymer today for chemical *improved oil recovery* (IOR*)* processes, such as polymer flood and/or polymer well treatments, is the synthetic partially hydrolyzed polyacrylamide (HPAM) and its derivatives. Several field projects have been carried out utilizing HPAM, and the observed trend is that these polymers show low shear stress stability and low salt tolerance. They are also sensitive to elevated reservoir temperatures. More robust, efficient and cost- effective thickeners are needed.

In this master`s thesis an characterization of modified HPAM, are carried out in low and high salinity brine at room temperature (22 ± 0.1^{o}C). By incorporation of a relative small amount of hydrophobic groups (i.e. 8-18 carbon atoms moieties) onto the hydrophilic chain of polyacrylamide in aqueous solutions, this provides significantly changes in the behavior of HPAM. A reorientation of the macromolecules in aqueous solutions due to polar and non-polar parts, results in a formation of hydrophobic associations between the incorporated hydrophobic groups. These modified HPAM polymers are referred to as *associating polymers*, due to the association occurring between hydrophobic groups within a macromolecule and between hydrophobic groups at neighboring macromolecules.

This characterization process involves shear viscosity measurements at different polymer concentrations and viscoelasticity measurements of entangled polymer solutions in different salinity brines. The purpose of this rheological characterization was to; detect thickening ability, shear stress stability, the strength of polymer gels and compare the elastic deformation response of gel solutions with increasing degree of hydrophobicity and increasing salinity of the brine.

In this study three polymers with the same polymer base with increasing degree of hydrophobicity, FP3630S < C319 < D118, were compared. In addition to an HPAM with lower molecular weight, but much higher degree of hydrophobicity, B192, was characterized.

Observations from shear viscosity measurements show improved thickening ability at high concentrations with increasing degree of hydrophobicity. A relative low content of incorporated associating groups seems to improve the thickening ability of HPAM with increasing salinity of the brine. Above a given concentration, CAC (critical association concentration), the associating macromolecules start to interact and form associating network. Formation of this gel structure seems to enhance the viscosity of the solution significantly.

In the untangled polymer concentration range, below C^* (critical overlap concentration), the viscosity seems to be reduce with increasing degree of hydrophobicity on HPAM. Increase of salinity in the brine, it observed to reduce the viscosity even further. These observations correspond well when the dominating interactions are the intramolecular hydrophobic interactions.

The yield point and gel point was measured for entangled gel solutions from viscoelastic measurements. The yield point indicates the maximum shear stress applied on the gel solution before it starts to deform, and after this threshold value the deformation response due to increasing shear stress was detected. The strength of the gel structure is observed to increase with increasing amount of associating groups (HPAM<C319<D118), due to reinforcement of the intermolecular hydrophobic. Salinity effect seems to reduce interactions in the gel network. For B192, the strength of gel structure is observed to be stronger than HPAM based polymers in low salinity brine, but the gel structure seems to be easier deformed. This may indicate that B192 has a different gel structure than HPAM based polymers, due to lower molecular weight. Increasing salinity of the brine seems to increase the strength of the interactions in the gel structure of B192, due to the high amount of associating groups and low degree of hydrolysis.

The gel point indicates the strength of the gel structure during a transition from viscoelastic liquid to viscoelastic solid or vice versa. The discussion about gel strength is the same as for yield point.

Nomenclature

Variables

A	Area, [cm^2]
C	Polymer concentration [kg/m^3]
^oC	Celsius degree
C^*	Critical overlap concentration [ppm]
C_i	Concentration of component *i* [mol]
C_p	Polymer concentration [ppm], [mg polymer/kg solution]
CAC	Critical association concentration [ppm]
cP	Centi Poise (1cP = 1mPa·s)
E_A	Area displacement efficiency, dimensionless
G	Shear modulus [Pa]
G^*	Complex shear modulus [Pa]
$G´$	Storage modulus [Pa]
$G_y^{´}$	Storage modulus at yield point [Pa]
$G´´$	Loss modulus [Pa]
I	Ionic strength [mol/kg]
K	Absolute permeability [m^2]
$K^{`}$	Power Law constant
K_H	Huggins Coefficient, dimensionless
$K_{r,i}$	Relative permeability of phase *i*, dimensionless
$K_{r,o}$	Relative permeability of oil, dimensionless
$K_{r,w}$	Relative permeability of water, dimensionless
L	Length [cm]
M	Mobility ratio, dimensionless
M	Molarity [mol solute/L solution]
MDa	MegaDalton (unit of molar weight) (1Dalton=1 g/mol)
Mol%	Percentage amount of mol of a chemical component
$mPa{\cdot}s$	Milli Pascal second
N	Power law exponent
$n^{`}$	Number of components in the solution

$OOIP$	Originally oil in place [barrels]
ΔP	Pressure difference in Darcy law [bar]
Q	Volumetric flow rate [cm^3/s]
S	Seconds
$tan\,\delta$	Damping factor, dimensionless
$wt\%$	Mass weight percent
z_i	Valence of component i

Greek letters

$\dot{\gamma}$	Shear rate [1/s]
$\dot{\gamma}_c$	Critical shear rate at the end of upper Newtonian plateau [1/s]
γ_y	Shear strain at yield point, dimensionless
δ	Phase shift angle [^{o}] (degrees between 0^o to 90^o.
η	Shear viscosity of a non- Newtonian solution
η^*	Complex shear viscosity [Pa/s]
η_s	Shear viscosity of solvent [Pa·s]
η_R	Reduced viscosity [cm^3/g]
η_{so}	Specific viscosity, dimensionless
η_I	Inherent viscosity [cm^3/g or ppm]
η'	Complex shear viscosity related to storage modulus [Pa/s]
η''	Complex shear viscosity related to loss modulus [Pa/s]
λ_c	Relaxation time
λ_o	Mobility of oil [m^2/mPa·s]
λ_w	Mobility of water [m^2/mPa·s]
μ	Viscosity [Pa·s]
μ_o	Zero shear viscosity [Pa·s]

μ_∞	Infinite shear viscosity [Pa·s]
$\sigma_{o/q}$	Interfacial tension between oil and water [N/m]
τ	Shear stress [Pa]
τ_y	Shear stress at yield point [Pa]
ω	Angular frequency [1/s]
ω_c	Angular frequency at gel- point (crossover) [1/s]
Δ	Difference, dimensionless

Abbreviations

AMPS	2-acrylamido- 2- methyl propane acid
API	American Petroleum Institute
bbl	Barrel
CIPR	Centre for Integrated Petroleum Research
CBY- model	Carreau- Bird- Ysauda Model
CP	Cone plate
DG	Double gap
EOR	Enhanced oil recovery
HPAM (FP3036)	Partially hydrolyzed polyacrylamide
HSHT	High salinity and high temperature
HTHP	High temperature and high pressure
IOR	Improved oil recovery
LVE- range	Linear viscoelastic range
LPS	Linked polymer solution
MCR	Modular Compact Rheometer
NCS	Norwegian continental shelf
NVP	N-vinyl- 2- pyrrolidone
PAM	Polyacrylamide
PDMS	Polydimethylsiloxane, fluid
PLM	Power Law model

PPM	parts per million, mass fraction (g/g)
R&D	Research and development
SSW	Synthetic sea water
TDS	Total dissolved solids
USD	United State dollars [$]

Unit conversion

$1Pa \cdot s = 10^3 mPa \cdot s$

$1mPa \cdot s = 1cP$

$1\ bbl = 0.159\ Sm^3$

$1Darcy = 9.87 \cdot 10^{-13}\ m^2$

$1\ ft = 0{,}348\ m$

Table of contents

1. Introduction

Global oil demand is expected to advance 1% a year to 105 million barrels a day by 2030 from 90 million barrels a day in 2012 (International Energy Agency, 2013). The expected increasing demand for oil must be meet through exploration of new hydrocarbon reservoirs and enhancing the oil recovery of available reservoirs.

Implementation of Enhanced oil recovery (EOR) techniques is a crucial contribution to the global need for energy. Today the oil recovery around the world lies between 30-40%, and considering the increasing world population and the global energy demand, this recovery efficiency is not satisfying. An increase in efficiency of the recovery process above 60% will be more adequate.

According to Wu et al. in 2012 (Wu et al., 2012), it is estimated that about 7000 billion barrels of oil are still remaining in the reservoirs worldwide today. And this amount of oil is the target value for EOR methods. To improve the flow efficiency at both macroscopic and microscopic levels using EOR technologies are very costly, and for most oil nations the crude oil price have to be high for the additional recovery to be economically beneficial (TOTAL E&P, 2008).

The oil market is mainly controlled by the increase in oil demand from the transport industry. According to a report to the Norwegian Parliament from the Ministry of Petroleum and Energy in 2011 (Olje og Energidepartement, 2011), more than half of the oil consumption is used as oil- based fuels. Even though there is an increasing interest in renewable energy, such as biofuel and electricity to substitute the use of fossil fuels in automobiles, this will not give a dramatic effect on the oil demand in the upcoming years.

On the Norwegian continental shelf (NCS) the average recovery efficiency from oil fields is 46%, and in Marsh 2013 the Norwegian Petroleum Directorate published that the total recoverable petroleum resources are estimated at 85.5 billion barrels of oil equivalents[1].

[1] http://www.npd.no/en/Topics/Resource-accounts-and--analysis/Temaartikler/Resource-accounts/2012/

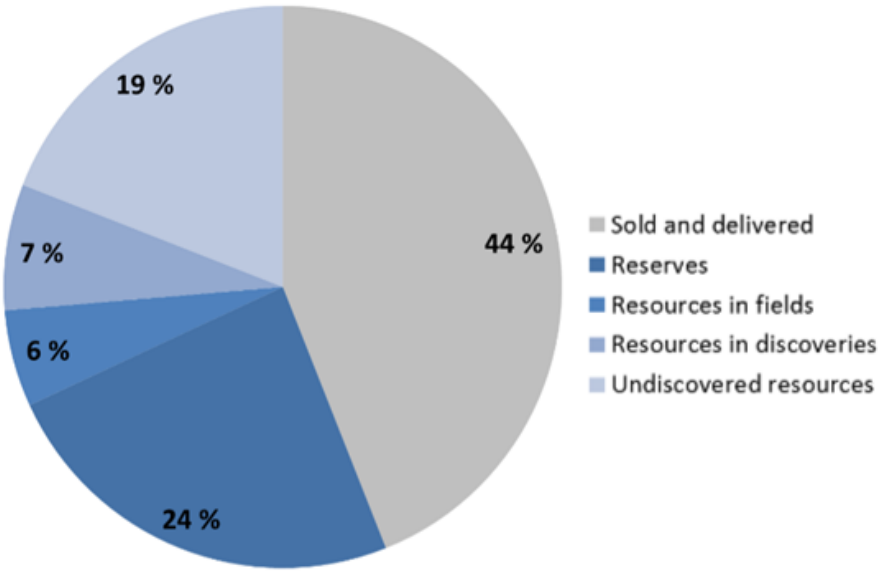

Figure 1.1 Recoverable resources on the NCS as of 31.12.12[2].

In addition to conventional oil recovery techniques, a chemical EOR approach can contribute to a more efficient recovery process resulting in a higher oil production. Polymers as viscosifying EOR agents were already considered in the early 1960‘s (Sorbie, 1991). By adding such thickening agents to the injection water, the viscosity will increase and the relative permeability of water will be reduced (Zolotukhin and Ursin, 2000). As a consequence of the increasing pressure difference due to the injected polymer solution, this can result in an accelerated oil production.

On the NCS conventional waterfloods have been very efficient because of the favourable mobility ratio. The reservoirs contain typically light oil with viscosities ranging from 0.5 to 2 mPa·s which implies that the oil and the water is almost equally mobile. Even though the reservoirs are highly heterogeneous, injecting water is still considered to be the most cost- and time efficient recovery method (Skarestad and Skauge, 2009).

The oil price controls the EOR activity on the NCS (Utvinningsutvalget, 2010), among other important parameters such as the increasing energy demand around the world, the economic growth and new technological developments. The market for Brent crude oil has varied a lot since the beginning of oil history on the NCS (Bolton, 2013, Olje og Energidepartement, 2011, Utvinningsutvalget, 2010), but since 2009 the oil price has been high. An oil price above 75 USD per barrel is considered high valued oil. In *figure 1.2* the development of the

[2] http://www.npd.no/en/Topics/Resource-accounts-and--analysis/Temaartikler/Norwegian-shelf-in-numbers-maps-and-figures/Recoverable-resources/

oil price through the last 26 years are shown. Exploration and production enhancements on the NCS are strongly influenced by the value of Brent crude oil.

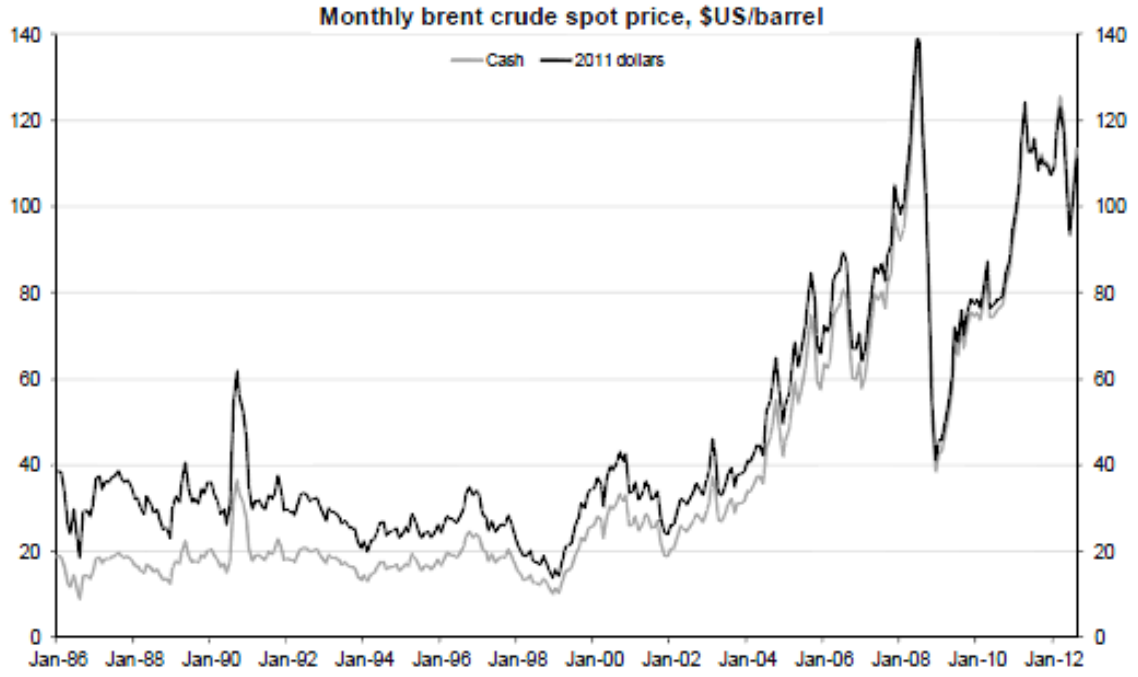

Figure 1.2 The global oil price development of Brent crude oil through the last 26 years (Bolton, 2013).

The value of the Brent crude oil has varied from 10 USD per barrels to 140 USD per barrels through the last twenty years. Since 1969 when the first oil was discovered in the Ekofisk field in Norway, the Norwegian petroleum industry was established right after. During the following decade and into the mid-nineties there were many big discoveries, such as the Statfjord field and the Troll field[3] (Olje og Energidepartement, 2011). Several Research and Development (R&D) projects were initiated to assure the Norwegian competence and competitive ability with the international market in the oil and gas sector[4,5]. The Oil companies and the authorities investigated the possibility for applying polymers, among others, to improve the oil recovery. During the middle of 1990`s the oil price dropped down to 15 USD per barrels. Together with the high prices for EOR chemicals, such as polymers,

[3] www.norskolje.museum.no

[4] http://www.regjeringen.no/nb/dep/oed/aktuelt/taler_artikler/minister/tidligere_olje_og_energiminister_enoksen/2007/building-a-sustainable-petroleum-industr.html?id=460505

[5] http://www.statoil.com/annualreport2011/en/ouroperations/businessareas/technology,projectsanddrilling%28tpd%29/pages/researchanddevelopment.aspx

the EOR projects were forced to termination (Skarestad and Skauge, 2009). In the beginning of 2000 the EOR activity took off, until the financial crisis lowered the value of the Brent crude oil in 2008. Since 2009 the oil price is stabilized on a high level, and together with increasing oil demand this has influenced the interest and activity for unconventional recovery techniques.

The most applied and studied polymer for EOR purposes around the world, is the conventional partially hydrolysed polyacrylamide (HPAM). This synthetic polymer is largely industrial available and has a lower price compared to other polymers, like the biopolymer Xanthan (Morel et al., 2008). In this study a modified HPAM is characterized due to their associating properties. These polymers are considered attractive for polymer flooding compared to HPAM, due to (Dupuis et al., 2011b):

1. A lower amount of polymer concentration is needed to achieve a given mobility (lower the costs).
2. They have an extended range of suitable reservoirs regarding salinity tolerance.
3. The mixing and pumping procedures are more facilitated due to rapid viscosity build-up and shear stability.

The enhanced thickening ability and elastic deformation response of associative polymers compared to classical water soluble polymers, makes the associating polymer solutions attractive for other IOR applications like near well treatments. The thickening capability and selective adsorption properties, highly concentrated associating polymer solutions can be injected for *in- depth gel formation.* These polymeric gels may be able to modify the injectivity and/ or production profile of a producing oil reservoir (Dupuis et al., 2011b).

2. Background

This chapter has the intention to create a better understanding of new modified polyacrylamide polymers, and a more sufficient aspect of associating polymers is considered for chemical EOR approach.

2.1 Enhanced oil recovery

Improved knowledge of sub terrain chemical and physical conditions, and the flow characteristics can improve the process of conventional recovery methods significantly. By implementing different *improved oil recovery* (IOR) measures like advanced modelling and simulation software, it is possible to characterize the reservoir and predict fluids flow and rock behaviour during production. Introducing high- resolution logging tools which gathers data close to the wellbore and seismic surveys which covers larger areas of the reservoir, the reservoir model can be improved. The resolution of these techniques are still low (Skarestad and Skauge, 2009). By including *enhanced oil recovery* (EOR) techniques in addition to advanced sub- sea technology and other production optimisation techniques, this could have a great impact on the efficiency and economic benefit of the recovery process on the Norwegian continental shelf (NCS) (Utvinningsutvalget, 2010).

All EOR methods have in common that a material is added to the reservoir, which is not necessarily originally in place. When adding a material, the reservoir is added energy to produce more hydrocarbons to the surface. Such EOR recovery methods are called unconventional methods, compared to primary and secondary oil recovery, which affects the whole reservoir and the oil production (Skarestad and Skauge, 2009). EOR techniques used in the petroleum industry can be distinguished between gas and water related EOR approach. Gas related EOR methods include injection of CO_2- and miscible hydrocarbon gas, whereas water related EOR includes chemicals like surfactants and polymers dissolved in the injection water and low salinity water injection. All EOR techniques have unique properties to reach out to different parts of the reservoir that was not yet been flooded by the water injection (Skarestad and Skauge, 2009).

2.1.1 Polymers for EOR

The most utilized polymers today are the synthetic and partially hydrolyzed polyacrylamide (HPAM), the modified natural polymers and the biological polysaccharide, Xanthan (Wu et al., 2012). The water – soluble polymers are very attractive for IOR purposes, and in this study mobility control through polymer flood in oil fields and production control by injection of a blocking polymer gel are considered.

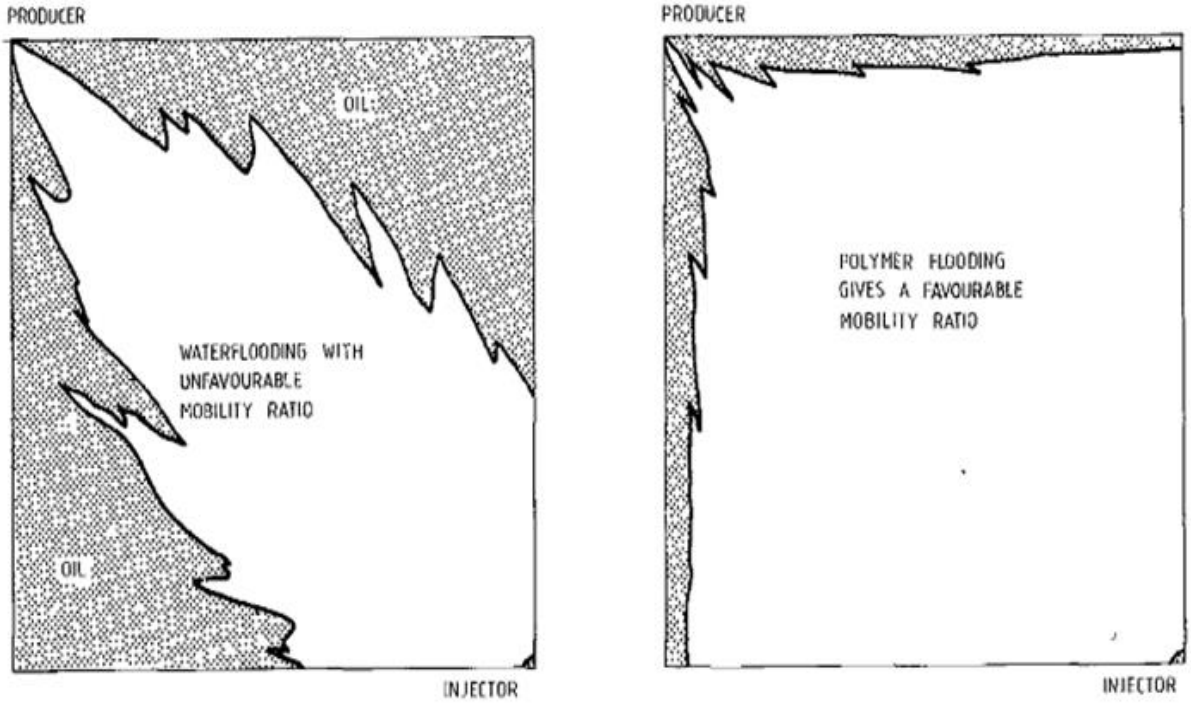

Figure 2.1 Comparison of area sweep efficiency (E_A) to an unfavorable waterflood (left) and a favorable polymer flood (right) from the injector to the producer (Sorbie, 1991).

In *figure 2.1* one of the most important parameter during oil production is illustrated by addition of polymers to the injection water, and that is the *mobility control (*Lee et al., 2009). When polymers are added to the injection water, this can result in a pressure build-up between the flooded area and the injection well in the reservoir. According to Darcy`s law, the pressure difference over the medium is related to the water solution`s viscosity and permeability. The lowest resistance to flow for the injected polymer solution will be anywhere besides the already existing "water channels". Darcy's law describes the permeability for a linear, horizontal flow. For incompressible fluid at constant volume rate in a core sample, Darcy's law can be defined as (Zolotukhin and Ursin, 2000):

$$Q = \frac{K \cdot A}{\mu} \cdot \frac{\Delta P}{L} \qquad \textbf{Eq. 2.1}$$

Where Q is the volumetric flow rate, K is the absolute permeability, A is the cross- sectional area, μ is the fluid viscosity, ΔP is the pressure difference over the medium and L is the length of the core sample.

Already in the early days of the oil production industry in the 1950‘s, extensive waterflood applications were applied after unveiling the down sides of pressure depletion methods. At the end of the 1950`s, the weaknesses and strengths of waterfloods in oil production were mainly explored (Sorbie, 1991). This led to extensive research and new developments of chemicals through the last 60 years (Lee et al., 2009). Water- soluble polymers, also called water thickeners, have the thickening ability to increase the viscosity of water due to its high molecular weight. Charged polymers will also be able to increase the hydrodynamic volume of the macromolecule even further, due to electrostatic repulsion between polymer coils and charged segments in the same coil (Wever et al., 2011).

For chemical EOR flooding the synthetic and anionic HPAM and its derivatives are the most common used polymers (Reichenbach-Klinke et al., 2011). This synthetic copolymer consists of acrylamide and acrylic acid, and has a typical high polymer weight between 2 to 20MDa (Sorbie, 1991). In *figure 2.2* the molecular structure of polyacrylamide (PAM) and HPAM are illustrated. Compared to HPAM; the modified natural polymers have a lower chemical and mechanical stability, and the biopolymers are more expensive and easier biological degradable during a polymer flood through the reservoir.

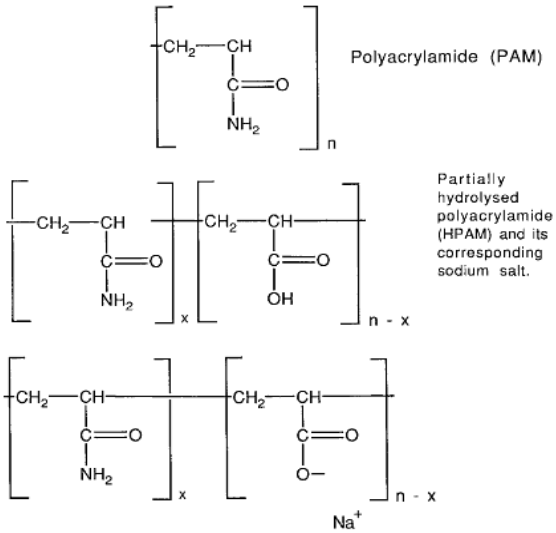

Figure 2.2 The primary chain structure of polyacrylamide (PAM) and partially hydrolysed polyacrylamide (Sorbie, 1991).

How easily a phase flows through a porous medium in a multiphase flow can be measured by its *mobility*. Single phase mobility, such as water, oil or gas, is defined as:

$$\lambda_i = \frac{K \cdot K_{r,i}}{\mu_i} \qquad \textbf{Eq. 2.2}$$

Where λ, μ, K and $K_{r,i}$ are the mobility, the viscosity, the absolute permeability and the relative permeability of the fluid i respectively.

The *mobility ratio* is defined the ratio between the mobility of the displacing fluid (water) and the displaced fluid (oil):

$$M = \frac{\lambda_w}{\lambda_o} = \frac{K_{r,w} \cdot \mu_o}{K_{r,o} \cdot \mu_w} \qquad \textbf{Eq. 2.3}$$

Where M and K_r are the mobility ratio and relative permeability respectively, and the subscripts o and w refers to oil and water (Sorbie, 1991).

To be more specific, a favourable mobility ratio between water and oil are often considered to be equal to or less than unity($M \leq 1$). This implies a stable displacement front between the fluids, and according to the Buckley – Leverett displacement theory, this ideal front is described as a shock- front (piston- like displacement). On the other hand, when the mobility ratio is greater than unity, this front becomes less sharp because the displacing fluid is more mobile than the displaced fluid ($M > 1$) (Lien, 2009).

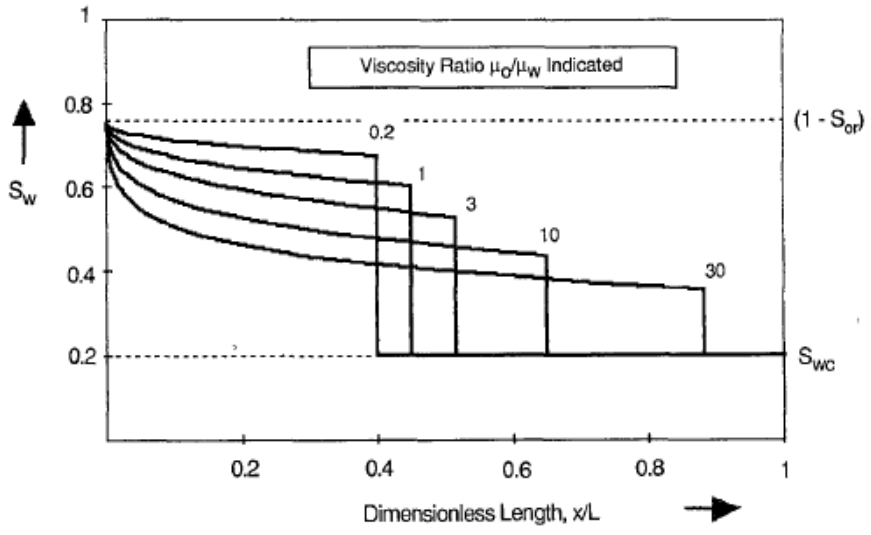

Figure 2.3 The Buckley- Leverett saturation front height is sharpest at favourable mobility ratio (Sorbie, 1991).

The *figure 2.3* illustrates the different outcomes of the displacement front at different mobility ratio. A mobility ratio above 10 is considered high, and the displacement front at this mobility

ratio is illustrated in *figure 2.3* as *"10" and "30".* A high mobility ratio cause the water to flow more easily towards the production wells compared to the oil. This unfavorable ratio leads to water bypassing oil, which results in a high residual oil saturation in the reservoir. A mobility ratio near unity is considered a low, and these displacement fronts at favorable conditions are illustrated in *figure 2.3* as "0.2", "1" and "3". A shock front of water sweeps the oil towards the productions wells, resulting in high water saturation after the flooding.

For a typical mobility control applications; polymers are considered when the viscosity of the oil is high (μ>5mPa·s), but also when the reservoirs are heterogeneous with oil- bearing layers at different permeabilities (Zolotukhin and Ursin, 2000). As mentioned in the beginning of this section, polymer gels can be utilized as a *near well diversion technique* to improve the production profile of an oil producing field. Polymer gels is injected to block thief zones, which is high permeability layers in the reservoir, and divert the water into new unswept areas of lower permeability. Injected polymer gels are illustrated in *figure 2.4.*

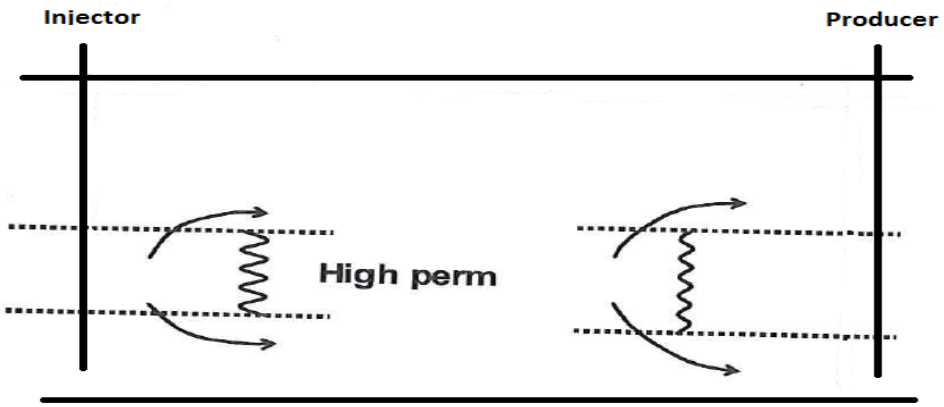

Figure 2.4 Polymer gels as near well diversion technique to improve injectivity and production performance (Skarestad and Skauge, 2009).

A reaction between a polymer and a cross linking agent the solution can swell many times their size and thereby block selected pore channels. Linked Polymer Solutions (LPS), BrightWater technology and Silicate gel are examples of such polymer gels (Skarestad and Skauge, 2009). These gels can be injected near the injection well to improve the injectivity performance, and near the production well to improve the production performance of the producers (Zolotukhin and Ursin, 2000). The success of the pore blocking using polymer gel, is related to the reservoir conditions and how this affects the performance of the gel (Skarestad and Skauge, 2009).

Comparing to conventional waterfloods on a timescale, polymer floods will accelerate the recovery process due to rapid viscosity build- up. Since the intention for all IOR measures is to improve the economic benefit of the recovery process, the polymer injections will contribute to a faster and higher oil production. An incremental recovery factor of 5% original oil in place (OOIP) or more is regarded as a successful polymer application (Rai et al., 2012, Singhal, 2011, Skarestad and Skauge, 2009).

2.1.2 Modifications on polyacrylamide

During the last two decades several polyacrylamide (PAM) - based polymers have been developed with improved rheological properties, to survive in high temperature and high pressure (HTHP) reservoirs (Wu et al., 2012).

There exist several important properties that have to be considered before a polymer flood. One of them is the solubility of polymer in the water solution. Polymers are often dissolved in brines on site, and thereafter injected into the reservoir. The polymer solutions may become inhomogeneous during mixing, where microgels and other insoluble associations can damage the formation and reduce the efficiency of the polymer solution when injected. A filtering process is required before any polymer flood to remove impurities and other unsolved particles that can contribute to an unwanted pore blocking (Sorbie, 1991). It is also important to take into consideration the exposure of rust, acid and other pollute chemicals the polymer solution can interact with on offshore platforms.

The molecule weight and chain distribution plays an essential role on the polymer flow characteristics in the porous media. The viscosity improvement and the expenses regarding the amount of polymers needed to improve the sweep efficiency have to be considered as well (Pope, 2007). Different molecular geometries will influence the performance and stability of the polymer solutions, and together with the properties of the porous media a thorough study is crucial to the outcome of the polymer application (Wu et al., 2012). Polymer retention mechanisms occurring during floods are probably the most important factor to evaluate the economically viable in given reservoir (Sorbie, 1991).

A rapid viscosity build- up and mixing process are also essential to the performance and the economical prospective considering polymer floods. A rapid mixing process using low concentrated polymer solution that easily achieve a desirable viscosity and homogeneity, is time- saving and economical (Singhal, 2011). Pre- wetting polymers are often received in powder form, and transported to offshore or onshore installations in 750kg sacs.

Figure 2.5 Transported polymer sacs ready to mix (Morel et al., 2012).

Another important rheological property of synthetic polyacrylamide polymers is the viscoelasticity. The ability to rearrange the molecular structure when exposed to mechanical stress is necessary to be able to sweep additional reservoir volumes, and thereby reach out to new areas of oil (Skarestad and Skauge, 2009).

The conventional HPAM solutions lose easily their viscosity at high temperatures and high salinity/ hardness, and this restricts the application of polymer floods in deep offshore oil fields. Polymer applications on the Norwegian continental shelf meet several restrictions and two of them are temperatures above 100^{o}C and the salinity. Strongly salinity oil reservoirs are considered to be 100 000 ppm (sea water 35 000 ppm) or higher, with a hardness of 2000 ppm or more (Singhal, 2011).

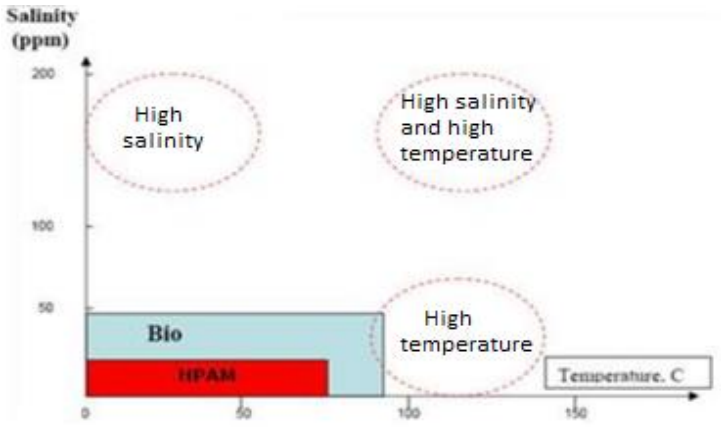

Figure 2.6 The conventional polymers like HPAM and Xanthan limitations regarding salinity and temperature[6].

[6] http://www.cipr.uni.no/projects.aspx?projecttype=11&project=54

An illustration of the limitations of conventional polymers like HPAM and Xanthan meet, regarding reservoir salinity and temperature are shown in *figure 2.6.*

As mentioned in the beginning, effective polymers have been designed to meet the requirements for HTHS reservoirs. Modifications on the polyacrylamide backbone are incorporations of groups that can improve the thermal stability of the macromolecule, and to provide a resistance to chemical degradation as the salinity of the brine increases.

To improve the thermal stability of the polymers, some of the implementations that have been done are reconstruction of the polymer backbone to a rigid ring structure, or incorporation of large side groups along the backbone (Wu et al., 2012). By incorporate large and rigid groups along the backbone, this steric effect will contribute to prevent the polymer molecules to coil-up and thereby maintaining the viscosity of the solution (Wu et al., 2012).

Incorporation of monomers like the 2- acrylamido- 2- methyl propane acid (AMPS) onto the polymer backbone, can contribute to reduce the sensitivity to ionic effects in the brine due to shielding of acrylic acid moieties. By incorporation of e.g. N- vinyl- 2- pyrrolidone (NVP) groups randomly on the polyacrylamide, an improvement in the thermal stability can be induced due to shielding of acryl amide moieties (Wu et al., 2012).

Introducing hydrophobic groups along the partially hydrolyzed polyacrylamide, these groups will induce an aggregation due to non- polar interactions in brines. This can result in a faster viscosity build- up and a more robust molecular structure due to strong intermolecular associations, compared to conventional HPAM solutions. In section 2.1.4 an introduction of such associative polymers is presented (Wu et al., 2012, Reichenbach-Klinke et al., 2011).

2.1.3 Hydrolysis reaction and salinity/hardness effect

HPAM is a chained polymer with repeating acrylamide and acrylic monomers, as illustrated in figure 2.2. In this thesis the conventional HPAM, SNF Flopaam 3036 (Lot Z 2340) was utilized. This polymer had a molecular weight between 16 to 20MDa, and a hydrolysis degree of 25- 30%. Hereafter in this study, this polymer is referred to as "HPAM".

A degree of hydrolysis around 25- 30 %, means that only 25% to 30% of the acrylamide moieties in the copolymer are hydrolyzed to acrylic acid (Reichenbach-Klinke et al., 2011). In *figure 2.7* the hydrolysis reaction of polyacrylamide (PAM) to HPAM is illustrated.

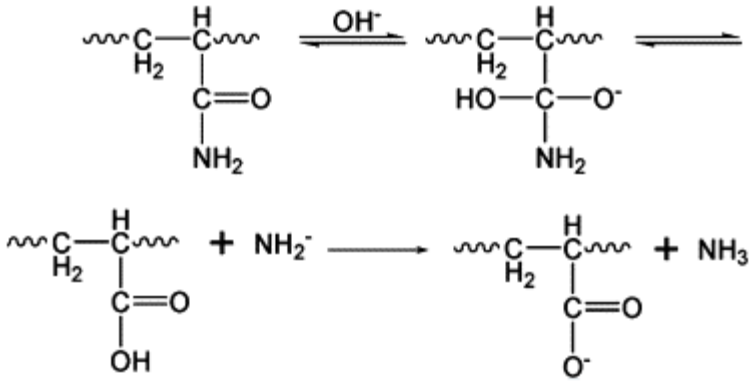

Figure 2.7 Hydrolysis reaction of polyacrylamide (PAM) to HPAM (Zhao et al., 2010).

In *figure 2.7* the hydrolysis reaction step by step is illustrated for one acrylamide monomer along the backbone. Some of the acrylamide monomers along the chain will react with surrounding water, and thereby substitute NH_2 with OH^- ions. Due to the negative charged acrylic acid monomers along the backbone, the repulsion between them stretches the polymer back bone out. This swelling occurring in the macromolecule structures increases the hydrodynamic volume of the polymer in the solution.

The degree of hydrolysis of polyacrylamide can affect the physical properties such as salinity and hardness sensitivities, mechanical stability and adsorption characteristics. A high degree of hydrolysis will induce unbalance in the repulsion between anionic carboxyl groups along the polymer backbone, where extensive screening may cause precipitation of polymers in the solution (Sorbie, 1991).

When salt is added the aqueous solution, the anionic carboxyl side groups will react with monovalent and divalent cations. The Coulomb repulsion between the negative charged groups on the polymer are less effective as the salinity in the brine increases, which reduces the swelling in the macromolecule (Reichenbach-Klinke et al., 2011).

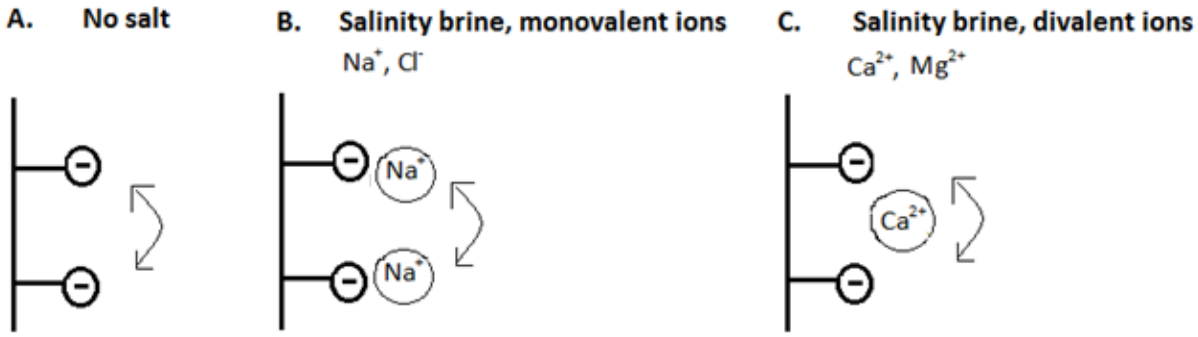

Figure 2.8 The anionic carboxyl side group simplified response to increasing salinity/hardness in the water solution.

In *figure 2.8 A*, the acrylamide and acrylic acid copolymer are dissolved in water without any salt. The interactions occurring between the anionic side groups cause electrostatic repulsion (Dupuis et al., 2010), which induce a swelling in the macromolecule. When the salinity increases by addition of monovalent salt ions into the water solution, as shown in *figure 2.8 B*, screening of the repulsion between the negative charged carboxyl groups occurs. As a consequence of the interactions between the positive charged monovalent ions and the side groups, the polymer molecules will start to coil- up. A further increase in the salinity and hardness of the brine by addition of divalent ions are illustrated in *figure 2.8 C.* The macromolecule are no longer in a stretched state anymore, the chains are now considered to be in a coiled state (Reichenbach-Klinke et al., 2011). In the presence of divalent ions, a precipitation of the polymer may occur. Precipitation of HPAM macromolecules in high salinity brine are related to the degree of hydrolysis. Above a certain level of acrylic acid in the copolymer, insoluble complexes between these anionic groups and divalent ions can be formed in the solution. When these segments precipitate out of the solution due to insolubility, the viscosity will drop (Reichenbach-Klinke et al., 2011).

Since HPAM is polyelectrolyte, the effect of salinity/hardness in the polymer solution is reducing the hydrodynamic volume of the macromolecules. This is illustrated in *figure 2.9.*

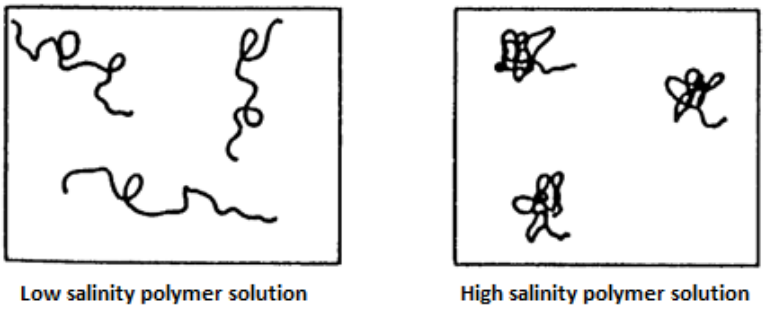

Figure 2.9 The long and flexible polymer backbone of HPAM coils- up when increasing the salinity/hardness of the solution (Sorbie, 1991).

The reaction rate of hydrolysis depends on the concentration of salt and hardness in the solution and temperature. Increasing salinity and hardness in an aqueous solution, or increasing the temperature, this may speed up the hydrolysis reaction *(Berg, 2010, Sorbie, 1991).* The relation between precipitation of HPAM macromolecules in the solution due salinity and temperature are illustrated in *figure 2.10.*

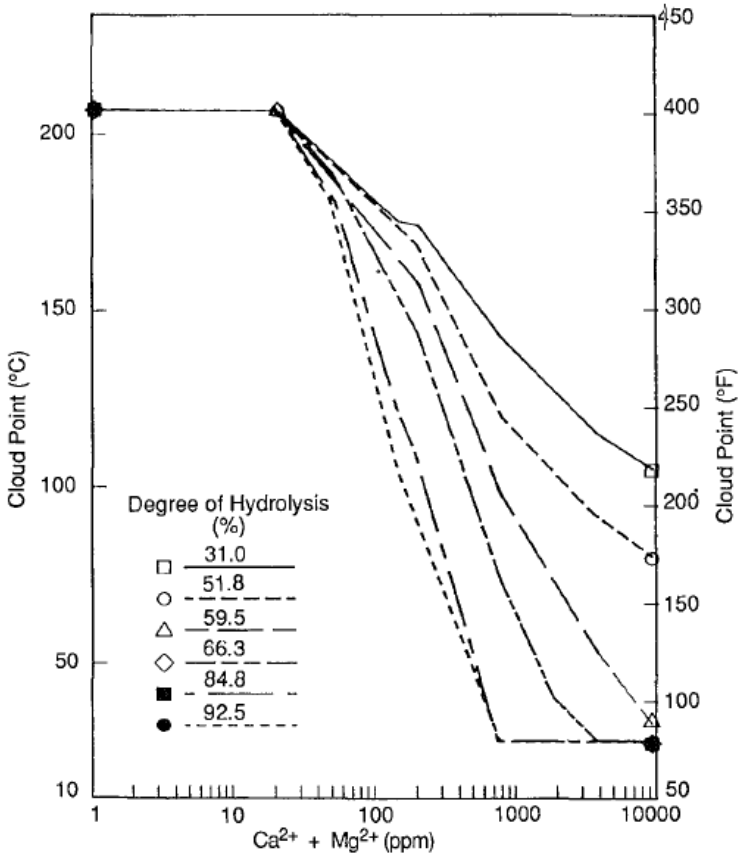

Figure 2.10 The relation between precipitation of HPAM due to increasing salinity and hardness in brine, and increasing temperature (Sorbie, 1991).

From *figure 2.10* increasing salinity cause a more rapid precipitation of HPAM with increasing degree of hydrolysis. The steepest precipitation slope is shown for HPAM with the highest degree of hydrolysis of 92.5% when salinity increases. Relating this observation to ambient temperature, the temperature of precipitation is increases as the degree of hydrolysis reduces. The temperature where the HPAM macromolecules precipitates in the solution, are often referred to as the solution *cloud point* (Sorbie, 1991).

Before any polymer applications the cloud point of the polymer solution must be evaluated to avoid precipitation on the chemical equipment during injection, or during the flow through the reservoir (Raney et al., 2011).

2.1.4 Associating polymers

Already during 1950`s the first design of partially hydrolyzed polyacrylamide containing hydrophobic groups was carried out (Argillier et al., 1996). In general a relative small amount of hydrophobic groups, i.e. 8-18 carbon atoms moieties (Wever et al., 2011) are incorporated into the charged hydrophilic backbone. According to an overview given by Seright et al. in 2011(Seright et al., 2011), less than 0.1 to 7 mol% are necessary to improve the thickening capability compared to non- hydrophobic containing HPAM in aqueous solutions.

To generate viscosity in the polymer solution, the thickening effect of these modified HPAM polymers do not rely only on the molecular weight and the Coulomb repulsion between the charged segments on the backbone. In addition, the incorporated hydrophobic groups can interact with each other between different chains and increase the hydrodynamic volume of the macromolecules (Reichenbach-Klinke et al., 2011, Seright et al., 2011, Buchgraber et al., 2009). Since the polyacrylamide backbone is soluble in aqueous brines, the hydrophobic groups will rearrange to minimize their exposure to the polar solvent (Chassenieux et al., 2010, Maia et al., 2009, Taylor and Nasr- El- Din, 2007, Taylor, 2003, Taylor and Nasr- El-Din, 1995).

The association effect depends on the properties of the aqueous solution like content, pH and temperature, and also the polymer structure, composition and concentration (Wever et al., 2011). The incorporated groups associate due *the intramolecular hydrophobic interactions* and *the intermolecular hydrophobic interactions.* Intramolecular hydrophobic associations occurs between hydrophobic groups within the macromolecule, whereas intermolecular hydrophobic associations are hydrophobic interactions occurring between neighboring macromolecules in the aqueous solution (Wever et al., 2011). In *figure 2.11* illustrates the different physical interactions occurring between hydrophobic groups.

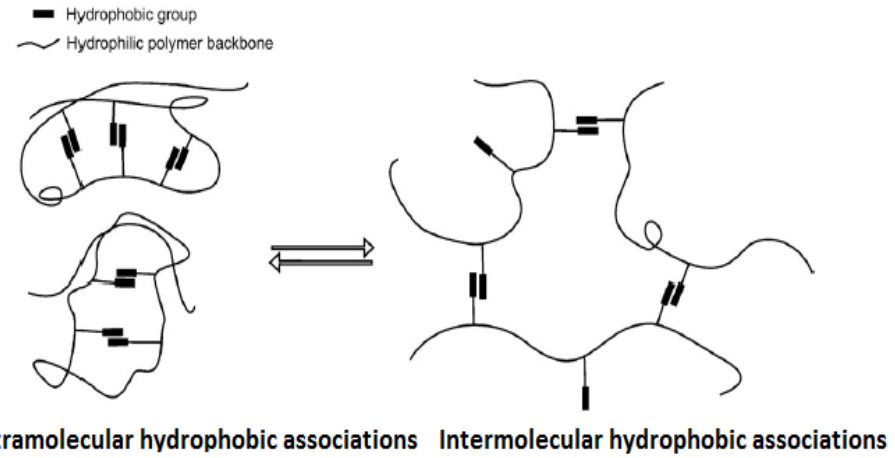

Figure 2.11 Intra- and intermolecular associations occurring between the hydrophobic groups (Wever et al., 2011).

According to McCormick and Johnson (McCormic and Johnson, 1988), concentrated solutions of these modified polymers may give rise to higher viscosities at low shear rates, they may also have higher salt tolerance, and show a less sensitivity to mechanical degradation compared to HPAM.

In the literature, these modified partially hydrolyzed polyacrylamide (Maia et al., 2009, Taylor, 2003, Lin et al., 2000, Taylor and Nasr- El- Din, 1995) is often referred to as *hydrophobically associating polyacrylamide* (HAPAM) (Wever et al., 2011, Maia et al., 2011, Lu et al., 2010, Argillier et al., 1996), *hydrophobically modified water- soluble polymers (HMWSP) (Dupuis et al., 2011a, Chassenieux et al., 2010)* or *hydrophobically associating polymers* (AP) (Seright et al., 2011, Reichenbach-Klinke et al., 2011, Buchgraber et al., 2009, Kujawa et al., 2006, Regalado et al., 1999). From hereafter, the modified partially hydrolyzed polyacrylamide is referred to as associating polymers.

An illustration of the chemical structure of an associating polymer with acrylamide and acrylic acid moieties are shown in *figure 2.12*. The hydrophobic group is dodecyl methacrylate.

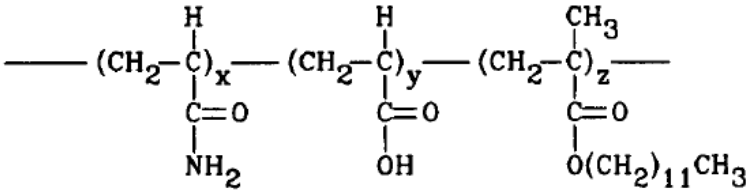

Figure 2.12 Hydrophobically associating acrylamide copolymer; x: 30-100, y: 0- 70, z: 0,01- 1 mol% (Taylor and Nasr- El- Din, 1995).

The association and rearrangement due to hydrophobic interactions, resembles to micelle formation by surfactants above it`s *critical micelle concentration* (CMC) (Taylor and Nasr-El- Din, 2007). The distribution of hydrophobic groups on the hydrophilic backbone has a great impact on association occurring, and the unique rheological properties that are formed (Jiménez-Regalado et al., 2004, Argillier et al., 1996). Above a given polymer concentration in aqueous solutions, a formation of a network of associating polymers is possible (Wever et al., 2011). This intermolecular association is an entropy driven process (Lin et al., 2000). It is the structure of the surrounding water molecules that becomes more disordered when the associating parts starts to interact and rearrange due to hydrophobicity.

From a paper by Kujawa et al. from 2006 (Kujawa et al., 2006), different properties can be changed to improve the thickening ability of associating polymers. They listed up changeable properties like the molecular weight, the chemical structure of the hydrophilic units, the nature and content of the hydrophobic groups and/or their distribution along the hydrophilic backbone.

There exists a classification of different associating polymers regarding the distribution of hydrophobic groups on the acrylamide backbone (Chassenieux et al., 2010, Dupuis et al., 2011a, Jiménez-Regalado et al., 2004):

1. *Associative polymers containing only one associating block (figure 2.13A)*
2. *Telechelic associative polymers (figure 2.13 B)*
3. *Multisticker associative polymers (figure 2.13 C)*
4. *Combined associative polymers*

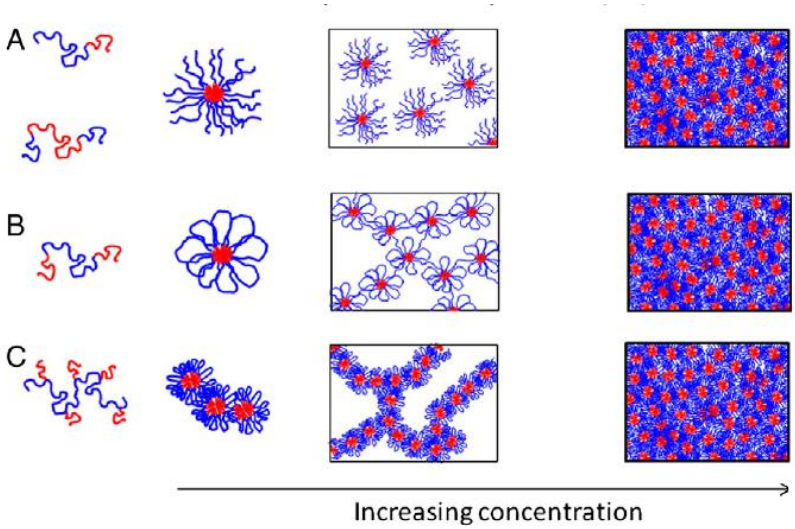

Figure 2.13 A simplified illustration of different associative polymers regarding the amount and distribution of the hydrophobic blocks (red) on the polymer backbone (blue) (Chassenieux et al., 2010).

The first class of associating polymer is illustrated in *figure 2.13 A*, where the synthetic polymer contain only one single hydrophobic group onto the hydrophilic chain. At a low polymer concentrations, the associative polymers flows freely with a Brownian motion in the solution. This means that there are no significant intermolecular associations occurring, since the macromolecules are not affected by the neighboring macromolecules (Taylor and Nasr-El- Din, 1995). This is illustrated in the *figure 2.14 "Free"*. This concentration range is referred to as *the diluted concentrated regime*, where the viscosity measured at these concentrations are dominated by the intramolecular hydrophobically interactions (Wever et al., 2011, Dupuis et al., 2009).

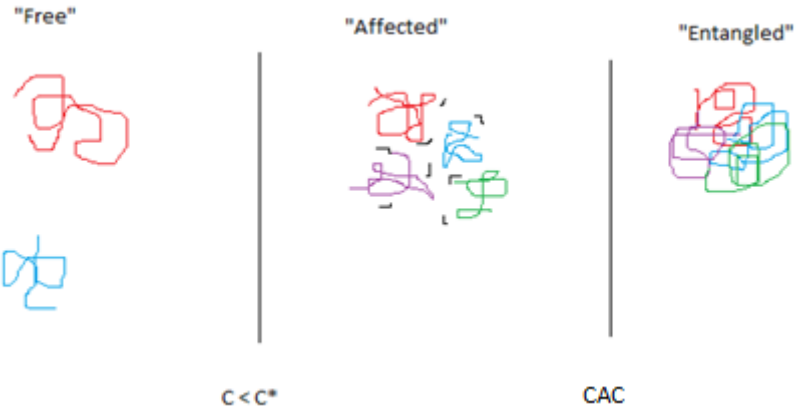

Figure 2.14 The behavior of associative polymers as the concentration increases in the solution.

A further increase in the polymer concentration will force the associating polymers together. At this concentration range the polymers motion in the brine are influenced by other polymers, and this is illustrated in the *figure 2.14 "Affected"*. An *affected* associating behavior occurs in a concentration range referred to as *the semi- diluted concentration regime* (Wever et al., 2011, Dupuis et al., 2009).

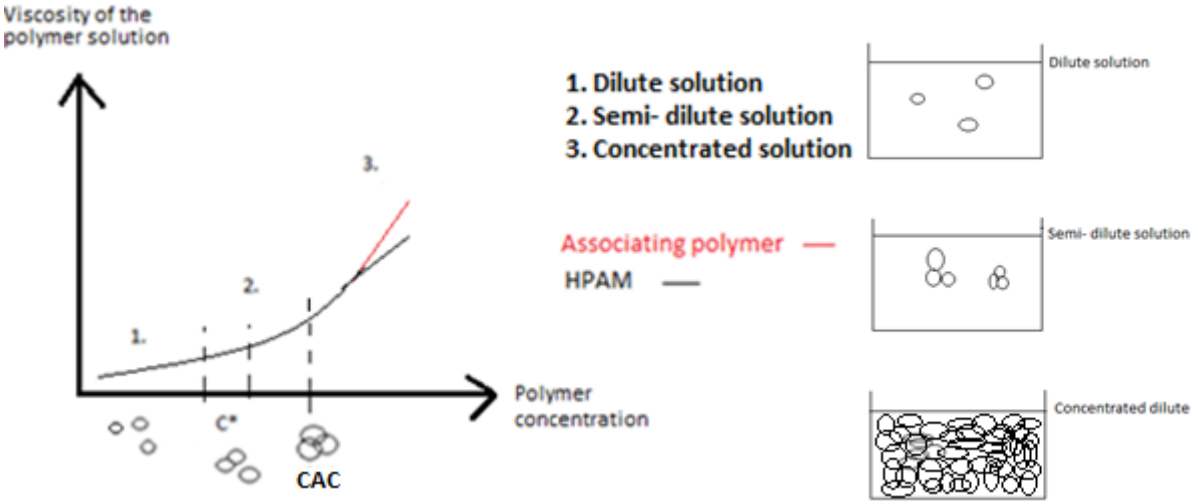

Figure 2.15 Schematic drawing of the change in the viscosity of associating polymer solutions (red) and HPAM, as the concentration increases. Different concentration regimes are denoted as "1": dilute solution, "2": semi- dilute solution, and "3": concentrated solution.

The critical overlap concentration, C^*, is the polymer concentration where the macromolecular structures starts to overlap. This concentration is often not an exact concentration, but rather a diffuse concentration range between the dilute regime and the *semi- diluted untangled regime* for the associative polymers (*figure 2.15_ 2*) (Dupuis et al., 2009).

The semi- diluted concentration range is divided into *untangled* and *entangled* regime depending on the concentration. In the semi- dilute untangled regime the associative polymers starts to associate and form typical "micelle"- like aggregations, due to the dominance of the intramolecular hydrophobic associations *(figure 2.13).* An increase in the polymer concentration results in an entangled regime, where extensive hydrophobic association between neighboring associating polymers leads to a formation of a transient network of polymers. This physical entanglement between polymer chains, are due to the strong intermolecular hydrophobic associations. This entanglement concentration is referred to *the*

critical association concentration, CAC, and is marked in the viscosity versus concentration plot (*figure 2.15 between "2" and "3"*) where the viscosity of the associating polymer solution increases significantly above this concentration (McCormic and Johnson, 1988).

Above CAC, this concentration range is referred to as *the concentrated regime*. At these concentrations the polymers are no longer able to move in the solution, they are said to be jammed in the solution (Chassenieux et al., 2010, Taylor and Nasr- El- Din, 1995).

The telechelic associative polymers are polymers containing hydrophobic groups typically located at both ends of the polymer backbone (*figure 2.13 B*) (Wever et al., 2011, Chassenieux et al., 2010, Jiménez-Regalado et al., 2004). Incorporation of more than one associating group can induce different types of associations when the polymer concentration increases. This is illustrated in *figure 2.16*.

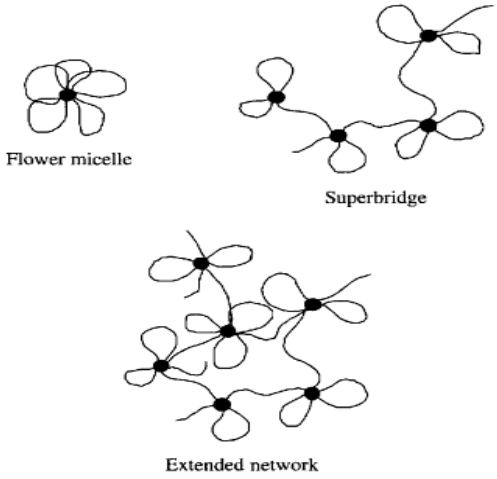

Figure 2.16 Schematic drawing of different types of association formed by the telechelic associating polymers (Ma and Cooper, 2001).

Figure 2.16 illustrates that associating polymers with hydrophobic groups are distributed at the end of the chains a flower- like assembling may be formed. The hydrophilic backbone creates a loop towards the solution. It is possible that an increase in the concentration will result in bridges between the flower cores (Wever et al., 2011). A network of associating polymers in the solution may be induced due to extensive formation of bridges between the cores as the concentration increases.

The third associative polymer class is the multisticker, which contain several hydrophobic groups along the hydrophilic backbone as illustrated in *figure 2.13 C*. These multisticker

polymers will more efficiently create bridges between the flower-like cores, even at low polymer concentration. A further increase in concentration may lead to a formation of a transient network as well, and the strength of the intermolecular interactions are higher compared to a network of telechelic associating polymers (Chassenieux et al., 2010, Jiménez-Regalado et al., 2004, Ma and Cooper, 2001).

The forth polymer class combines the hydrophobic localization to the telechelic and the multisticker, and is refer to the combined associated polymers (Jiménez-Regalado et al., 2004). This type of distribution of hydrophobic groups may result in stronger association and a much higher viscosity increase of the solution. The strength of the associations depends on the hydrophobic group, the position on the polymer backbone, and the polymer mobility in the solution (Jiménez-Regalado et al., 2004).

2.1.5 Salinity/hardness effect on associating polymers

The behavior of the associative polymers in salty brines depends on the dominance of the attractive association of the hydrophobic groups, compared to the repulsive electrostatic interaction between the charged units along the molecular backbone (Maia et al., 2011, Kujawa et al., 2006).

The sensitivity of salinity of associating polymer solutions is presented in several papers (Maia et al., 2011, Dupuis et al., 2011a, Pancharoen, 2009, Gouveia et al., 2008, Taylor and Nasr- El- Din, 2007). The papers from 2011 by Reichenbach- Klinke et al. (Reichenbach-Klinke et al., 2011) and Wever et al (Wever et al., 2011) are also about the salinity effect on associating polymers. The salinity effect on the viscosity of the associating polymer solution compared to HPAM solutions is observed to be related to the dominance of hydrophobic associations. The classical behavior of HPAM solutions due to electrostatic screening is a reduction in the viscosity as the salt concentration increases. This electrostatic screening is also observed in associating polymer solutions. Above the critical overlap concentration (C^*) in the semi- diluted concentration regime, the polymers are affected by each other and interactions occurs between the hydrophobic groups of neighboring polymers. The salinity strengths the intermolecular hydrophobic associations occurring, and a more polar solvent increases the viscosity of the solution.

In the concentrated regime, increasing salinity increases the viscosity of associating polymers up to a certain level due to intermolecular hydrophobic interactions. Above a given salinity concentration in the solution, the polymers starts to precipitate or form a pseudo gel- structure (Dupuis et al., 2011a, Kujawa et al., 2006, Taylor, 2003).

According to an overview given by Taylor and Nasr- El- Din from 2007 (Taylor and Nasr- El-Din, 2007) the salinity effect of associating polymers in the diluted concentration region follows the same trend as HPAM solutions. Below the critical overlap concentration (C^*), the viscosity decreases as the salt concentration in the solvent increases. This is due to an enhancement in the intramolecular hydrophobic associations, which reduces the hydrodynamic volume of the associating polymer even further than HPAM solutions. Similar observations have been observed several times (Maia et al., 2011, Gouveia et al., 2008).

In June 2009 Monrawee Pancharoen (Pancharoen, 2009) finished his thesis at Stanford University, where he characterized several associating polymers and compared these to the conventional HPAM. The chemicals he used from SNF Floerger were FP 3630, SuperPusher D118, S255 and SuperPusher B192. In this thesis the same polymers were studied, except of S255. SuperPusher C319 was utilized instead. He performed shear viscosity measurements of these polymer solutions at constant temperature, and thereafter compared these viscosities after addition of salts. His results showed that the viscosity of associative polymers was less affected to an increase in the salinity from 2wt% and 10 wt% NaCl brines, compared to the HPAM.

In this thesis associating polymers were delivered from SNF Floerger, and the properties of these polymers and HPAM as presented in *table 3.4* in section 3.1.3. Hereafter, the three different SuperPusher polymers utilized during this study are referred to as C319, D118 and B192.

2.2 Polymer rheology

Rheology is a study of the flow behavior and properties, and deformation of all kinds of materials exposed to external stress. When materials are under deformation stress they all show a viscoelastic behavior, which is a mixture of viscous and elastic properties (Berg, 2010). Viscosity is a measure of a fluids resistance to deform under influence of an external force. In general, the viscosity of polymer solutions will not be the same at all time. The viscosity value is highly influenced by the fluids nature, ambient temperature and the amount of force applied. Sir Isaac Newton defined the dynamic viscosity as (Newton`s Law of viscosity):

$$\mu = \frac{\tau}{\dot{\gamma}} \qquad \textbf{Eq. 2.4}$$

Where μ is the viscosity, τ is the shear stress, and $\dot{\gamma}$ is the shear rate in laminar flow. The SI-unit of the dynamic viscosity is "Pascal · second" [Pa · s], but the field unit used in the petroleum industry is centipoise [cP] after Jean Poiseuille. The viscosity unit centipoise is the same as "milliPascal · second".

2.2.1 Shear viscosity

Fluids can be divided into several classes based on their behavior compared to the shear rate applied. A *flow curve* is a plot of shear rate versus shear viscosity, and can be used to determine which class a certain fluid belongs to. The viscosity of Newtonian fluids is independent of the shear rate, i.e. the viscosity is constant. Typically Newtonian fluids are water and mineral oils (Schramm, 1998). Most fluids are Non- Newtonian, and their shear flow behavior is always changing. The viscosity is therefore dependent upon the shear rate, and polymer solutions acts as Non- Newtonian fluids at sufficiently high concentrations (Sorbie, 1991). *Figure 2.17* show a standard shape of the complex flow behavior for dilute flexible chain- like polymer solutions, with four distinct regions.

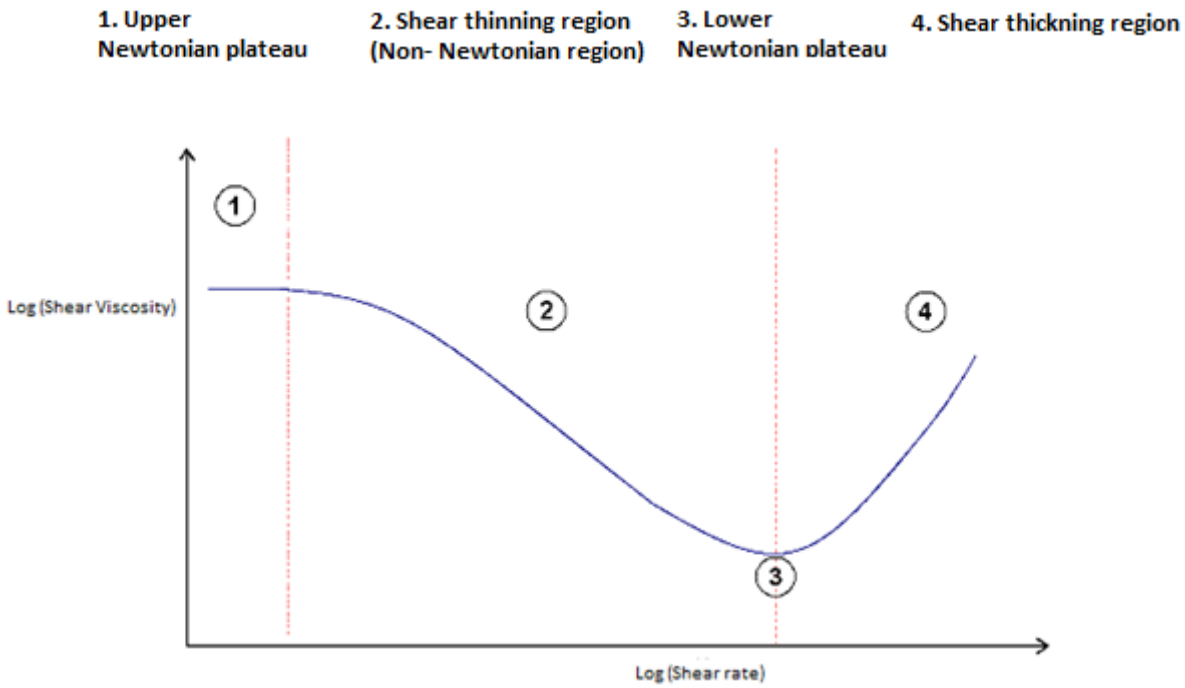

Figure 2.17 Schematic viscosity curve of a polymer solution as a function of shear rate where each number represents a specific region (Lunestad, 2011).

The rheological characterization of polymer solutions must include determination of their viscosity in both shear and extensional flows, since these macromolecules are subjected to both shear and extensional stresses inside an oil reservoir (Chauveteau, 1986). Polymer solutions at low concentration can act as non- Newtonian time- independent fluids (Sochi, 2010), which indicates that the strain rate at a given point only depend on the instantaneous stress at that point.

The four distinct regions in the flow curve illustrated in *figure 2.17* are described below:

1. ***The upper Newtonian plateau*** (Sochi, 2010)**:** This region is also called the plateau of the zero- shear viscosity (μ_0). At low shear rates, the viscosity is constant, i.e. independent of shear rate. This behavior can be explained through the phenomenon *Superposition of two processes* (Anton Paar, 2008).

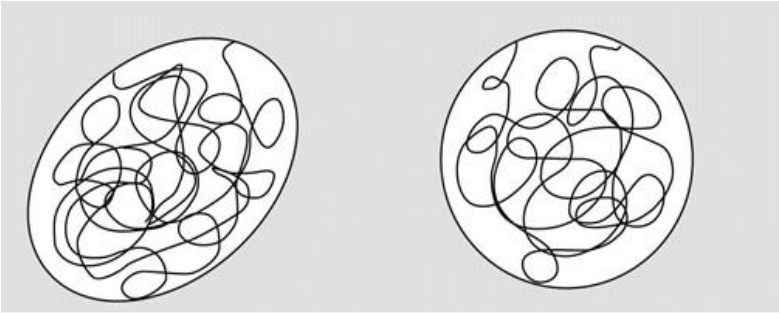

Figure 2.18 Illustration of Superposition of two processes at low shear rate (Anton Paar, 2008).

In the low- shear range the macromolecules will start to orient them- self towards the flow, which cause disentanglements. Since the shear force acting on the polymer solution is so weak, the polymers are still able to re- entangle because of their viscoelastic properties. These two processes cancel each other out, leading to an area on the flow curve with no change in the total viscosity value.

Chauveteau and Yasuda defined a *transition zone* between the Newtonian region (1) and the shear- dominated region (2) at high shear rates. A critical shear rate ($\dot{\gamma}_c$) defined at the end of the upper Newtonian plateau, was estimated to be equal to the inverse proportion of the rotational relaxation time (λ_c). The *relaxation time* is characteristic for a specific polymer solution, and is defined as the response time for the macromolecules to rearrange back to the originally configuration after the shear stress stops. A long relaxation time indicates a high elasticity in the polymer, caused by the strong interactions in the molecular chains (Sorbie, 1991).

2. ***The shear thinning region:*** After the critical shear rate defined at the relaxation time for the polymer, the viscosity starts to decrease with increasing shear rate. This non-Newtonian behavior is also referred to a *pseudoplastic* behavior (Sochi, 2010). Now the shear forces starts to break up the equilibrium structure, and uncoils the macromolecules. This results in a deformation in shear direction, which reduces the flow resistance of the polymer solution.

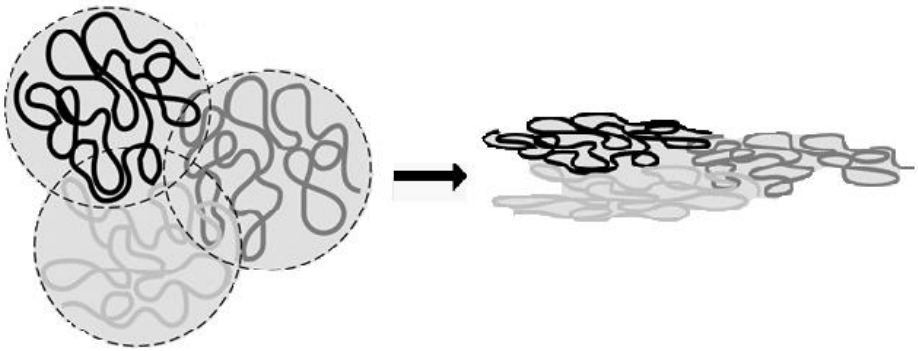

Figure 2.19 Disentanglements of flexible chain- like polymers under shear stress (Anton Paar, 2008).

3. ***The lower Newtonian Plateau:*** At this shear rate region the viscosity of the polymer solution is at its lowest value(μ_∞), due to the strong deformation forces acting on of the macromolecules. All the macromolecules in the solution are now stretched out to an aligned conformation and oriented to the shear direction.

4. ***The shear thickening/ dilatant region:*** Odell et al. in 1987 (Odell et al., 1987) reported observations on extremely dilatant effects occurring at high shear rates.

This shear thickening character occurs in any turbulence flows, like thus occurring in the porous media. This viscoelastic effect on the polymer occurs beyond a critical shear rate which is characteristic for a given polymer type, molecular weight and solvent. There exist some disagreement about how this viscosity enhancement phenomenon occurs compared to pure solvent; but two of the most supported theories are the *coil- stretch transition, and the development of transient entanglement network.*

The most supported hypothesis is the one where the viscosity increases due to stretching of random- coiled molecules. The high shear flow is now regarded as an extensional flow and the stretching continues until the macromolecules are torn apart. A more recent hypothesis to explain this viscoelastic effect is a formation of a transient aggregation network, due to collision of the polymer molecules. As the shear rate increases, the collision frequency increases as well. Since these macromolecules have very flexible chains, they will start to aggregate. This entanglement is thereafter followed by a disentanglement process, which takes longer time. And it is this transient aggregation that may induces the viscosity enhancement.

In an overview paper by Sochi in 2010 (Sochi, 2010), he listed up three broad classifications of non- Newtonian fluids. As described above, polymers at low concentrations can be typically time- independent fluids. They can also be classified as viscoelastic or time-dependent fluids, since no sharp distinction exist between them in this classification. A polymer solution can have different characteristically properties that allows it to cover all three of the classifications. At different polymer concentrations, the flow behavior depending on shear rate and shear time may differ.

Viscoelastic fluids are fluids that are partial elastic upon the removal of a shear stress. Such materials have properties that can be typical of both viscous fluids and elastic solids (Sochi, 2010). Some fluids, like polymer solutions, may be time- dependent or *thixotropic* non-Newtonian solutions. The shear viscosity of such fluids will decrease not only with increasing shear rate, but also with time at constant shear rate. The higher shear stress applied, the faster is the structure- breakdown process (Berg, 2010).

2.2.2 Models for shear flow

In 1991 Sorbie (Sorbie, 1991) listed up several proposed empirical functions to describe the complex shear behavior for non- Newtonian fluids. The most applied and simplified mathematic model for shear thinning behavior in viscometric flows is the *Power Law Model* (PLM), also referred to as the Ostwald- de- Waele model. The viscosity function in the PLM is given by the expression:

$$\mu(\dot{\gamma}) = K^{'}\dot{\gamma}^{n-1} \qquad \textbf{Eq. 2.5}$$

Where $\mu(\dot{\gamma})$ is the shear dependent viscosity, $\dot{\gamma}$ is the shear rate, and $K^{'}$ and n are empirical constants. The constant n is known as the Power Law index, and when $n < 1$ this results in a non- Newtonian flow behavior showing a monotonically decreasing shear thinning response at $\dot{\gamma}>0$ (Sochi, 2010). For a Newtonian fluid, $K^{'}$ is the constant viscosity and n is equal to unity.

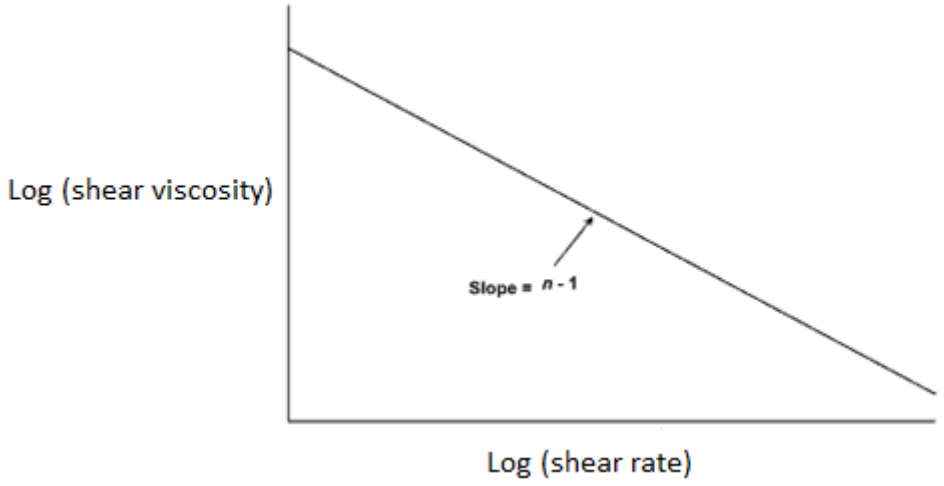

Figure 2.20 The Power- Law Model validity is only in the shear thinning region (Sochi, 2010).

The PLM is unfortunately not valid in the upper Newtonian plateau or in the lower Newtonian plateau, as illustrated in *figure 2.17*. Because of these limitations, the model is just able to produce results in the shear thinning or shear thickening area depending on the Power law index.

A more adequate model for the whole shear range is a four- parameter rheological model. The *Carreau- Bird- Ysauda Model* (CBY Model) includes region 1 to 3 illustrated in *figure 2.17*, and is expressed like this:

$$\mu(\dot{\gamma}) = \mu_{\infty} + \frac{(\mu_0 - \mu_{\infty})}{\left[1+(\gamma\dot{\lambda}_c)^2\right]^{\frac{1-n}{2}}} \qquad \textbf{Eq. 2.6}$$

Where $\mu(\dot{\gamma})$ is the shear dependent viscosity, μ_{∞} is the infinite shear viscosity, $\mu_0$is the zero-shear viscosity, $\dot{\gamma}$ is the shear rate, λ is a time constant and *n* is the Power Law index. The time constant (λ_c) is the relaxation time for a given polymer solution. The disadvantage about this empirical model is that it neglects the shear thickening region.

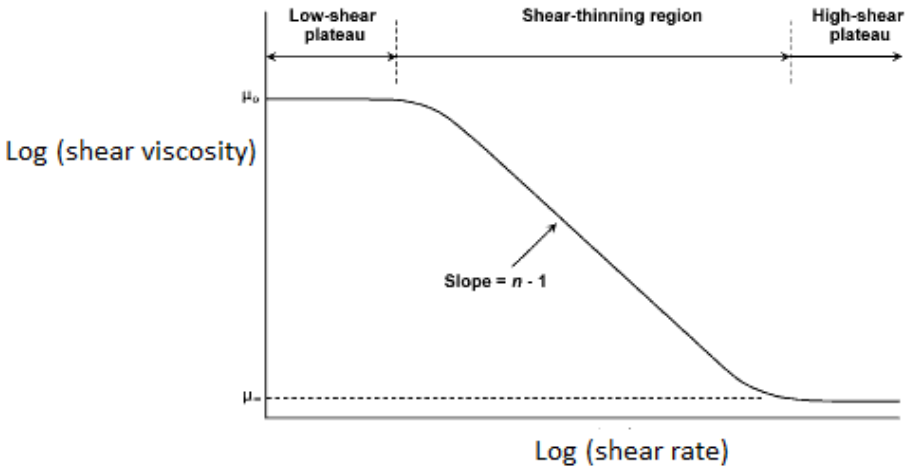

Figure 2.21 The validity of the Carreau- Bird- Ysauda Model (Sochi, 2010).

Several mathematic models have been proposed to describe this complex behavior of non-Newtonian fluids in one or more of these regions, but these involves more parameters and demands therefore a more precise input data.

2.2.3 Intrinsic viscosity and Huggins coefficient

The viscosifying properties of polymer solutions are given in relation with the molecular size and conformation, and the ability to expand in a given solvent. In dilute polymer solution the most important characterizing viscosity parameter, is the hydrodynamic volume of the macromolecules. This volume is referred to as the *intrinsic viscosity* of the polymer solution (Maia et al., 2005). An increase in the hydrodynamic volume will result in an increase in the intrinsic viscosity of the solution. The intrinsic viscosity can be defined as the *reduced viscosity* as the polymer concentration goes to zero (Sorbie, 1991):

$$[\eta]_o = lim_{c\to 0} \frac{\eta - \eta_s}{\eta_s c} = lim_{c\to 0} \frac{\eta_{sp}}{c} = lim_{c\to 0}\, \eta_R \qquad \textbf{Eq. 2.7}$$

Where $[\eta]_o$ is the intrinsic viscosity at zero polymer concentration [cm^3/g], η is the non-Newtonian shear viscosity of the solution [Pa·s], η_s is the solvent viscosity [Pa·s], c is the polymer concentration [g/cm^3]. η_{sp} is the *specific viscosity* (dimensionless unit) and η_R is the *reduced viscosity* [g/cm^3]. The SI- unit for intrinsic viscosity is [cm^3/g], but the unit [1/ppm] is often preferred.

The *reduced viscosity* is defined as the ratio of the specific viscosity to the polymer concentration (Sorbie, 1991):

$$\eta_R = \frac{\eta_{sp}}{c} \qquad \textbf{Eq. 2.8}$$

Where η_{sp} is the specific viscosity (dimensionless unit) and c is the polymer concentration of the solution [g/cm^3].

The *specific viscosity* is a dimensionless viscosity parameter defined as the *relative viscosity* minus unity (Sorbie, 1991):

$$\eta_{sp} = \eta_o - \eta_\infty = \frac{\eta}{\eta_s} - \frac{\eta_s}{\eta_s} = \eta_r - 1 \qquad \textbf{Eq. 2.9}$$

Where η_o is the viscosity of the solution at the upper Newtonian plateau [Pa·s], η_∞ is the viscosity of the solution at very high shear rates [Pa·s], and η_r is the relative viscosity (dimensionless unit).

The *relative viscosity* is also a dimensionless viscosity parameter, and is defined as the ratio between the viscosity of the polymer solution to the viscosity of the solvent (Sorbie, 1991):

$$\eta_r = \frac{\eta}{\eta_s} \qquad \textbf{Eq. 2.10}$$

Where η is the non- Newtonian shear viscosity of the polymer solution [Pa·s], and η_s is the solvent viscosity [Pa·s].

Sorbie et al. (Sorbie, 1991) related the intrinsic viscosity to the *inherent viscosity* as the polymer concentration goes to zero:

$$[\eta]_o = lim_{c\to 0} \frac{ln(\frac{\eta}{\eta_s})}{c} = lim_{c\to 0} \frac{ln(\eta_r)}{c} = lim_{c\to 0}\, ln(\eta_I) \qquad \textbf{Eq. 2.11}$$

Where $[\eta]_o$ is the intrinsic viscosity at zero polymer concentration with the unit [cm^3/g], and η_I is the inherent viscosity with the SI- unit [cm^3/g].

The inherent viscosity is defined as the ratio between the logarithmic value of the relative viscosity and the concentration of the solution (Sorbie, 1991):

$$\eta_I = \frac{ln(\eta_r)}{c} \qquad \textbf{Eq. 2.12}$$

Where the relative viscosity (defined in **Eq. 2.10**) is a dimensionless viscosity parameter, and the polymer concentration, *c*, has the unit [g/cm^3].

The intrinsic and inherent viscosity can be measured through viscometry at different concentrations. Since they are limited to zero polymer concentration, the viscosity is determined by extrapolation from the plot. In *figure 2.22* this extrapolation technique is illustrated, and it is only valid at low polymer concentrations such as in the dilute regime where the rheological flow behavior of the polymer solution is Newtonian (Chauveteau, 1986).

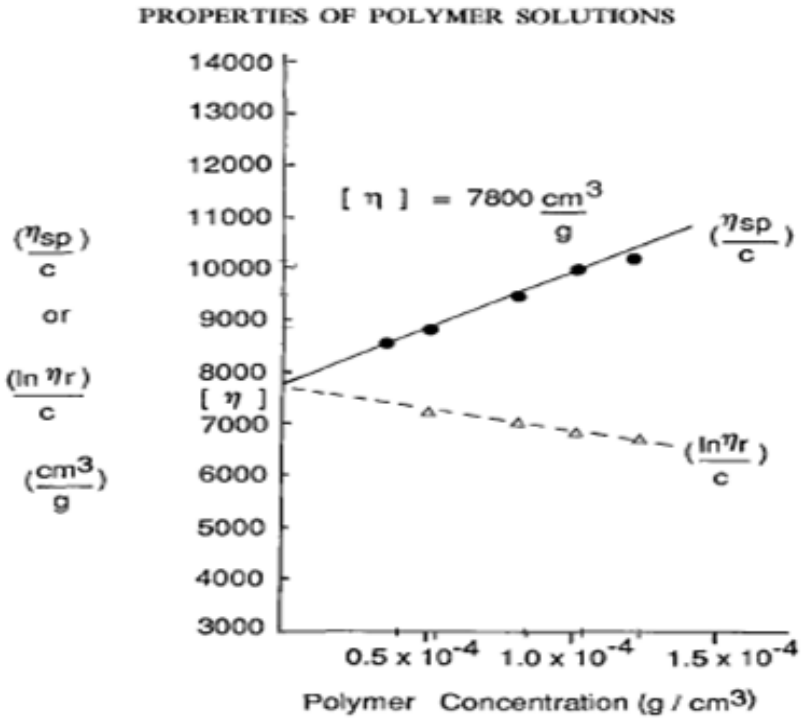

Figure 2.22 Determination of the intrinsic viscosity (Sorbie, 1991).

The most used parameter to characterize the hydrodynamic interactions between polymer-polymer, polymer- solvent and solvent- solvent in a shear flow, is the *Huggins constant* or *the Huggins coefficient.* In 1942 Huggins suggested a relationship that links the viscosity and concentration in the Newtonian region of a pseudoplastic solution (Chauveteau, 1986), and this relation is defined like this (Sorbie, 1991):

$$\frac{\eta_{sp}}{c} = [\eta] + K_H[\eta]^2 c \qquad \textbf{Eq. 2.13}$$

Where η_{sp} is the specific viscosity (dimensionless unit), c is the polymer concentration [g/cm^3], η is the solution viscosity [Pa·s] and K_H is Huggins coefficient (dimensionless unit).

The value of the Huggins coefficient indicates how well the polymers are dissolved in a solvent, considering the intra- and inter- chain effects in the solution. If the interactions are neither attractive nor repulsive at short distances, the Huggins coefficient depends only on the particle conformation in solution. According to Maia et al. in 2005 (Maia et al., 2005) larger values like 0.5- 1 typically indicates that polymers are in poor solvents, caused by contractions of the polymer chains due to intramolecular association (attractive forces). In a paper by Volpert et al. in 1998 (Volpert et al., 1998) they defined a Huggins coefficient value of 0.4 ± 0.1, as a *good* solvent conditions for polymers. In good solvent there exist no specific interactions in the polymer solution (Chauveteau, 1986).

By relating the intrinsic viscosity to associating polymers, the intrinsic viscosity of the solution is regarded as proportion to the reciprocal of the density of the polymer solution. The smaller $[\eta]_o$ is, the denser (less swelled) are the macromolecules in the solution (Dupuis et al., 2011a). By incorporation of hydrophobic groups on the acrylamide backbone, the intrinsic viscosity is supposed to decrease as the hydrophobicity increases, or the length of the hydrophobic unit increases. Due to intramolecular hydrophobic associations that most likely dominate in the diluted concentration range, the hydrodynamic volume reduces as the intrachain bonds between the hydrophobic groups increases (Kujawa et al., 2004). According to new experimental insights on associating polymers from 2011 by Dupuis et al. (Dupuis et al., 2011a), this observation was not confirmed due to too low hydrophobic units (≤0.5 mol%) along the backbone. They concluded that formation of significant amounts of intrachain bonds in the diluted concentration range may be possible above a particular amount of incorporated hydrophobic units.

Relating the Huggins coefficient to associating polymer solutions, experimental studies carried out by Dupuis et al. in 2011 (Dupuis et al., 2011a) observed good solvent conditions in neutral brines. Increasing the hydrophobicity, the Huggins coefficient was observed to be above unity. This seems like there exist attractive interactions occurring between the hydrophobic groups within the macromolecule, which makes the polymer less soluble in the solvent. This corresponds well with the experimental observations carried out for Kujawa et al (Kujawa et al., 2004), regarding the dominance of the attractive intramolecular hydrophobic associations.

Estimating the intrinsic viscosity and Huggins coefficient, only low polymer concentrations are valid. These parameters can be found using polymer concentration in the diluted concentration regime below the critical overlap concentration, $C < C^*$. Several models have been proposed to estimate the critical overlap concentration, C^*, directly from the intrinsic viscosity. In a paper by Chauveteau in 1986 (Chauveteau, 1986) he suggested the *Simha overlap parameter*:

$$C^* = \frac{0.7}{[\eta]_0} \qquad \textbf{Eq. 2.14}$$

Where C^* is the critical overlap concentration for a given polymer solution [ppm] and $[\eta]_0$ is the intrinsic viscosity at zero- polymer concentration [1/ppm].

In 1991 Sorbie et al. (Sorbie, 1991) suggested that this relationship would be better estimated through this definition:

$$C^* = \frac{1}{[\eta]_0}$$ **Eq. 2.15**

2.2.4 Viscoelasticity

This subchapter covers fundamental details about linear viscoelasticity. For more extensive discussion look up the sources; Barnes et al. (1989) (Barnes et al., 1989).

All materials have a mixture of viscous and elastic portions that determine their rheological state and behavior. When they are exposed to a deformation stress or temperature changes, it is possible for a material to change their physical behavior from elastic state to a more liquid and easier flowing state. It is due to breakage of intermolecular interactions that holds the elastic structure together, that may transform the material to a more viscous state.

Polymeric fluids show viscoelastic effects above the critical overlap concentration (C^*), and several models exist to describe the observed viscoelastic phenomena that occurs during flows. These models are not able to describe all aspects of the rheological behavior, but according to a paper by Sochi in 2010 (Sochi, 2010) they all have in common one characteristic parameter of time to account for the fluid memory. The relaxation time (λ_c) is a characteristic parameter of a particular polymer system, and is correlated to viscoelastic studies through the *yield point*.

The models for viscoelasticity are divided into linear and nonlinear studies, and the most supported fluid model is *linear viscoelastic Maxwell model*. This model has several limitations, but is devoted to the study of viscoelastic materials under very small strain. Under sufficiently low deformation where the displacement gradients are very small, the flow regime can be described as a linear relationship between shear stress and shear strain (Sochi, 2010).

In oscillatory experiments the viscoelastic behavior of a system can be characterized through the response of deformation and sliding forces. A viscoelastic study of a fluid can be carried out by subjecting stress (or strain) through a rotational viscometer that varies periodically in time (Berg, 2010). Robert Hooke defined the elasticity law, and applied for oscillation the deformation energy can be expressed like this:

$$G = \frac{\tau}{\gamma} \qquad \textbf{Eq. 2.16}$$

Where G is the shear modulus, τ is the shear stress and γ is the shear strain. The SI- unit of shear modulus is Pascal [Pa]. This shear modulus describes the viscoelastic behavior of a

material, and is divided into the elastic portion and the viscous portion. This elastic part of the viscoelastic behavior is called *storage modulus, G´,* and the viscous part is called *loss modulus, G´´*. The balance of the two portions in viscoelastic behavior of a material is given through the *damping factor, tan δ*. The damping factor of a solution is defined as the relationship between the viscous and the elastic portion:

$$tan\,\delta = \frac{G''}{G'} \qquad \textbf{Eq. 2.17}$$

Where tan δ is a defined parameter, *G´´* is the loss modulus and *G´* is called the storage modulus.

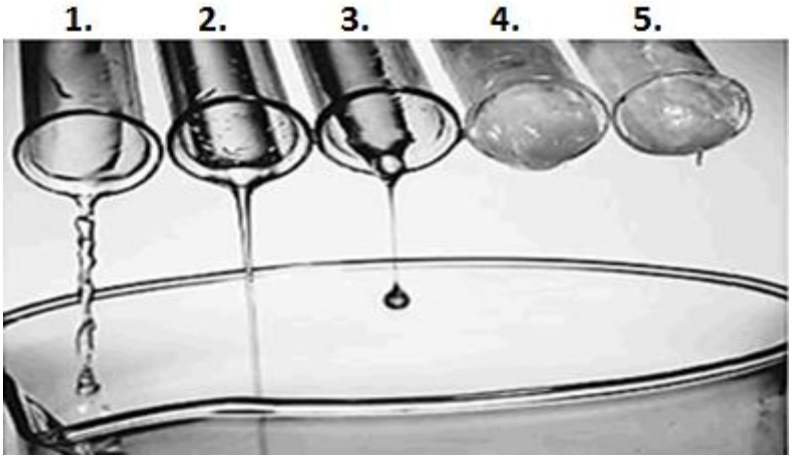

Figure 2.23 Materials with different viscoelastic properties at a given condition (Anton Paar, 2008).

As illustrated in *figure 2.33*, the measured complex viscoelasticity of a material, can give us an indication of the molecular configuration and the processing flow behavior. The viscoelastic properties of a material can be described through to the value of the damping factor at a given condition (Anton Paar, 2008):

1. **Ideally viscous liquids, tan δ >> 1:** When the damping factor of a material is much larger than unity, this indicates that the viscous behavior dominates over the elastic portion (G´´>> G´). Such liquids have a liquid- like structure, and flows very easily as illustrated in *figure 2.23_1*.
2. **Viscoelastic liquids, tan δ > 1**: For a viscoelastic liquid the damping factor is just above unity, this indicates that the viscous portion is still dominating over the elastic part (G´´> G´). These liquids have a liquid- like structure as well as illustrated in *figure 2.23_2*.

3. **Viscoelastic liquid/solid, tan δ = 1:** When there exist an equal balance between the viscous and elastic portion in the flow behavior ($G'' = G'$), the state of a material is a mixture of liquid and solid. At this specific condition, the damping factor is equal to unity. During viscoelastic measurements, this characteristic condition is found at the *gel point.* At these conditions the flow behavior of the solution, is equally dominated with liquid and gel- like character (*figure 2.23_3*).
4. **Viscoelastic solids, tan δ < 1:** A viscoelastic solid have a gel- like character during flow, and require some energy to start moving. The damping factor is below unity, which indicates that the viscous portion is lower than the elastic portion (G´> G´´). Typical behavior of such viscoelastic solids is illustrated in *figure 2.23_4.*
5. **Ideally elastic solids, tan δ << 1:** When the elastic portion is strongly dominating over the viscous portion, these rigid solids require a lot of energy to initiate flow (G´>> G´´). Their gel- like character is provided by strong interactions within the material, resulting in a damping factor much lower than unity. The flow behavior is illustrated in *figure 2.23_5.*

To characterize the viscoelastic behavior of polymer solutions at different concentrations; an *amplitude sweep* and a *frequency sweep* were carried out. An amplitude sweep or strain sweep was carried out first to detect the *linear viscoelastic (LVE) region* of the polymer solution. In the amplitude plot the storage and loss moduli are given as a function of shear strain or shear stress. A classical amplitude sweep on a highly concentrated polymer solution is illustrated in *figure 2.21*.

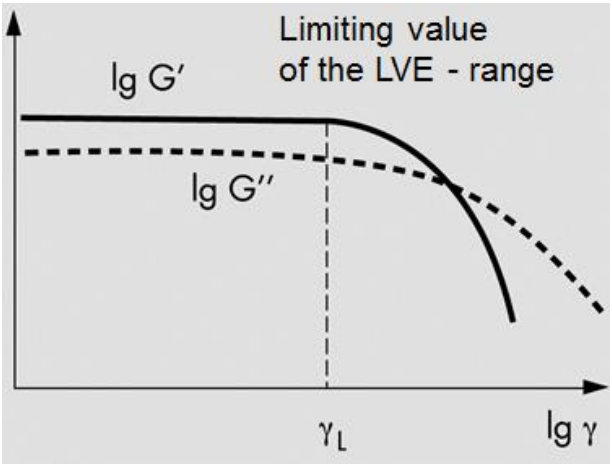

Figure 2.24 Typical logarithmic amplitude plot of the viscoelastic behavior of a polymer solution (Anton Paar, 2008).

Above the critical overlap concentration regime of a polymer solution, the storage modulus will dominate over the loss modulus. The damping factor is then below unity (tan δ < 1), which indicates that polymer solutions have a gel structure.

The *linear viscoelastic (LVE-) range* of a given polymer solution, can be determined from an amplitude sweep. The LVE- range is the linear viscoelastic plateau for a given condition at a constant angular frequency, and is detected on the dominating shear modulus of the solution. At the end of this linear plateau, the characteristic *yield point* of the solution can be estimated. This point can be related to the *relaxation point* from shear viscosity measurements of polymer solutions.

This yield point of a concentrated polymer solutions (polymeric gels) represent the highest shear stress (τ_y) applied at a given condition, without breaking the interactions holding the gel- structure together. The dominating storage modulus at yield point ($G_y^{'}$), represent the strength of the intermolecular forces acting in the gel – like network of the solution.

When the external forces exceed the interactions in polymeric gels, the gel- like network starts to break into a solution of small clusters and isolated macromolecules (Kujawa et al., 2006). For typical Maxwellian fluids, this elastic deformation shows a declining response after yield point on the storage modulus curve, as illustrated in *figure 2.24*. The two moduli shown in *figure 2.24*, illustrates the balance between deformation force and sliding force. Since concentrated polymer solutions are in solid state, applied stress cause dominance of deformation up to yield point. Hence, the sliding force starts to dominate. The crossover point between the storage and loss moduli indicates a total dominance of viscous portion. Any additional stress will push the solution around in the measuring cup, with no resistance.

According to a viscoelasticity study performed by Kujawa et al. in 2006 (Kujawa et al., 2006) of associating polymers above CAC (critical association concentration), the yield point is increasing with increasing hydrophobicity. Above CAC the amount of chain overlap and entanglements prevent the network of polymers to disrupt, and increasing the amount or length of the hydrophobic groups the intermolecular hydrophobic associations enhances. In addition upon salt, the effect is related to polymer concentration and dominating hydrophobic

association. In concentrated solutions above CAC, the observed salinity effect is not that pronounced. Increasing the salinity of the solution above a critical salt content, the polymer solutions may starts to separate into a turbid elastic gel with low viscosity.

From a viscoelasticity study carried out by Regalado et al. (Regalado et al., 1999), they also observed an significant change in the viscoelastic behavior above a given concentration when incorporating only a few hydrophobic groups on a hydrophilic backbone of HPAM. When temporary hydrophobic intermolecular associations occurs above this concentration and a formation of a associating network is formed, this seems to contribute to a reduction in the process of polymer diffusion (decomposition) and an increase in the zero- shear viscosity.

After the linear viscoelastic region was defined, the second oscillation test was carried out. It is crucial to determine the LVE- range of the polymer solution before performing a frequency sweep, because of the deformation of the network- structure occurring after a critical shear stress. According to Anton Paar (Anton Paar, 2008), the limit of the LVE- range for a concentrated polymer solution is usually set at a shear strain (γ_L) of 10%.

In a frequency sweep the storage and loss modulus is given as a function of the angular frequency at constant amplitude, this logarithmic plot is illustrated in *figure 2.25.* The complex viscosity (η^*) is also represented in the same plot, as a function of angular frequency at constant amplitude.

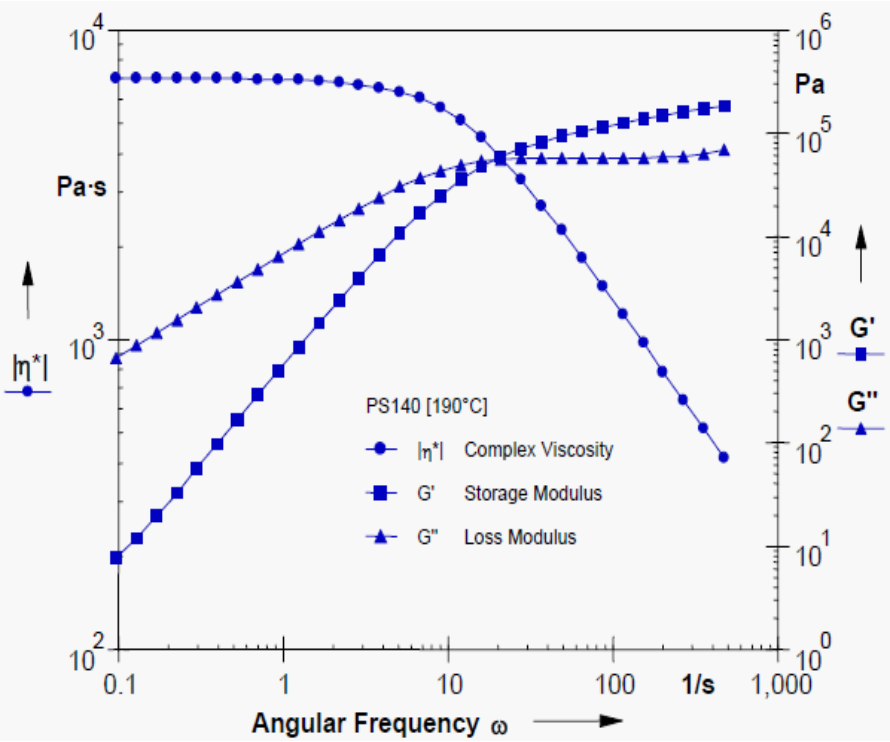

Figure 2.25 A typical logarithmic frequency plot of a concentrated polymer solution (Anton Paar, 2008).

Figure 2.25 show a classical G´´ (ω), G´ (ω) and $\eta^*(\omega)$ curves for an entangled polymer solution, as the angular frequencies decreases. At low angular frequencies these vary in accordance with the Maxwell model (Kujawa et al., 2006, Caputo et al., 2004, Jiménez-Regalado et al., 2004). This linear viscoelastic model states that G‘(ω) varies proportional to ω^2, while the G´´ (ω) varies proportional to ω.

There exist a relationship between the storage and loss moduli as a function of angular frequency, and this relation is given through the *complex shear modulus* ($G^*(\omega)$). This relationship is illustrated in a vector diagram in *figure 2.26.*

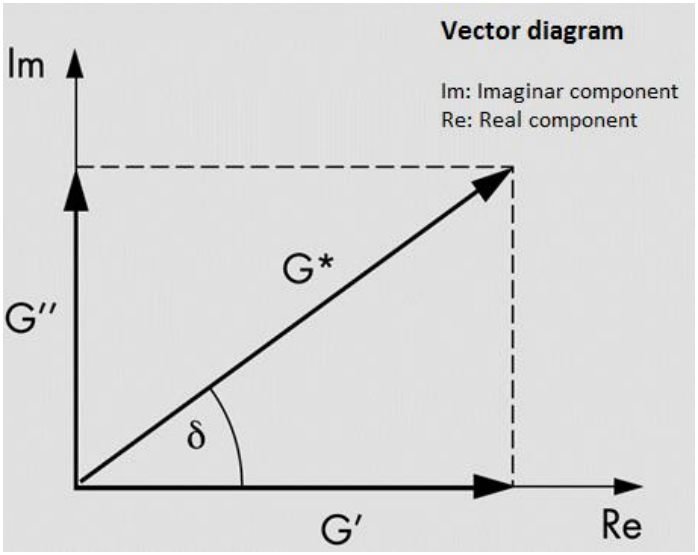

Figure 2.26 The vector diagram shows the relationship between the complex shear modulus and the storage and loss moduli (Anton Paar, 2008).

In *figure 2.26* the two moduli that represent the elastic and viscous portion of the viscoelastic behavior, are illustrated as two vectors. The complex shear modulus is the sum of the two vectors, and a contact angel δ [^{o}] is marked between the complex modulus and the loss modulus. δ [^{o}] is referred to as the *phase shift angle*, and the angles varies between 0^{o} to 90^{o} degrees. Through the damping factor, denoted as $\tan\delta$, it is possible to characterize the dominating behavior (Anton Paar, 2008).

The complex shear modulus is defined as:

$$G^*(\omega) = G'(\omega) + i \cdot G''(\omega) \qquad \textbf{Eq. 2.18}$$

Where $G'(\omega)$ is the storage modulus as a function of angular frequency given as a real component of the complex shear modulus, and $G''(\omega)$ is the loss modulus as a function of angular frequency given as an imaginary component of the complex shear modulus.

The complex shear modulus can also be defined through the complex shear viscosity, η^* as follows (Anton Paar, 2008):

$$\eta^* = \frac{G^*}{\omega} \qquad \textbf{Eq. 2.19}$$

In vector form, the complex viscosity can be defined as the real and imaginary components as functions of angular frequency. The relationship is defined as:

$$\eta^* = \eta' + i \cdot \eta'' \qquad \textbf{Eq. 2.20}$$

Where the relation to the storage and loss moduli is given as:

$$\eta' = \frac{G''}{\omega}$$ **Eq. 2.21**

$$\eta'' = \frac{G'}{\omega}$$ **Eq. 2.22**

The complex viscosity ($[\eta^*]$), is given defined in **Eq. 2.19** as a relationship between the complex shear modulus for oscillation and the angular frequency at constant amplitude. This function connects the study of viscoelastic behavior of entangled polymer solutions to the upper Newtonian plateau shown in *figure 2.17* in section 2.2.1. At low angular frequency, the zero- shear viscosity (μ_0) can be extrapolated from the measured complex viscosity at zero angular frequency. This relation can be expressed like this (Anton Paar, 2008):

$$[\eta^*] = \lim_{\omega \to 0}[\eta^*(\omega)]$$ **Eq. 2.23**

Where the complex viscosity is given as $[\eta^*]$, and $[\eta^*(\omega)]$ is the complex viscosity given as a function of the angular frequency, ω.

According to the viscoelasticity study of Regalado et al. (Regalado et al., 1999), for entangled polymer solutions the functions of zero- shear viscosity as a function of shear rate ($\eta(\dot{\gamma})$) and complex viscosity as a function of angular frequency ($\eta^*(\omega)$) seems to coincide. And the transition zone between the Newtonian plateau and the shear thinning region given as the relaxation time ($\dot{\gamma}_c$) of the polymer system, corresponds point in a frequency sweep where the two moduli at a given angular frequency cross over each other ($G''(\omega_c) = G'(\omega_c)$).

This crossover point is an important characteristic parameter, and is referred to as the *gel point* of a polymer solution. The value of the relaxation time indicates the strength of the intermolecular forces acting in the gel- like network structure. At gel point a transition occurs from liquid phase to solid (gel) phase, as the deformation stress decreases. This transition is the revers phase transition that happens at yield point.

The limitations of the Maxwell model are shown in the classical frequency plot of the two moduli in *figure 2.26*. Already before the gel- point the linear relationship starts to deviate. Angular frequencies above the gel- point of the polymer solution are not valid for the Maxwell model, since these curves are non- linear.

3. Experimental

This chapter will give you an introduction of the experimental methods that were used, along with the instruments to interpret the results.

3.1 Chemicals

3.1.1 Salts

For preparation of saline polymer solutions and the corresponding brine solutions, different salt were used. Only sodium chloride was added in the brine containing 0.5 wt% NaCl. This brine was prepared by first making a 15 wt% NaCl stock solution, and let this 1 liter solution stand at least 12 hours on stirring. The following day was this stock solution filtrated through a 0.45µm vacuum filter, in order to remove unwanted particles from the brine. After filtration was the stock solution diluted to 0.5 wt% NaCl in a quantum of 5- 10 liters, using distilled water. By making this brine in such a huge quantum, the uncertainties of weighing is reduced to 0.1g.

The high salinity water consisted of different salts. The salts added in this solution are listed up in *table 3.1*, where the concentration parts per million (ppm) is given as g/g. Hereafter the two brines are referred to as *low* and *high salinity brines*.

Table 3.1 Properties of salts used in the high salinity brine, in total 5 kg.

Type	*Mass [g/5 kg]*	*Concentration of salt [ppm]*	*Molar concentration [mol/l]*	*Manufacturer*	*Purity [%]*
NaCl	325.00	65000	1.11	Sigma- Aldrich, Switzerland	≥ 99.5
$CaCl_2*2H_2O$	75.00	15000	0.10	Riedel- de Haën, Germany	≥ 99.0
$NaHCO_3$	10.00	2000	0.024	Fluka Analytical, Germany	≥ 99.0
Na_2SO_4	2.50	500	0.0035	Riedel- de Haën, Germany	≥ 99.0
KCl	100.00	20000	0.27	Fluka Analytical, Germany	≥ 99.0
H_2O (distilled water)	4487.50	0	0	-	-
Total	**5000.00**	**102500**		-	-

The density of 1 kg/L is utilized during calculations of molar concentrations, and no more precise density measure of the solutions is required.

The high salinity brine was also made in a quantum of 5 liter to reduce the uncertainties of weighing. After addition of distilled water, this mixture of salts was let overnight on stirring to make it as homogeneous as possible. After more than 12 hours on stirring the high salinity brine had a pale appearing compared to the low salinity brine, as the picture in *figure 3.1*shows.

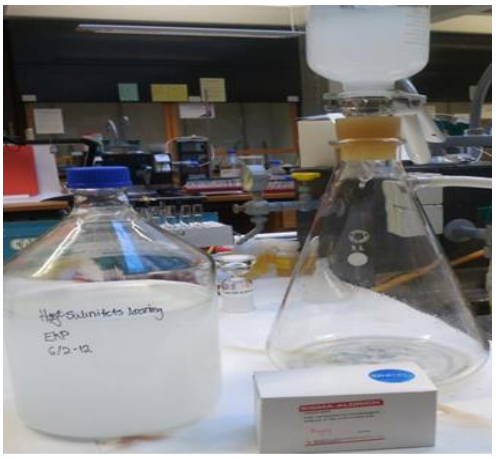

Figure 3.1 Filtration of high salinity brine through a 0.45µm filter.

The following day, the brine looked homogeneous in spite of the pale appearance. No precipitation had occurred through the night. Using a 0.45µm vacuum filter to remove impurities and insoluble salt, a filter change every 10 to 15 minutes was essential. Compared to the filtration process of the low salinity solution, the filter got blocked very easily due to accumulation of compounds. After the filtration process the high salinity solution was as clearly as the low saline brine.

Table 3.2 The ionic strength of the two solvents.

Component	***Molecular weight [g/mol]***	***Composition at 1 liter solvent***			
		Low salinity [mol]	***Low salinity [ppm]***	***High salinity [mol]***	***High salinity [ppm]***
Na^+	22.99	0.086	1967	1.14	26198
Ca^{2+}	40.08	-	-	0.10	4089
K^+	39.10	-	-	0.27	10489
Cl^-	35.45	0.086	3033	1.58	56174
HCO_3^-	61.02	-	-	0.024	1453
SO_4^{2-}	96.07	-	-	0.0035	338
TDS [ppm]		-	**5000**	-	**98742**
Ionic strength [mol/kg solution]		-	**0.086**	-	**1.72**

TDS is a shortening for *total dissolved solids*, and in *table 3.2* this value is very high compared to synthetic sea water. The ionic strength presented for each solvent in *table 3.2*, are calculated through this definition:

$$I = \frac{1}{2}\sum_{i=1}^{n`} c_i \cdot z_i^2 \qquad \textbf{Eq. 3.1}$$

Where I is the ionic strength of the solution, with the SI- unit [mol/kg], $n`$ is the number of components in the solution, c is the concentration of given component i in the solution and z is the ionic charge number of component i.

3.1.2 Reference fluid for viscosity measurements

A polydimethylsiloxane (PDMS) solution manufactured by Sigma- Aldrich was used as a standard calibration solution during viscosity measurements on the rheometer. This PDMS test was carried out frequently to detect deviation at 20 ± 0.1^{o}C.

Table 3.3 Properties of the standard calibration fluid at 20 ^{o}C± 0.1^{o}C.

Standard fluid for viscosity measurements		
Product name	***Manufacturer***	***Shear viscosity [mPa ·s]***
PDMS200	Sigma- Aldrich, Switzerland	5.25 ± 0.10

3.1.3 Polymers

The most applied polymer today for chemical IOR processes, are the synthetic HPAM and its derivatives. The reference polymer utilized in this experimental thesis, was the Flopaam partially hydrolyzed polyacrylamide manufactured by SNF Floerger, France. Compared to other conventional polymers like the biological Xanthan, this polymer is known to have low shear stress stability due to flexible chains.

After a high amount of shear stress applied on an entangled HPAM solution cease, the decomposition process of the macromolecules happens more rapid compared to entangled associating polymers solution. In addition to physical chain entanglements, an associating network of macromolecules is formed in the solution due to intermolecular hydrophobic interactions (Dupuis et al., 2011b). If the amount of shear stress was high enough, the weak intermolecular network of physical entanglements in HPAM solution is broken up and polymer backbones may be torn apart. In contrast to associating polymers, the backbones may still be intact and the associating polymer network may be reformed or decomposed to associating clusters. A viscosity drop is observed for HPAM, whereas in an associating polymer solution the viscosity may be built up to its original level before shear was applied due to the associating network (Reichenbach-Klinke et al., 2011).

During preparation of polymer solution the shear rate has to be high enough to create a homogenous solution without causing degradation. The stirring rate was determined from recommendations from the producer and researchers at CIPR. HPAM is also sensitive to chemical degradation, where exposure to iron and oxygen may induce a rapid chemical attack.

During preparation, storage and measurements the temperature was set within the stability range of the polymer solution. An increase in the ambient temperature may accelerate the hydrolysis process of the acrylamide monomers.

The associative polymers utilized in this experimental thesis were SuperPusher C319, SuperPusher D118 and SuperPusher B192 manufactured by SNF Floerger, France. All applied chemicals were used as received and the known properties of the polymers are shown in *table 3.4.* SNF Floerger has informed that these polymers have purity between 88- 92 %.

Table 3.4 Properties of SNF Floerger polymers

SNF Floerger Polymers					
Product name	***Appr. Molecular weight [MDa]***	***Hydrolysis degree [mole %] at room temperature***	***Hydrophobic content***	***Relative hydrophobic content***	***Batch***
FLOPAAM 3630S	~ 16 - 20	25-30	Non	-	Lot Z 2340
SUPERPUSHER C319	~ 16 - 20	25-30	Low	1	Lot X 3433
SUPERPUSHER D118	~ 16 - 20	25-30	Medium	2	Lot RG 2567/ 5-6-7
SUPERPUSHER B192	8-12	15	High	5 - 6	Lot GC 3157/ 14

3.2 Preparation procedure

3.2.1 The API stock solution procedure

The preparation of all polymer stock solutions during this thesis, regardless of type of polymer and solvent, followed the American Petroleum Institute (API) standard procedure described in chapter 2.3, RP 63, 1st ed. 1990. Some adjustments were made regarding the amount and type of pre- filtered solvent, and the stirring rate and time.

The standard concentration for a stock solution was 5000 ppm. Polymer solutions in the semi-diluted concentration regime were prepared by the following procedure:

1. 480g pre- filtered brine was first weighed in an 800ml beaker.
2. Accurately 2.800g polymer powder was thereafter weighed in a tray.
3. The pre- filtered brine was then placed on a magnetic stirrer, where an increasing stirring rate induced a vortex. When the vortex extended to about 75 % towards the bottom, the stirring speed was set.

Figure 3.2 The vortex created by magnetic stirring.

4. The polymer powder was then added slowly just below the vortex shoulder. This careful sprinkling process was carried out during 30 seconds.
5. Right after the addition of the polymer granulate, the stirring speed was reduced to the lowest possible rotation. This step, together with step 4 is crucial to the homogeneity of the polymer solution. A careful addition of the polymer power, followed by a

sufficient stirring rate can avoid gel formation and precipitation. The lowest possible stirring speed is set where the polymer particles still float in the solution.

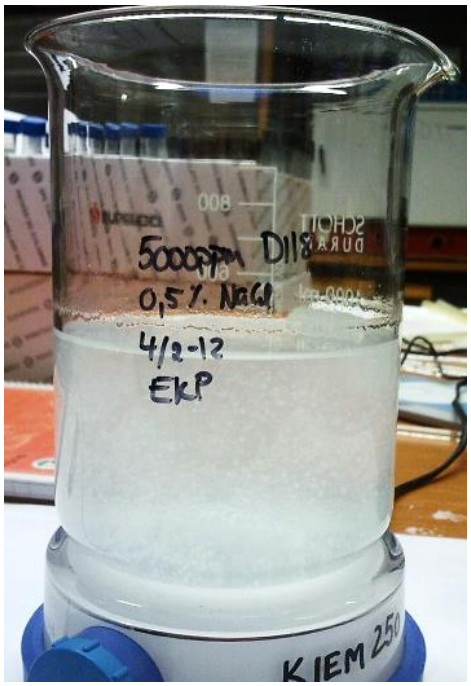

Figure 3.3 Polymer powder floating around in the solution.

6. To avoid oxidation of the polymer solution a parafilm is placed at the top of the beaker.
7. The tray is thereafter measured for the second time to detect how much of the polymer powder that actually was added to the solution.
8. The polymer solution was left on adequate stirring overnight. The following day the solution was transferred to a Duran flask with a cork sealed by a parafilm.

All polymer solutions that were made during this thesis were stored without stirring in about seven days after mixing, after recommendations from CIPR. The highest concentrated solutions of HPAM, C319 and D118, with a polymer concentration of 5000ppm, dissolved in low salinity brine were stored on stirring overnight after mixing. 5000ppm solution of B192 dissolved in the same brine was placed on the magnetic stirrer over two nights. Decreasing solubility was expected with increasing hydrophobicity, and the difficulties concerning solubility of concentrated B192 was more pronounced compared to the two other associating polymers.

A further increase in the salinity and hardness of the brine was expected to enhance the hydrophobic aggregation. That was why all 5000ppm associative polymer solutions dissolved in high salinity brine, were placed on a magnetic stirrer over two nights instead of one night.

Figure 3.4 A homogenous polymer stock solution after mixing overnight (5000ppm solution of D118 in low salinity brine).

In spite of two nights on stirring, the 5000ppm solutions of the B192 in both brines did not seem homogeneous at all. Several viscosity measurements were carried out for 5000 ppm B192 dissolved in low salinity brine. Since samples of the solution were most likely not representable for the whole solution, an average value of these measurements is presented in the results. Difficulties arise during sampling of B192 dissolved in high salinity brine.

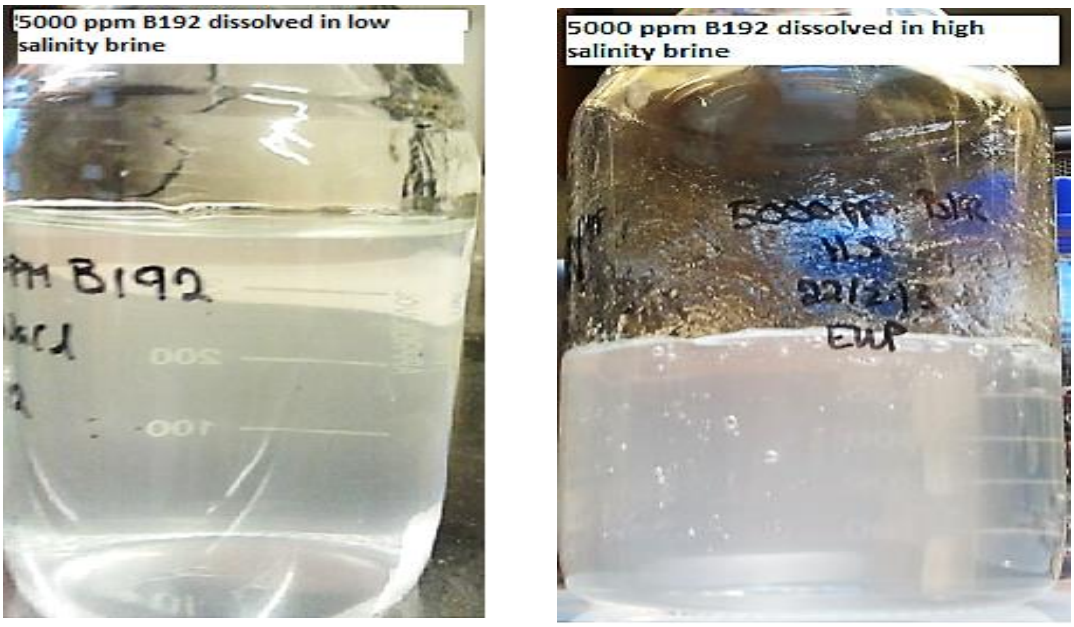

Figure 3.5 High degree of hydrophobicity cause a dramatic thickening ability, this is illustrated for 5000ppm solutions of B192 in the low salinity brine (left) and high salinity brine (right).

All the 5000ppm solutions were thereafter diluted to desired polymer concentrations. The API dilution procedure of stock solutions was carried out in the same way for all diluted polymer solutions in different brines. A given amount of the 5000ppm solution was diluted with low or high salinity brine, and thereafter placed on magnetic stirring overnight. A solution was never diluted more than ten times it initial concentration. For all diluted solution of B192 in low saline brine, the stirring time lasted over two nights to achieve solubility.

After the diluted solutions from the 5000ppm solution were mixed, they were vacuum filtrated through a 40µm filter to remove precipitations and/or microgels. The filtration time varied on the brine, the polymer composition and concentration. The vacuum suction was barley noticeably during filtration of D118 and B192, since formation of foam made the process run very fast. Somewhat higher suction was needed during filtration of HPAM and C319 solutions, without causing mechanical degradation of the polymers.

Figure 3.6 is a picture of a filtrated diluted solution of C319 dissolved in high salinity brine. This filtrated solution has a clear and homogeneous appearance, and was identical to the appearance of the filtrated HPAM and C319 dissolved in low salinity brine. During filtration the filter had to be changed frequently, due to accumulation.

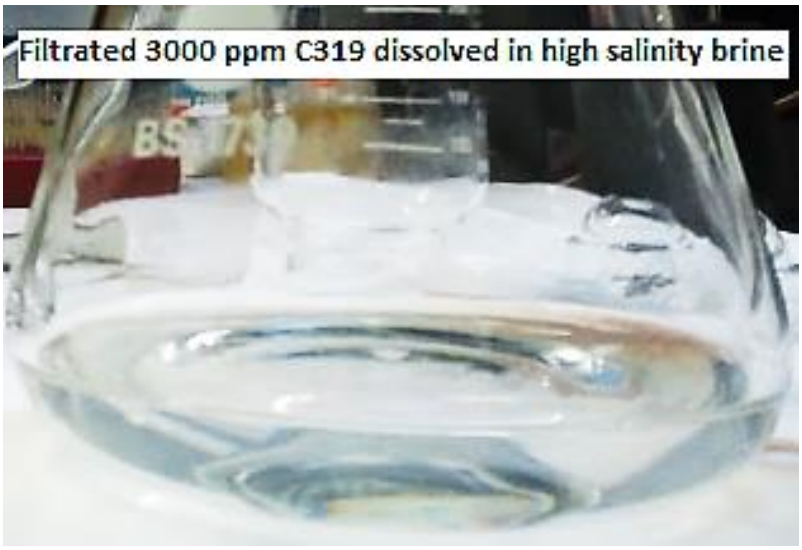

Figure 3.6 Filtrated 3000ppm solution of C319 in high salinity brine.

Increasing hydrophobicity and salinity, the filtration process run faster. During filtration of associative polymer solutions containing medium to high amount of hydrophobic groups, foam was created. Compared to the filtration of HPAM and C319, there was observed less accumulation on the filter. Pictures of the filtrated D118 and B192 in low and high salinity brine respectably, are shown in *figure 3.7*. An extensive formation of foam is observed for SuperPusher B192, which resulted in a shorter filtration time.

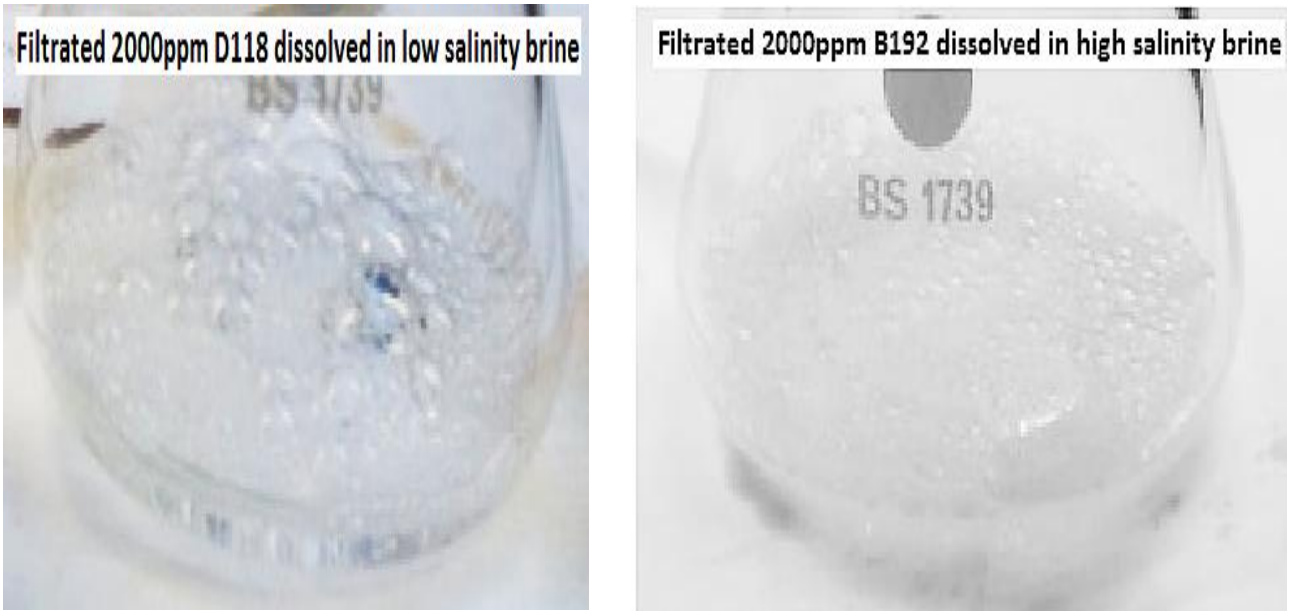

Figure 3.7 Filtrated 2000ppm solutions of D118 (left) and B192 (right) in low salinity brine.

The filtrated HPAM and C319 solutions were left to gain equilibrium overnight before use. Whereas D118 and B192 filtrated solutions were placed on the magnetic stirrer for about 20

to 30 minutes, before stored overnight after filtration. The intention was to reduce the amount of foam in the solution, by reforming the hydrophobic interactions between the chains that contribute to the thickening ability (Reichenbach-Klinke et al., 2011).

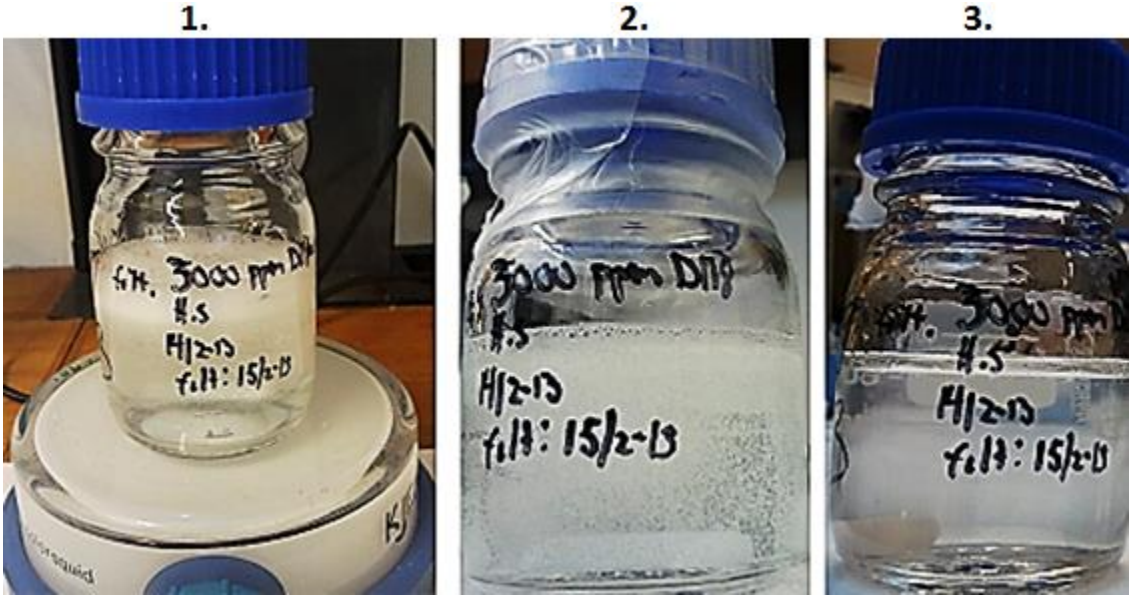

Figure 3.8 Filtrated 3000ppm solution of D118 placed on stirrer (**1.**), after 30 minutes (**2.**), the solution was stored overnight (**3.**).

The pH value of the brine was measured and always adjusted to 6.8 before mixing with the polymer. It was very important that the pH of these polymer solutions was held at a neutral value between 6 and 8, since they are polyelectrolytes. An excess of hydrogen ions or hydroxyl ions in the solvent, have a tendency to react with the carboxylate functional groups on the molecular backbone of the polymer. At neutral pH the viscosity of the polymer solution is immediate affected by electrostatic effects (Sorbie, 1991) occurring in the solvent, especially at low salinity brines.

Before any viscosity measurements of the polymer solutions, the pH had to be measured. A diluted NaOH with a concentration of 0.1M was used to adjust the pH value of the polymer dissolved in low salinity brine to 6.8. The high salinity brine acted as a solid buffer during addition of diluted HCl with a concentration of 0.1M. The acid concentration had to be adjusted to 1.0M to be able to change the pH. After reaching a sour environment outside the buffer zone, a couple of droplets of 1.0M NaOH were necessary to increase the pH of the solution again. After five minutes waiting time, the pH value had increase up to the initial value again. During this waiting time a precipitation of the associating polymer had occurred in the solution, a picture of this is shown in *figure 3.10* for C319 dissolved in high salinity

brine. Since the high salinity brine acted as a buffer and the precipitation occurred during pH adjustment, a pH value between 6 and 8 of the polymer solutions was accepted prior to viscosity measurements.

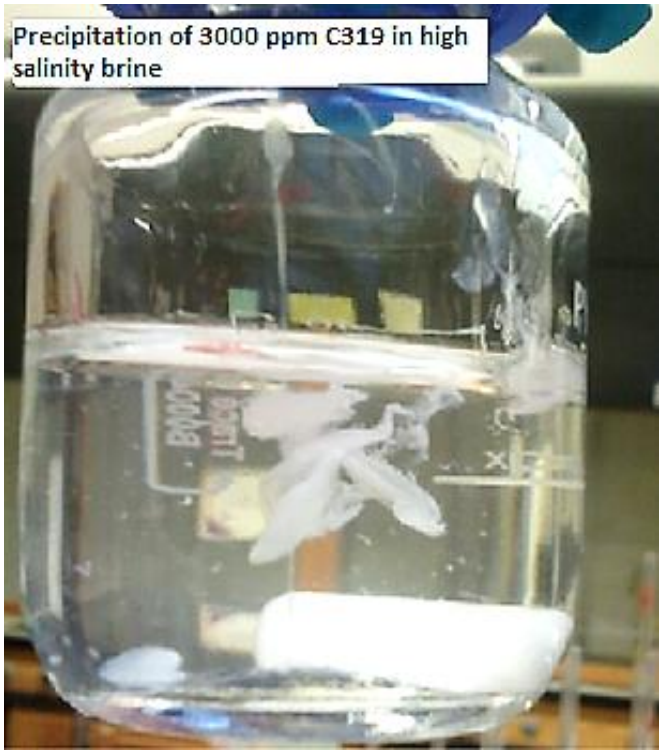

Figure 3.9 Precipitation of 3000ppm solution of C319 diluted in low salinity brine, pH= 7.53.

During preparation, storage and measurements a stable temperature was set to reduce uncertainties and other source of errors. The whole experiment was carried out at room temperature, T= 22 ^{o}C.

From February 25 to May 6 in 2013 (10 weeks) the rheometer at CIPR was out of order, before a replacement was in place. Due to time limitations, the storage procedure of B192 and 600ppm and 100ppm solutions of SuperPusher C319 in high salinity brine was changed. After preparing the polymer solutions for the second time, the solutions were now stored in a refrigerator for about 3 weeks before measurements were carried out. A degradation check was performed at room temperature and compared to earlier shear viscosity measurements of the 5000ppm solution of C319 in high salinity brine. Some degradation was observed, but the deviation was approved.

3.2.2 Regarding concentrations

In this thesis all concentrations are in parts per million (ppm) or weight percent (wt%). These units are preferred instead of molar concentrations because it is more frequently used in previous reports, and thus easier to compare the results. The salinity content of the brines is in this thesis presented as weight percent of the solution. A more common concentration unit for salt used in the chemical industry is molar (*M*).

The concentration range was changed during this thesis, because there were some uncertainties in the beginning about the concentrations that should be more evaluated than others regarding the association phenomenon.

In *table 3.5* the polymer concentration ranges that were studied during this experimental thesis are presented due to the new adjustments.

Table 3.5 Presentation of the different polymer concentration ranges.

Adjustments regarding concentrations	***Polymer type and brine***	***Polymer concentrations***
1. Concentration range at the beginning	HPAM, C319 and B192 dissolved in low salinity brine	5000 ppm solution - Diluted to 2000 and 3000 ppm solutions - Filtrated 2000 ppm solution was diluted to 600 and 1000 ppm solutions - 1000 ppm solution was diluted to 100 and 150 ppm solutions - 600 ppm solution was diluted to 200 and 300 ppm solutions - 100 ppm solution was diluted to 25 and 50 ppm solutions
2. New adjustment due to knowledge about C^* and CAC	D118 dissolved in low salinity brine	5000 ppm solution - Diluted to 2000 ppm solution - Filtrated 2000 ppm solution was diluted to 1000 and 1500 ppm solutions - 1500 ppm solution was diluted to 300 and 600 ppm solutions - 1000 ppm solutions was diluted to 100 and 200 ppm solutions
3. New adjustment due to Newtonian trend of high concentrated solutions	D118 and C319 dissolved in high salinity brine	5000 ppm solution - Diluted to 2000 and 3000 ppm solutions - Filtrated 2000 ppm solution was diluted to 1000 and 1500 ppm solutions - 1000 ppm solution was diluted to 100 and 600 ppm solutions
4. New adjustment due to extremely viscous 5000ppm solution	B192 dissolved in high salinity brine	5000 ppm solution - Diluted to 2000 and 1000 ppm solutions - Filtrated 2000 ppm solution was diluted to 1500 ppm - Filtrated 1000 ppm solution was diluted to 100 and 600 ppm solutions

3.3 Experimental apparatus and equipment

3.3.1 Physica MCR300 Rheometer

The rheology measurements were performed by a Modular Compact Rheometer, Physica MCR300 by Anton Paar. In *figure 3.10* a picture of this rheometer is shown. The MCR300 is equipped with different measurement geometries, whereas two of them are the double gap geometry and the cone plate geometry. The presumed viscosity of the solution decides which of the two geometries that was utilized. The viscosity of the fluid sample can be calculated from the measured torque (moment of force) during a steady rotation of one of the surfaces of the fluid. The uncertainty of the rheometer is given as the overall uncertainty of the viscosity measurements measured at given reference shear rates. At reference shear rate for diluted solutions below 200ppm the uncertainty was ± 0.01 mPa·s, and at reference shear rate for polymer solutions with concentrations above 200ppm the uncertainty was ± 6.1 mPa·s.

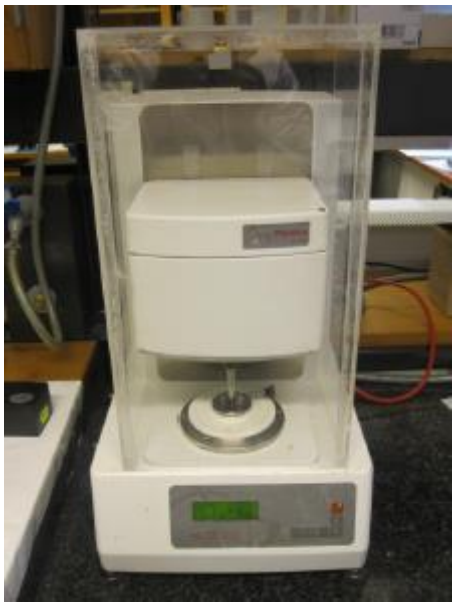

Figure 3.10 MCR300 Rheometer by Anton Paar covered by a Plexiglas.

The cone plate geometry (CP-75) is preferred for samples with a presumed viscosity higher than 10 mPa·s (e.g. polymer stock solutions and concentrated solution), with a TEK 150P-C measuring cell. The cone plate setup consists of a sample plate stator and a slightly coned plate rotor with a distance of 0.05mm gap between them. For samples with a presumed viscosity (μ) below 10 mPa·s (e.g. diluted polymer solutions and brines), the double gap geometry (DG- 26.7) is utilized with a TEZ 150P-C measuring cell. The double gap geometry

setup consists of two sets of measuring surfaces, and consists of a concentric cylinder stator and an open- end cylinder rotor. In *figure 3.11* the two rheometer geometries are illustrated.

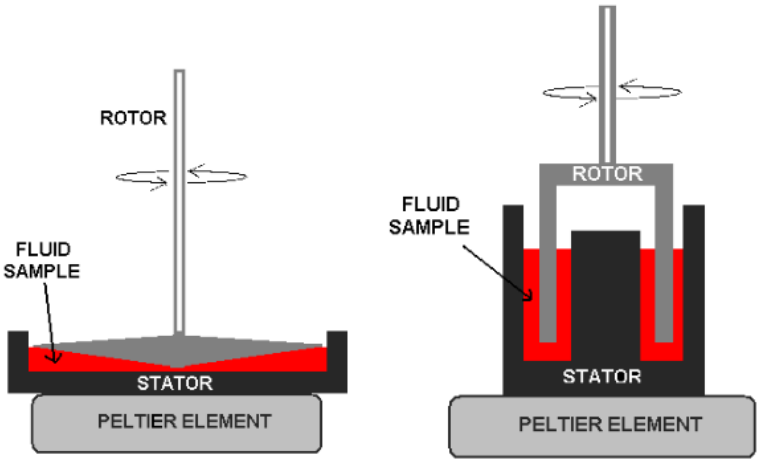

Figure 3.11 Cone plate geometry is illustrated on the left, and the double gap geometry is illustrated to the right (Lunestad, 2011).

The MCR300 instrument has a Peltier element with water cooling and electric heating which controls the ambient temperature of the fluid sample. The viscosity measurements carried out on the rheometer was performed at 22 ^{o}C, and the apparatus had an uncertainty of 0.1 ^{o}C. About five minutes waiting time was set before any measurements, to gain an equilibrium temperature between the Peltier apparatus and the fluid sample. As illustrated in *figure 3.10*, a Plexiglas was covering the rheometer to protect the fluid sample from debris and air fluctuations that can interfere with the measurements.

The sampled volume required for the DG measuring cell was 3.8 ml, and for the CP measuring cell 3.1 ml was used. The required sampled volume was dispensed with a pipette onto the cup or plate. For each measurement performed on the rheometer, only fresh samples of the solution were used since a measured sample becomes mechanically degraded at high shear rates. Some difficulties arise for very viscous fluid samples regarding use of the pipette to sample the required volume from the solution, and thereafter injecting it into the plate (*figure 3.12*).

Figure 3.12 Difficulties when sampling the extremely viscous 5000ppm solution of B192 in the high salinity brine.

Precautions were made regarding how the samples should be specific injected into the cup or plate, since the rotor speed is extremely influenced by the resistance fluids cause when they are contacted. It is from this rotor speed the rheometer software measures the torque, and thereafter calculates the shear rate. From the calculated shear rate, the shear viscosity of the sample is estimated. When injecting a sample onto the plate, it is very important that the sample is placed in the middle like a pancake. Then the sample seems to be equally spread out on the plate when the stator is pushed down to a 0.05mm gap distance. When the sample is injected into the cup, no sample must be placed on the top of the stator. This can result in incorrect measurements of the sample, since some volume is missing from the cup and the liquid that are contacted with the rotor may cause a higher resistance to the rotor speed.

A sampled volume of 4.1 ml was used for PDMS reference testing of the viscosity at $20^{o}C \pm 0.1^{o}C$ on the double gap measuring geometry. The viscosity testing of the PDMS was carried out several times before, during and after viscosity measurements of polymer solutions. The purpose of this Newtonian fluid was to detect irregularities in the rheometer, and thus enhancing the credibility of the viscosity measurements of the polymer solutions. An accepted viscosity measure of PDMS reference fluid is noted in section 3.2.1. The viscosity settings on DG measuring cell were 60 measuring points detected over 600 seconds at a constant shear rate of 100 (1/s).

The cleaning process before any measurement on the rheometer was crucial, and was carefully carried out. All parts that were in contact with the fluid sample, had to be cleaned and dried before injecting a new fluid sample. The cleaning process started by taking out all the removable parts that were contacted. The rotor, the plate and the disassemble cup were

thereafter washed gently with soap and water, rinsed three times with distilled water before rinsed one time with acetone. The parts were gently wiped off by a soft paper before totally dried using pressurized air.

Common to all rheology measurements performed on the MCR300 in this thesis; an Air Check test, leveling of the rheometer with a tubular spirit level and five minutes checking time of temperature equilibration at constant 22 ± 0.1^{o}C before any measurement. The Air check test was performed at 22 ± 0.1^{o}C using the CP- geometry at a zero- gap distance between the rotor and the plate. During the Air check test 120 measuring points were detected every two seconds during a measuring interval of 240 seconds. Quite often did the air check test show irregularities during the measurements over time, and therefore was a motor adjustment of the CP system necessary. After the calibration adjustment, another air check test was performed to check if the irregularities were removed. If they were, the viscosity or the viscoelastic measurements of the fluid samples could begin.

Two parallels were always carried out on the rheometer of a polymer solution to make the results more credible. Some of the very viscous solutions, like the stock tank solutions and other highly concentrated solutions, several parallels were necessary since the sampled amount from the solution seemed inhomogeneous and gel- like.

During shear viscosity measurements of the polymer solutions, the recorded values were approved by the Rheoplus software when the status of the measurement was denoted as "Dy_auto". All of the shear viscosity measurements processed in the results is approved values. In the viscoelasticity measurements carried out for the different polymer solutions, there were a great number of not approved recoded measurements. The approved viscoelasticity measurements were denoted as "DSO", whereas measurements below the limitations of the rheometer were denoted as "TaD". During the amplitude sweep of the polymer solutions, only the stock tank solutions had all of the measuring points approved. In the frequency sweep most the stock solutions had all measurement points approved, but some of them lacked approval of the two first recoded points. The same trend was found in both viscoelasticity sweep tests; the numbers of approved measurements were lowered as the polymer concentrations were reduced. That is why no viscoelasticity measurements were carried out for polymer solutions with concentrations below 600 ppm. These solutions behaved like Newtonian fluids during the shear viscosity measurements, and no viscoelasticity measurements were carried out since they had no viscoelastic property.

3.3.2 Shear viscosity measurements

The shear viscosity measurements performed by the MCR300 was controlled by Anton Paar's software Rheoplus. Different settings were made to detect the viscosity as a function of shear rate, time and polymer concentration. The settings on the rheometer and the concentration range were changed during this thesis, because it was not clarified in the beginning which part of the viscosity range and concentration range that should be thorough studied.

The first shear viscosity measurements were carried out for HPAM polymers dissolved in low salinity brine. The viscosity range was divided into four intervals, and some changes were necessary between the two different measuring geometries.

Table 3.6 Shear viscosity settings for HPAM dissolved in low salinity brine.

Interval number	***CP settings*** ***(μ > 10 mPa·s)***	***DG settings*** ***(μ < 10 mPa·s)***
1. First interval	41 measuring points were taken during a logarithmic increase in the shear rate range from 0.01 to 100 (1/s). The measuring time for each point varies logarithmically from 10 seconds for the lowest shear rate, and up to 30 seconds for the highest shear rate.	Equal to CP
2. Second interval	6 measuring points every 10 seconds at constant shear rate of 10 (1/s).	6 measuring points were detected every 30 seconds at constant shear rate of 10 (1/s).
3. Third interval	21 measuring points were detected during a logarithmic increase in the shear rate range from 10 to 1000 (1/s). The measuring time for each point varies logarithmically from 10 seconds for the lowest shear rate, and up to 30 seconds for the highest shear rate.	Equal to CP
4. Fourth interval	11 measuring points were detected during a linear increase from 1000 to 5000 (1/s). The measuring time for each point varies logarithmically from 10 seconds for the lowest shear rate, and up to 30 seconds for the highest shear rate.	6 measuring points were taken during a logarithmic increase in the shear rate from 1000 to 3500 (1/s). The measuring time for each point was the same as for CP.

It is due to the limitation of the rheometer using DG geometry that the fourth interval is different from CP settings. The maximum shear rate on DG is set at 3500 (1/s). The data

points of HPAM dissolved in low salinity brine were sampled using averaging 500 recorded values.

New changes were made in Rheoplus, before measuring the C319 dissolved in low salinity brine. The new adjustments in the setting of CP and DG geometries are shown in *table 3.7*. At that time these adjustments gave a more genuine measure of the polymer solutions. It was also necessary to change the settings regarding how the data points were sampled, and they were now sampled as the last 10% of the recorded values at equilibrium.

Table 3.7 New shear viscosity settings for C319 dissolved in low salinity brine.

Interval number	***CP settings*** ***($C_p \geq 1000$ ppm)***	***DG settings*** ***($C_p < 1000$ ppm)***
1. First interval	41 measuring points were taken during a logarithmic increase in the shear rate range from 0.01 to 100 (1/s). The measuring time for each point varies *now* logarithmically from 100 seconds for the lowest shear rate, and up to 10 seconds for the highest shear rate.	Equal to CP
2. Second interval	6 measuring points every 10 seconds at constant shear rate of 10 (1/s).	6 measuring points were detected every 10 seconds at constant shear rate of 10 (1/s).
3. Third interval	21 measuring points were detected *every* 10 seconds during a logarithmic increase in the shear rate range from 10 to 1000 (1/s).	Equal to CP
4. Fourth interval	11 measuring points were detected *every* 10 seconds, during a linear increase from 1000 to 5000 (1/s).	6 measuring points were taken every 10 seconds during a logarithmic increase in the shear rate from 1000 to 3500 (1/s).

New adjustments had to be made before measuring the associative polymer solutions of C319, D118 and B192 dissolved in high salinity brine, and D118 dissolved in low saline brine. The viscosity range and concentration range at this time was now more specific, leading to fewer concentrations below 600 ppm. According to the viscosity measurements carried out for the associative polymers C319 and B192 dissolved in low salinity brine, an assumption was made that the critical overlap concentration (C^*) range was between 200ppm and 400ppm and the critical aggregation concentration (CAC) ranged from 600ppm to 2000ppm. In previous settings of viscosity measurements, the shear rate range was divided into four intervals. The

new setting consists of only two intervals and these are presented in *table 3.8*. The settings regarding how the data points were sampled are the same before.

Table 3.8 New shear viscosity settings for D118 dissolved in low salinity brine, and C319 and B192 dissolved in high salinity brine.

Interval number	***CP settings*** ***($C_p \geq 1000$ ppm)***	***DG settings*** ***($C_p < 1000$ ppm)***
1. First interval	41 measuring points were taken during a logarithmic increase in the shear rate range from 0.1 to 1000 (1/s). The measuring time for each point varies *now* logarithmically from 30 seconds for the lowest shear rate, and up to 10 seconds for the highest shear rate.	Equal to CP
2. Second interval	17 measuring points were recorded every 10 seconds during a linear increase in the shear rate range from 1000 to 5000 (1/s).	17 measuring points were detected every 10 seconds during a linear increase in the shear rate range from 1000 to 3000 (1/s).

After the shear viscosity measurements of the polymer solutions were finished, the recorded data was transferred to Excel sheets in order to make proper graphs of the measured samples.

Since polymer solutions are non- Newtonian fluids, the shear viscosity of the bulk solutions have to be compared at a constant shear rate. The reference shear rate chosen for all of the different polymer solutions is within the shear thinning region, as illustrated in *figure 2.17* in section 2.2.1. It was very important to not choose a reference shear rate that was too low or too high since the polymer solutions show Newtonian flow behavior at these shear rate ranges. For low viscous solutions, the limitation of the rheometer by Anton Paar has to be considered.

In previous reports, different reference shear rates have been utilized to characterize the shear viscosity of non- Newtonian polymer solutions (Lunestad, 2011, Nordli, 2010, Pancharoen, 2009). In this study, the reference shear rates at 10 (1/s) and 100 (1/s) was both chosen. The shear viscosity measured at reference shear rate 10 (1/s) give a more realistic viscosity measure of the polymer solution, considering a typical flow rate of 1 ft. per day in a reservoir. For low concentrated polymer solutions (25ppm to 200ppm) a shear viscosity measured at 10 (1/s) may not be credible. The shear viscosity measurements carried out at low shear rates is most likely surface tension of the liquid. Therefore a reference shear rate of 100 (1/s) chosen for the diluted polymer concentrations.

The rheometer had clear limitations at low and high shear rates, as illustrated for low and high salinity brine. In *figure 3.13*, a flow curve (shear viscosity as a function of shear rate) is shown for both brines using DG- geometry on the rheometer.

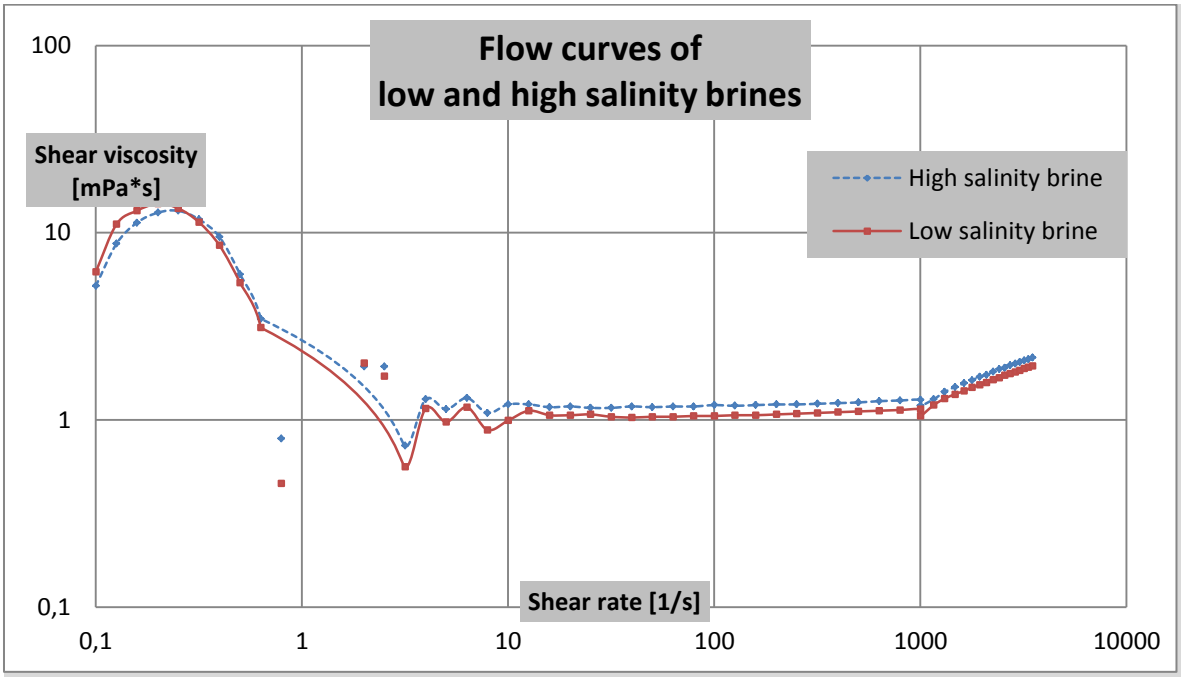

Figure 3.13 Shear viscosities as a function of increasing shear rate of low (red) and high (dotted blue) salinity brines at 22± 0.1 ^{o}C.

Through shear viscosity measurements at room temperature with increasing shear rate, the flow curves of both brines are detected. Their flow behavior is quite similar to each other, but the shear viscosity of high salinity brine is higher than low salinity brine. The shear viscosity measurements of the brines seem very unstable at low shear rates, before they stabilize. This indicates that, for low viscous solutions with dominating Newtonian flow behavior, the detected data at shear rates below 10 (1/s) seems to be surface tension between solution in measuring cup and air. For diluted polymer solutions with unstable measurements at low shear rates, these data is eliminated from the flow curves.

The Newtonian flow behavior is shown from 10 (1/s) to 100 (1/s), before an increase in the shear viscosity is observed. This increase in shear viscosity at high shear rates indicates turbulence. For highly concentrated and elastic polymer solutions, a viscosity increase is also observed around 1000 (1/s). As the shear rate increases above 1000 (1/s), these viscoelastic solutions started to climb out of the measuring area between the cup and the spindle. This climbing effect of polymer solutions may be due to the Weissenberg effect (rod climbing

effect) (Anton Paar, 2008) or phase transition between viscoelastic liquid and viscoelastic solid phase. When the shear measurement was finished, most of the sampled volume was detected on the top of the sample rather than in the measuring cup as illustrated in *figure 3.14.*

Figure 3.14 Unstable measurements at high shear rates due to Weissenberg effect or phase transition of concentrated polymer solutions. 5000ppm solution of C319 in low salinity brine is photographed.

3.3.3 Viscoelastic measurements

By changing the settings in the Rheoplus software, the viscoelastic properties could be detected for different polymer solutions and brines. The viscoelastic properties were measured through an amplitude (strain) sweep, where the strain is given as a function of storage and loss modulus. A frequency sweep was carried out after the amplitude sweep, where the angular frequency is given as a function of complex viscosity, storage and loss modulus, and phase shift angel.

The settings in Rheoplus for the amplitude sweep and the frequency sweep are presented in *table 3.8* and *table 3.9* respectably.

Table 3.8 Settings in the amplitude sweep at 22 ± 0.1^{o}C.

Interval	***CP and DG settings***
1. First interval	19 measuring points were taken during a logarithmic increase in the shear strain range from 0.1 to 3000%. The angular frequency was set at a constant shear rate of 10 (1/s), after recommendation from the producer Anton Paar regarding polymer solutions.

Table 3.9 Settings in the frequency sweep at 22 ± 0.1^{o}C.

Interval	***CP and DG settings***
1. First interval	18 measuring points were taken during a logarithmic increase in the angular frequency range from 300 to 0.1 (1/s). The shear strain was set at 10%, after recommendation from the producer Anton Paar regarding polymer solutions.

3.3.4 The pH- meter

During this thesis two different pH- meters have been utilized at 22^{o}C, but the twinpH B-212 from Horiba was only used for pH measurements of B192 dissolved in the low salinity brine. The main pH- meter was the one from Hach- Lange showing two decimal units on the display, and had an accuracy of ± 0.1pH. Before any pH measurements on both pH- meters, a pH calibration was performed using the producers own solutions of different pH values. On the Hach- Lange pH- meter, the results of the calibration did always display a percentage success around 92% to 94%.

Figure 3.15 the pH- meter from Hach- Lange with ISFET and glass pH probe.

The *Ion- Sensitive Field Effect Transistor* (ISFET) at the end of the probe is a silicon chip, which contains a final layer with affinity for hydrogen (H^+) ions only. This surface sensor is illustrated in *figure 3.16*. Hydrogen ions near or at the sensor in the solution, cause electrical effect that is detected. From this electrical effect the pH value of the solution is estimated.

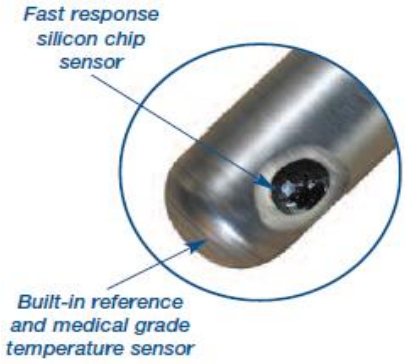

Figure 3.16 ISFET Technology on the pH meter from Hach- Lange[7].

[7] http://www.hach.com/h-series-h160-portable-ph-meter-starter-kit/product-downloads?id=7640516412

The pH- meter from Hach- Lange was much easier to utilize compared to the twinpH meter. The pH of polymer solutions and brines was measured by placing the pH measuring probe into the solution. The pH measuring area on the probe was covered by thin glass that was very fragile, so it was crucial that the probe was carefully placed into the solution during the measurements.

Figure 3.17 The twinpH from Horiba.

Before starting preparation of the polymer solutions of B192 dissolved in low salinity brine, the pH- meter from Hach- Lange was damaged at CIPR and sent to reparation. It was replaced with the twinpH, which only displayed one decimal unit (*figure 3.17*). The uncertainty of the pH measurements given by the producer of Horiba was ± 0.1pH. To measure the pH of these solutions, a given amount was sampled and injected into the measuring cup on the twinpH.

3.3.5 Weighing scales

Four different weighing scales have been utilized during preparation of polymer solutions and brines. To reduce the uncertainty of weighing of polymer powders, salts, polymer solutions and large quantum of brines different weighing scales have been used to provide a more accurate measure of the solute and solvent.

The different types and technical specifications of the weighing scales are presented in *table 3.10*.

Table 3.10 Different types of weighing scales utilized.

Type	*Resolution*	*Minimum weight [g]*	*Maximum weight [g]*	*Deviation [g]*	*Manufacturer*
AB 204-S	Fine	0.01	220	0.0001	Mettler Toledo
PB 3002S	Medium	0.05	3100	0.01	Mettler Toledo
SG 16001g	Coarse	-	16100	0.1	Lab- Tec

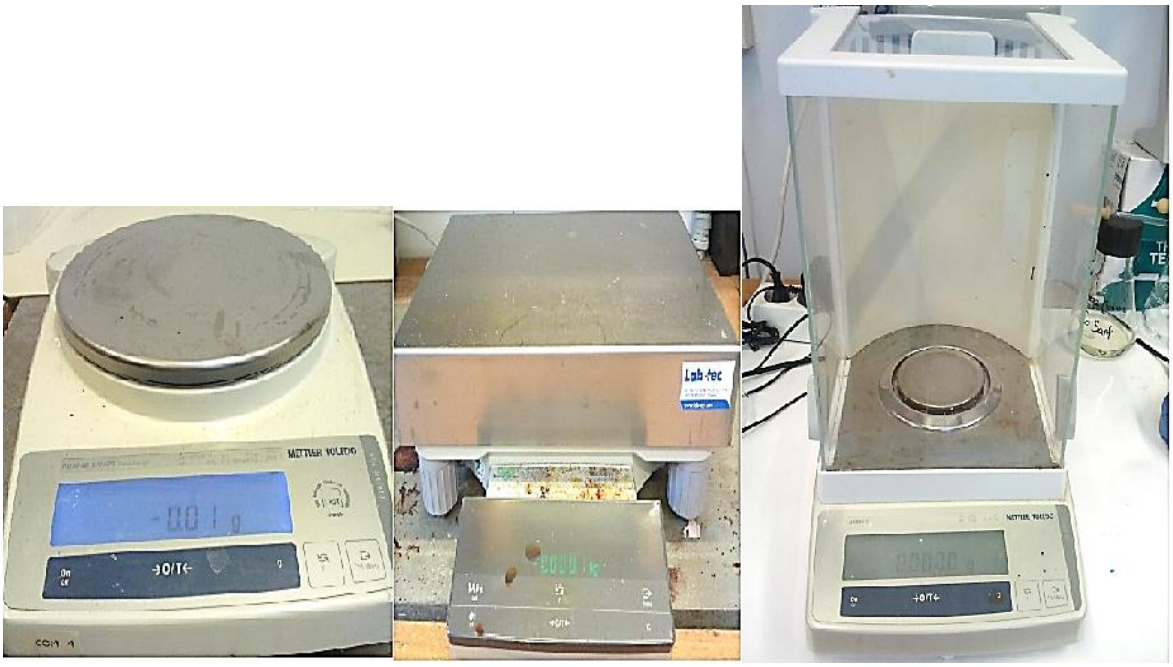

Figure 3.18 Weighing scales. Left: PB 3002S, middle: SG 16001g, right: AB204-S.

The main source to deviation of polymer solutions and brines is the preparation procedure. That is why the uncertainties during the weighting process contribute very little to the reproducibility of the solutions, and that is why they are neglected. It is the preparation procedure that has the highest impact on the viscosity of the solutions. There exist several

different procedures of how high salinity brines can be added and how the mixing process of the polymer solutions can be done (Wever et al., 2011, Maia et al., 2005). In this study the given salt concentration in the brine was already fixed before mixing it with a polymer, according to previous papers will this give a more homogenous mixture than increasing the salt concentration gradually in an already mixed polymer solution (Maia et al., 2005).

The largest impacted on the viscosity of the solution that exceeds the uncertainties of the preparation procedure and the accuracy of the rheometer, is the sampling process from the solution. Highly viscous solutions may be inhomogeneous, even though they seem uniform, and the sampled volume from the solution may not be representable. This will be the highest uncertainty concerning reproducibility and credibility of these experimental results. To provide a higher credibility of the measurements carried out in this thesis; two identical parallels were always carried out. In *appendix section A.1*, a list of uncertainties is presented.

4. Results and discussion

The main objective of this experimental thesis is to characterize the rheology properties of associating polymers from SNF Floerger. C319, D118 and B192 were dissolved in different brines at constant room temperature conditions. HPAM was only dissolved in the low salinity brine, due to precipitation at higher salinity.

4.1 Shear viscosity measurements

From the shear viscosity measurements on the MCR 300 Rheometer, the characteristic flow behavior of each polymer at different concentrations and brines are recorded. The intrinsic viscosity, the Huggins coefficient, and the critical overlap concentration (C^*) and critical association concentration (CAC) of the polymer solutions were estimated.

4.1.1 Characteristic flow behavior

HPAM dissolved in high salinity brine was not measured in this study, but the effect on increasing salinity of the brine was measured and discussed in the master thesis of Monrawee Pancharoen in 2009 (Pancharoen, 2009). He concluded that the effect of increasing salinity on HPAM solution was more pronounced compared to the associative polymer solutions, which showed a higher viscosity reduction due to increasing salinity.

The shear viscosity of HPAM and the associating polymers where measured at different shear rates. The highest shear viscosities were recorded for the highest concentrated polymer solutions, and the non- Newtonian flow behavior was strongest for these polymer solutions. The viscosity build- up property of polymer solutions is quite favorable during a polymer flood through the reservoir. The non- Newtonian flow behavior is quite adequate during polymer floods. As the shear rate decreases during propagation towards the production well, the viscosity is increasing. For diluted polymer solutions, the shear viscosity is lower compared to higher concentrated solutions and this shrinks the shear thinning region. The flow behavior of the polymer solutions at different concentrations in different brines as the shear rate increases, are shown in the logarithmic plots of shear viscosity as a function of shear rates. The *flow curve* of D118 in both brines is presented in *figure 4.1*, the rest of the flow curves are presented in *appendix section A.2.* A selected concentration range with polymer concentrations of 600ppm, 1000ppm, 2000ppm and 5000ppm solutions are presented. For HPAM; only polymer concentrations of 600ppm, 1000ppm and 5000ppm

solutions were prepared and therefore presented in this specific concentration range. In *appendix section A.2* measured shear viscosities of the solutions at reference shear rate of 10 (1/s) in the shear thinning region is presented.

Before the shear viscosities of different polymer solutions are discussed as the shear rate increases, the schematic flow behavior illustrated and described in *figure 2*.17 in section 2.2.1 is important to have in mind.

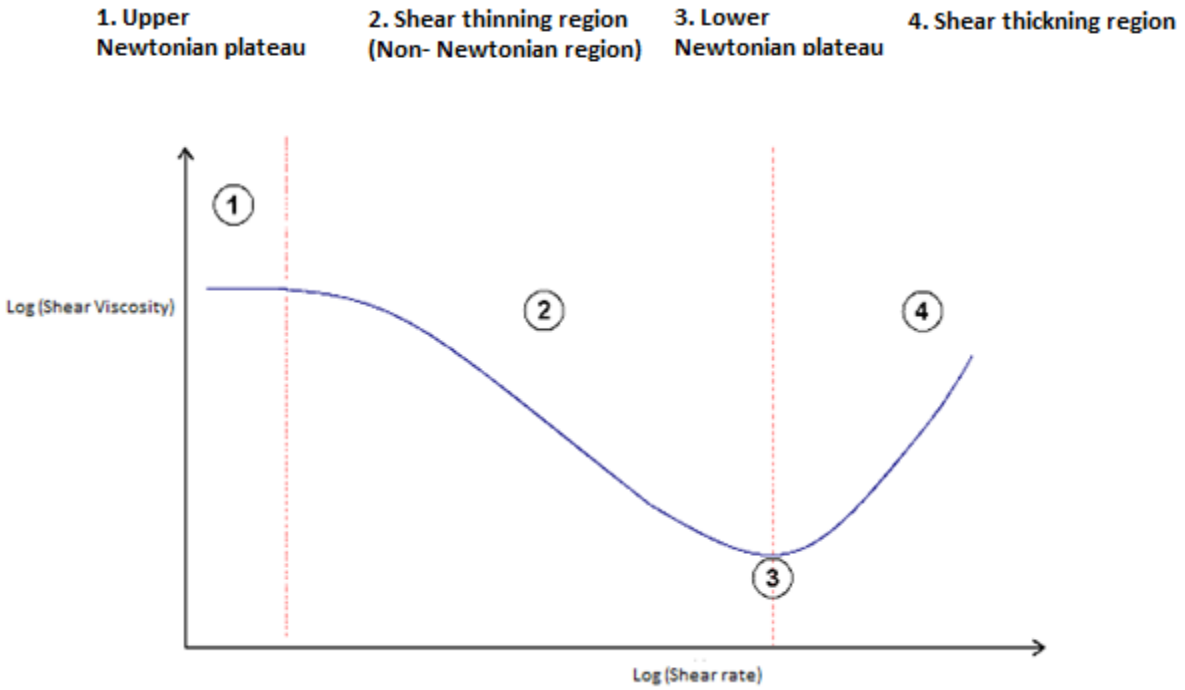

Figure 2.17 Flow curve illustration with four distinct regions from section 2.2.1.

Observations:

The flow curve of D118 dissolved in low and high salinity brine carried out at 22 ± 0.1°C is presented in *figure 4.1*.

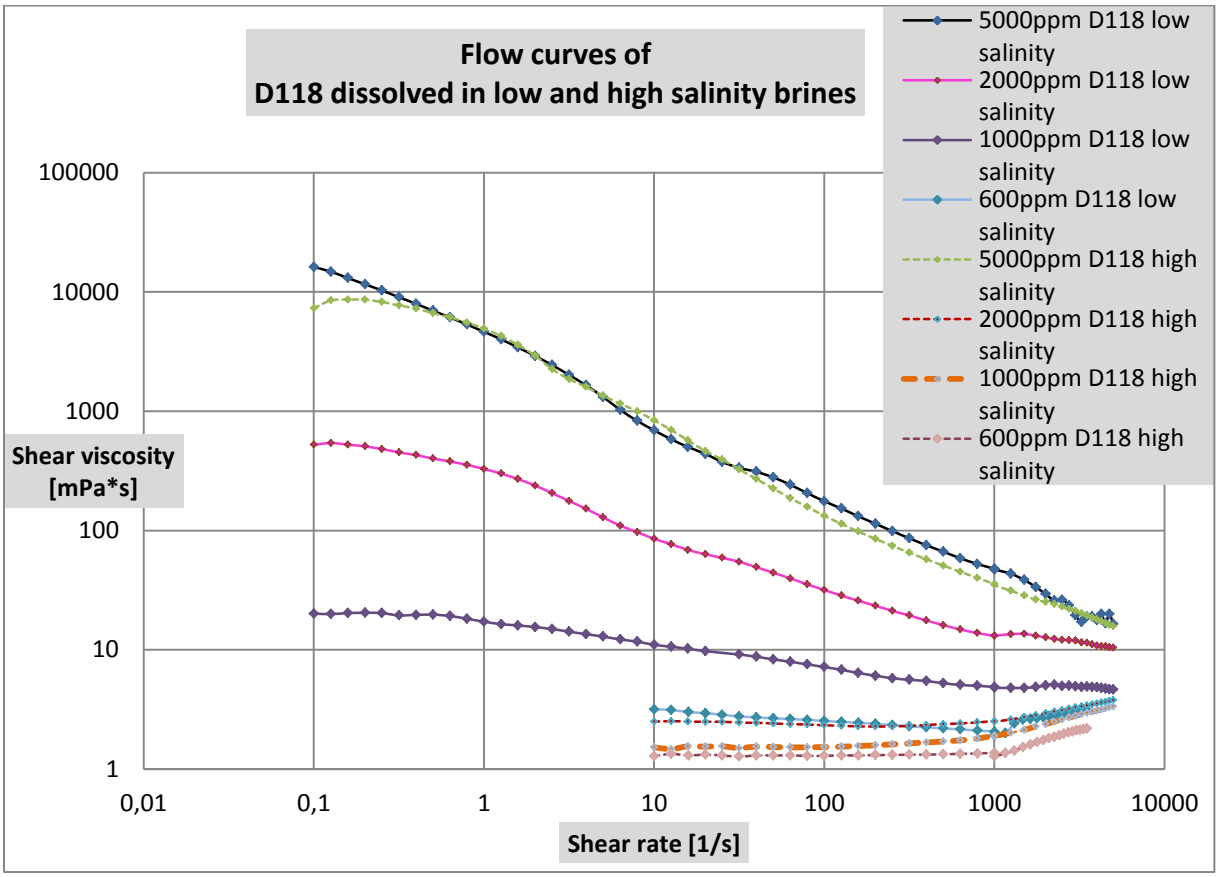

Figure 4.1 Shear viscosities as a function of shear rate of different concentrated polymer solutions (different colors) of D118 dissolved in low (solid line) and high (dotted line) salinity brines (22 ± 0.1°C).

The expected flow behavior of HPAM based polymer solutions, are an increase of shear viscosity due increasing polymer concentration and electrostatic repulsion (Sorbie, 1991). This corresponds well with observations from this study; in low salinity brine the polymer backbone stretches out due to electrostatic repulsion. Increase of the polymer concentration seems to force the chains to overlap in the solution and induce higher viscosity (*Appendix section A.2*).The hydrodynamic volume and amount of the HPAM macromolecules in the solution seems to determine the viscosity. Dissolving HPAM in high salinity brine was not carried out, since in the presence of salt screens the negative charged segments on the

backbone. The hydrodynamic volume of the polymer reduces until they precipitates (Reichenbach-Klinke et al., 2011).

Shear thinning regions were observed, and the decreasing slope is steepest for 5000ppm solution. This corresponds well with the *Power Law index* (*n*), where this index diverts to unity as the viscosity reduces. At unity, $n = 1$, there exist no shear thinning region, and the solution is now characterized with a Newtonian flow behavior.

Incorporation of a small amount of hydrophobic groups on the backbone of HPAM, like C319 solutions in the same low salinity brine, the viscosity increased for concentrated solutions of 2000ppm and 5000ppm. The same observations are observed for D118 in low salinity brine, with a higher amount of hydrophobic groups incorporated. As presented in *table 3.4* in section 3.1.3, the properties of HPAM, C319 and D118 are all the same except the amount of hydrophobicity. These observations seems to correspond well with earlier viscosity studies carried out on associating polymers (Maia et al., 2011, Dupuis et al., 2011a, Reichenbach-Klinke et al., 2011, Wever et al., 2011). Above a critical polymer concentration, where the macromolecules are physically entangled (CAC), a significant viscosity build- up is observed for associating polymers due to increasing degree of hydrophobicity. They explained this increase as a dominance of intermolecular hydrophobic associations that forms an entangled network of associating polymers that enhanced the hydrodynamic volume of the solution.

For B192, with a lower molecular weight and much higher degree of hydrophobicity, the same trend was observed for 2000ppm and 5000ppm solutions compared to HPAM based polymer solutions in low salinity brine.

For polymer concentrations below 2000ppm, the slope on the shear thinning region is less steep. Through the Power Law index, an observation from HPAM based polymer solutions in low salinity brines is that this index increases as the polymer concentration decreases and the hydrophobicity increases (HPAM<C319<D118). The macromolecules in these solutions may be entangled as well, but the intermolecular associations seem to be less efficient compared to the 2000ppm and 5000ppm solutions.

Polymer concentrations of 600ppm and 1000ppm of B192 in the low salinity brine, follows the same trend as HPAM based polymers with increasing amount of associating groups. Decreasing polymer concentration seems to reduce the steepness in the shear thinning region.

The Power Law index from the slope of the shear thinning region, seem to be almost unity for diluted B192 solutions (HPAM<C319<D118<B192).

No viscosity measurements of HPAM without any associating groups were carried out in high salinity brine, due to precipitation. By a small increase of the degree of hydrophobicity, a viscosity build- up is observed. The shear viscosities of 5000ppm solution of C319 in high salinity brine is significantly higher compared to HPAM, but lower than 5000ppm solution in low salinity brine. A shear thinning behavior is also observed in high salinity brine, compared to the Newtonian behavior of HPAM in high salinity brine.

A further increase in the degree of hydrophobicity, the viscosity of 5000ppm solution of D118 in high and low salinity is observed to be approximately the same. These observations seems to indicate the efficiency of associating polymers as thickening agents, and corresponds well with earlier experimental studies (McCormic and Johnson, 1988). Above a critical concentration, the associating polymers exhibit higher viscosities, higher salinity tolerance and have a more marked shear- thinning behavior at higher shear rates than HPAM without any associating groups.

In high salinity brine, the viscosities of 5000ppm solution of B192 was observed to be higher than in low salinity brine up to a given shear rate. This trend seems to indicate that the thickening ability in entangled associating polymer solutions, enhances with increasing degree of hydrophobicity (HPAM<C319<D118<B192). At a given shear rate, the viscosities of B192 in low salinity brine was higher than in high salinity brine. This may indicate that due to different polymer composition of B192 compared to HPAM based polymers, B192 seems to be more sensitive to shear stress in the high salinity brine.

The observed viscosity reduction from the 5000ppm solutions and down polymer concentration of 2000ppm in high salinity brine, was observed to drop more with increasing degree of associating groups (C319<D118<B192). The same trend was observed for the shear thinning region that seems to be less marked with increasing degree of hydrophobicity.

Conclusions:

The viscosity of an associating polymer will be significantly higher at higher polymer concentration compared to HPAM. The thickening ability seems to be more efficient at higher concentrations and increasing amount of associating groups (HPAM<C319<D118<B192). The associating behavior due to intermolecular hydrophobic interactions seems to provide a higher salt tolerance. Even a small amount of hydrophobic groups seems to induce a less sensitivity to salt.

The effect on increasing salinity corresponds well with earlier studies on associating polymers flow behavior (McCormic and Johnson, 1988), where the viscosity of the solutions are strongly related to the physical interactions occurring in the solution. In the concentration where the viscosity of a solution is much higher than other polymer concentrations like 2000ppm and 5000ppm, there macromolecules in the solution seems to be entangled. Increasing salinity of associating polymer solutions where the polymers are entangled seems to strengthen the dominating intermolecular hydrophobic associations.

Below polymer concentrations of 2000ppm, the viscosities are often relatively lower than 2000ppm and 5000ppm. These solutions may also be entangled, but the association occurring is not that significant since there exist fewer macromolecules in the solution. This result in a lower effect of hydrophobic association compared to higher polymer concentrated solution, where the polymers are closer together and forced to physical entangle.

As mentioned in section 3.3.2, for some highly viscous solutions like the 5000ppm solution of B192, viscoelastic effects was observed at high shear rates. These highly concentrated polymer solutions started to climb out from the measuring region between the cup and the spindle at sufficient shear rates. From the flow curves of these 5000ppm solutions, the observed shear viscosities in the low salinity brine seems to decrease with a straight decreasing slope for B192. The shear viscosities of HPAM, C319 and D118 seem to divert from this straight line to some extent. In high salinity brine, the shear viscosity measurements seems to divert less with increasing degree of hydrophobicity (C319>D118>B192). It seems like the impact on the shear viscosities, due to the climbing effect or the phase transition process that occurs at high shear rates, may be related to the increasing degree of

hydrophobicity and gel structure. The more elastic the polymer solution is, it seems like the more effected is the polymer solution to the climbing process.

4.1.2 Intrinsic viscosity, Huggins coefficient and C*

The intrinsic viscosity is the one of the most important viscosity parameters for diluted polymer solutions. This parameter is directly related to the hydrodynamic volume of the macromolecules in the solution (Sorbie, 1991). During this study, the diluted concentration range was estimated to be polymer concentrations below 200ppm. The intension was to choose a range where the macromolecules in the solution were still untangled, and no intermolecular association occurred.

From section 2.2.3, the intrinsic viscosity was defined as the reduced viscosity goes to zero-polymer concentration:

$$[\eta]_o = lim_{c\to 0}\frac{\eta-\eta_s}{\eta_s c} = lim_{c\to 0}\frac{\eta_{sp}}{c} = lim_{c\to 0}\,\eta_R \qquad \textbf{Eq. 2.7}$$

Where $[\eta]_o$ is the intrinsic viscosity at zero- polymer concentration [cm^3/g], η is the non-Newtonian shear viscosity of the solution [Pa·s], η_s is the solvent viscosity [Pa·s], c is the polymer concentration [g/cm^3]. η_{sp} is the *specific viscosity* (dimensionless unit) and η_R is the *reduced viscosity* [g/cm^3]. The SI- unit for intrinsic viscosity is [cm^3/g], but the unit [1/ppm] is often preferred.

No correspondence where found between the experimental data of HPAM and the inherent viscosity. Estimation of intrinsic viscosity was performed through extrapolation from the plot of reduced viscosity as a function of polymer concentration.

The Huggins coefficient is another important characteristic parameter of the polymer solution. The value of this coefficient indicates how well the polymer is dissolved in the solvent, regarding the interactions between polymer- polymer, polymer- solvent and solvent- solvent in a shear flow (Sorbie, 1991).

The Huggins coefficient is dependent on the slope of reduced viscosity as a function of polymer concentration, and the relation is given through **Eq. 2.13** in section 2.2.3:

$$\frac{\eta_{sp}}{c} = [\eta] + K_H[\eta]^2 c \qquad \textbf{Eq. 2.13}$$

Where $\eta_{sp,}$ c, η and K_H are the specific viscosity (dimensionless unit), the polymer concentration [g/cm^3], the viscosity of the solution [Pa·s] and the Huggins coefficient respectably.

The critical overlap concentration, C^*, can then be estimated through calculations using **Eq. 2.14** and **Eq. 2.15** in section 2.2.3:

$$C^* = \frac{0,7}{[\eta]_0} \quad \textbf{Eq. 2.14}$$

$$C^* = \frac{1}{[\eta]_0} \quad \textbf{Eq. 2.15}$$

Where C^* is the critical overlap concentration for a given polymer solution and $[\eta]_0$ is estimated intrinsic viscosity at zero- polymer concentration (Sorbie, 1991).

Observations:

It was not possible to use this extrapolation technique to estimate the intrinsic viscosity of the associating polymers, since irregular viscosity measurements were detected. This resulted in a negative slope in the diluted concentration range (*appendix section A.3)*. This technique was only possible to utilize for HPAM solutions dissolved in low salinity brine.

A graphic approach was utilized to estimate the intrinsic viscosity of the associating solutions. It seems like the behavior of associating polymers deviates from HPAM without any associating groups, and the viscosity may be dominated by random clusters of macromolecules.

In *figure 4.2* the reduced viscosity as a function of polymer concentrations in the diluted region is shown. The shear viscosity measurements at reference shear rate of 100 (1/s) was measured at 22 ± 0.1^{o}C. The intrinsic viscosity of associating polymer solutions was estimated from the plot by making an averaging line of the measured reduced viscosities at polymer concentrations of 50ppm, 100ppm, 150ppm and 200ppm. This line was extrapolated to zero- polymer concentration. In the diluted concentration range of D118, only polymer concentrations of 100ppm and 200ppm were carried out.

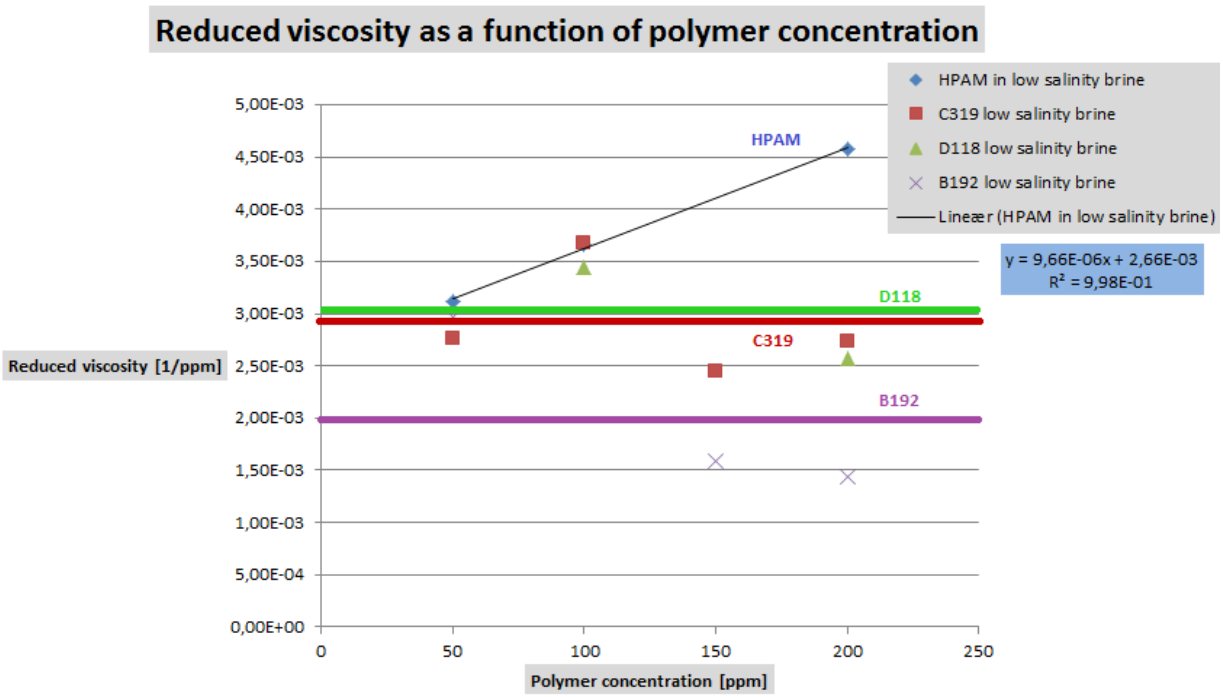

Figure 4.2 The linear relationship between reduced viscosity and polymer concentration for all polymers dissolved in low salinity brine in the diluted concentration range at 22 ± 0.1°C.

In *figure 4.2*, the linear relationship between the reduced viscosity and polymer concentration of HPAM and associating polymer solutions in low salinity brine is presented. HPAM follows the linear increasing trend as the polymer concentration increases, and the through the equation of the trend line (blue equation) the intrinsic viscosity, Huggins coefficient and critical overlap concentration can be estimated. For the associating polymer solutions, the intrinsic viscosity is estimated through an averaging line between the measured reduced viscosities that extrapolates to zero- polymer concentration.

The estimated properties of HPAM, are compared to the experimental study carried out by Nordli in 2010 (Nordli, 2010) and Lunestad in 2011 (Lunestad, 2011) at CIPR. The same HPAM polymer was utilize at 22°C in their experimental master study. The properties and salinity of the low salinity brine was also the same, with a 0.5 wt% of NaCl.

In *table 4.1* the intrinsic viscosity, Huggins coefficient and C^* is presented for all the polymer solutions dissolved in low salinity brine. In addition the estimated properties of Nordli (Nordli, 2010) and Lunestad (Lunestad, 2011) are also presented to compare these results to HPAM.

Table 4.2 Estimated properties of polymer solutions in low salinity brine at 22 ± 0.1°C; intrinsic viscosity, Huggins coefficient and critical overlap concentration.

Polymer type	***Salinity of brine***	***Intrinsic viscosity*** $[\eta]_o$ ***[1/ppm]***	***Huggins coefficient,*** K_H *[-]*	***Critical overlap concentration,*** C^* ***[ppm]***	
				$C^*=1/[\eta]_o$ ***[ppm]***	$C^*=0,7/[\eta]_o$ ***[ppm]***
HPAM	Low	0.0027	1.37	376	263
Nordli, FP3630	*Low*	*0.0056*	*0.06*	*179*	*125*
Lunestad, FP3630	*Low*	*0.0056*	*0.08*	*179*	*125*
C319	Low	0.0029	-	344	241
D118	Low	0.0030	-	333	233
B192	Low	0.0020	-	501	351

Comparing the estimated properties of HPAM to Nordli and Lunestad, some differences are observed. The calculated Huggins coefficient and C^* using viscosities measured at reference shear rate of 100 (1/s) at 22 ± 0.1°C, a doubling of the calculated Huggins value is observed. The slope in the linear expression of the trend line of HPAM was observed to be much lower in this study. Both, Nordli and Lunestad, have used polymer concentrations up to 1500ppm which is not in the diluted concentration range of HPAM. Using only diluted polymer solutions below 200ppm, improves the credibility of the estimation of intrinsic viscosity carried out during this study.

The calculated Huggins coefficient is above unity for HPAM in this study, and this indicates that the macromolecules are in a poor solvent due to dominating attractive interactions between dispersed macromolecules (Chauveteau, 1986). A *good* solvent has a Huggins coefficient of 0.4 ± 0.1, in such solvents there exist no specific hydrodynamic attractive or repulsive interactions that dominate (Volpert et al., 1998).

Comparing the estimated properties of HPAM to Nordli and Lunestad; their values are much lower. The difference is related to the chosen polymer concentration range used to estimate the intrinsic viscosity. The intrinsic viscosity of HPAM seems to be relatively too low

regarding the effect of salinity on polyelectrolytes. Even though the estimation procedure in this study is different from Nordli and Lunestad, the low intrinsic viscosity gives in turn a low Huggins coefficient. Since the salinity in the solvent is so small, an equal balance between the attractive and repulsive hydrodynamic interactions of the macromolecules in the solution was expected. An intermediate value of the intrinsic viscosity from Nordli and Lunestad to this estimated value intrinsic viscosity from this study will probably be a more realistic value ($\sim$0,0043 [1/ppm]).

The concentration where the polymer chains in the diluted polymer solution starts to overlap, C^*, a very high critical overlap concentration is estimated for HPAM in this study. These concentrations are high as a consequence of the low estimated intrinsic viscosity. A doubling in the concentration is observed in the experimental master study of Nordli (Nordli, 2010) and Lunestad (Lunestad, 2011).

Comparing the associating polymer solutions in low salinity brine, the estimated intrinsic viscosity of the solution was approximately the same for C319 and D118. Even though these two polymers have equal chemical properties, the increasing degree of hydrophobicity in the diluted concentration range seems to not affect the hydrodynamic volume of the macromolecules in this solvent significantly.

The expected observation was a lower intrinsic viscosity of D118 relative to C319, due increasing amount of intramolecular hydrophobic interactions, which reduces the hydrodynamic volume of the macromolecules in low salinity brine. A similar odd observation was also observed by Dupuis et al. (Dupuis et al., 2011a). They concluded that significant changes in the intrinsic viscosities were related to the amount of incorporated hydrophobic groups in the diluted concentration range. Relating this observation to this study, it seems like the relative amount of hydrophobic groups on D118 which is known to be twice as much as C319, is not that different. The actual amount of incorporated hydrophobic groups on the hydrophilic chain in mol% is not notified by the producer (SNF Floerger). Dupuis et al. observed that a given amount of hydrophobic groups are needed to induce significant amounts of intrachain bonds. It seems like from this observation that the relative amount of hydrophobic units in mol% of the polymer molecule is not that different on C319 to D118.

The intrinsic viscosity of B192 in the diluted concentration range corresponds well with earlier observations. Increasing degree of hydrophobicity will significantly reduce the hydrodynamic volume of the macromolecules in low salinity brine.

The critical overlap concentrations estimated for C319 and D118 are approximately the same due to the estimated intrinsic viscosity. Compared to HPAM, the expected critical overlap concentrations with increasing hydrophobicity should be higher due to hydrophobic intramolecular associations (McCormic and Johnson, 1988). From the estimated C^* of C319 and D118, this corresponds well with the estimated critical overlap concentrations of HPAM carried out by Nordli (Nordli, 2010) and Lunestad (Lunestad, 2011). An averaging value of the critical overlap concentration between 200 to 300 ppm for the estimated concentration carried out in this study to Nordli and Lunestad, corresponds well with increasing degree of hydrophobicity.

The critical overlap concentration of B192 is much higher than the others due to the low intrinsic viscosity. This corresponds well with experimental studies of associating polymers (Dupuis et al., 2011a, Kujawa et al., 2004), where associating polymer with high hydrophobicity (192) is observed to have strong intramolecular hydrophobic interactions. The solubility in a polar solvent like this low salinity brine, reduces as the degree of hydrophobicity increases. And an estimated Huggins coefficient would most likely be highest for B192 in this study.

Conclusions:

It was observed that for associating polymer solution in low salinity brine, the extrapolation technique of intrinsic viscosity through the linear relation given in **Eq. 2.13**, was not adequate due to negative slope. In low concentrated associating polymer solutions, some irregularities are observed in the measured viscosities compared to HPAM. It seems like some kind of association occurs, it might by random formation of clusters that differs from the behavior of HPAM.

The estimated intrinsic viscosity of HPAM in this study was carried out using the linear relation between intrinsic viscosity, Huggins coefficient and polymer concentration (**Eq.**

2.13). Comparing this estimated intrinsic viscosity of HPAM to the estimated value carried out during the experimental master study of Nordli (Nordli, 2010) and Lunestad (Lunestad, 2011), it is relative lower. The observed difference was due to different concentration ranges was utilized. The credibility of the intrinsic viscosity estimated in this study is higher, since the linear relation through **Eq. 2.13** is only valid below critical overlap concentration (C^*). Estimation of the critical overlap concentration before utilizing this extrapolation technique may provide an even better credibility of the estimated intrinsic viscosity, since the diluted concentration range will be more defined.

Using an average intrinsic viscosity of HPAM, the estimated viscosity in this study compared to Nordli and Lunestad, a reduction in the intrinsic viscosity is observed with increasing hydrophobicity. The estimated intrinsic viscosities of C319 and D118 are not that different as expected. Since only the relative amount of hydrophobicity is known, the actual amount of hydrophobic groups in mol% of the macromolecule may be too low to create significant number of intermolecular hydrophobic bonds. The estimated intrinsic viscosity of B192 follow the expected tend.

The critical overlap concentration is found to be increased with increasing hydrophobicity, since increasing amount of intramolecular hydrophobic associations reduces the hydrodynamic volume of the polymer. A higher polymer concentration is needed to initiate overlapping chains in the solution.

4.1.3 Shear viscosity as a function of polymer concentration

In section 2.1.4 about associating polymers *figure 2.15* illustrates how shear viscosity of HPAM compared to associating polymer solutions, are expected to behave when the polymer concentration increases.

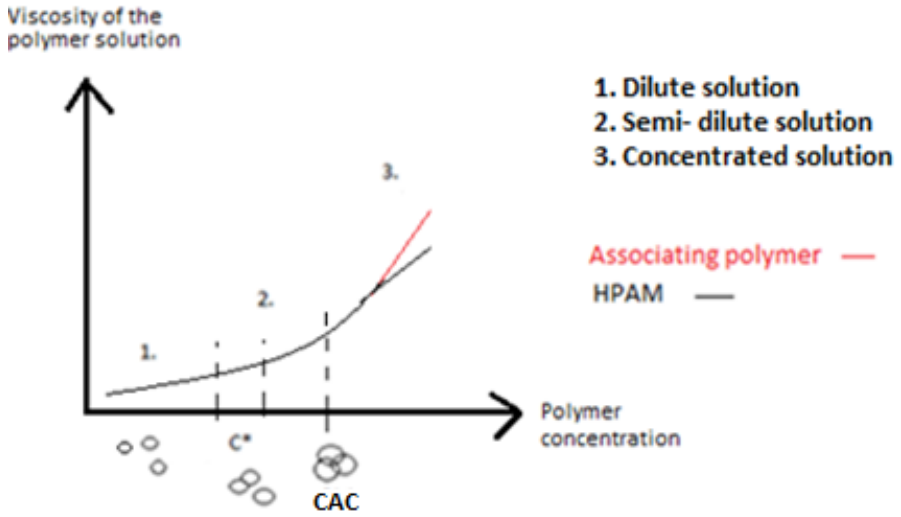

Figure 2.15 Viscosity build up due to increasing polymer concentration. Expected increase of HPAM is shown as a back line, and an expected viscosity increase of associating polymer as red line.

The increase in *figure 2.15* show an improved viscosity change at higher polymer concentrations of associating polymers compared to HPAM. The numbers 1, 2 and 3 corresponds to the characteristic concentration ranges with distinctive physical and chemical interactions occurring.

A graphic approach to determine the critical overlap concentration (C^*) and the critical aggregation concentrations (CAC) was carried out. Due to unstable shear viscosity measurements at low concentrations and at concentrations around CAC of associating polymers, this determination procedure was quite difficult and no clear differences in these concentrations was observed due to salinity changes. In *appendix section A.4* the graphic approach on C319 and D118 in low salinity is illustrated, and the result of the C^* and CAC of the polymer solutions in low and high salinity brines are presented.

Observations:

In *figure 4.3*, the shear viscosities of polymers measured at a given reference shear rate in low and high salinity brine is given as a function of polymer concentration. For polymer concentrations from 25ppm to 200ppm, a reference shear rate of 100 (1/s) was utilized to estimate the shear viscosity of the solution. Polymer concentrations above 200ppm and up to 5000ppm, a reference shear rate of 10 (1/s) was utilized. The specific concentration range for each polymer is listed in *table 3.5* in section 3.2.2.

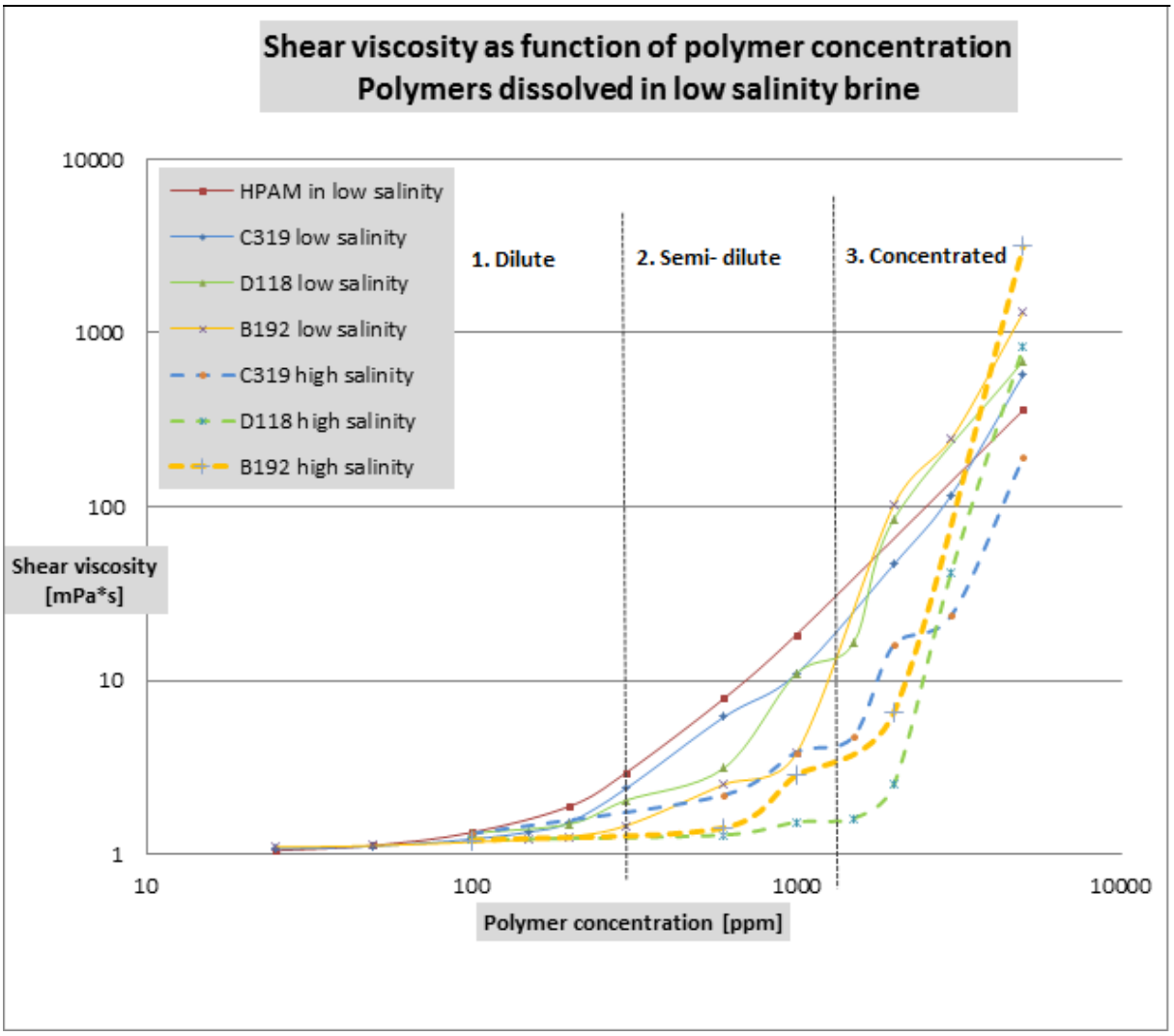

Figure 4.3 Relationship between shear viscosity and polymer concentrations in low (solid curves) and high (dotted curves) salinity brines at 22 ± 0.1°C.

In *figure 4.3*, the double logarithmic plot of shear viscosity as a function of polymer concentration is shown. From *figure 2.15*, the expected increasing viscosity behavior of

HPAM and associating polymer is similar until a given polymer concentration, where the viscosities of associating polymers increases even more.

In *figure 4.3*, the three different concentration regions were estimated. The back dotted lines have the intension simplify the effect of hydrophobicity and salinity effects. The first dotted line at polymer concentration of 200ppm is an illustrating border between diluted concentration range and semi- diluted concentration range. The second dotted line at higher polymer concentration (above 1000ppm) is illustrates the border between the semi- diluted and the concentrated concentration range. These border lines are in reality more diffuse (Dupuis et al., 2009).

Below the first border line in the diluted concentration range, the viscosities measured at these concentrations seems to decrease with increasing degree of hydrophobicity (HPAM>C319>D118>B192). This observations corresponds well with earlier experimental studies (Wever et al., 2011), that below the critical overlap concentration (C^*) where the macromolecules are untangled, the dominating interactions occurring in associating polymer solutions is intramolecular hydrophobic interactions. Increasing hydrophobicity in untangled polymer solutions, the hydrodynamic volume of the macromolecules will decrease (Reichenbach-Klinke et al., 2011). The sensitivity to salinity in untangled polymer solutions seems to reduce the viscosities (Wever et al., 2011).

Between the two dotted lines, the polymer concentration range is referred to as the semi-diluted concentration range. These border lines are just an illustration where the different concentration ranges may exists, due to the increasing viscosities measured at different concentrations. This intermediate concentration range includes both untangled polymer solutions at the lower polymer concentration end, and entangled polymer solutions at higher polymer concentrations. Common to such polymer solutions is that the macromolecules are all *affected* by each other in the solution, as the concentration increases the chains will start to overlap (Dupuis et al., 2009). The steepest slope on the curve, or the highest viscosity build-up as the concentration increases, is observed to be HPAM in low salinity brine. The steepness of the curve decreases with increasing degree of hydrophobicity in low salinity brine (HPAM>C319>D118>B192). At the end of the semi- diluted concentration range, the steepness of the curves of D118 and B192 increases more rapid compared to HPAM and C319. At this end of the semi- diluted concentration range, between 600ppm to 2000ppm, the

critical aggregation concentration (CAC) is expected to be found due to the rapid viscosity increases observed in low salinity brines.

Some variations in the shear viscosities of the associating polymer solutions are observed in both brines in the semi- diluted concentration rang. Compared to HPAM without any associating groups, the shear viscosities at increasing polymer concentrations seem more stable. This variation may be due to random formation of clusters, which results in irregular viscosity increase with polymer concentration.

As the salinity increases, the viscosities of associating polymers seems to still be lower than the viscosity measured in low salinity brine at the beginning of the semi- diluted concentration range. Around 600ppm, some changes in the viscosities are observed for C319 and B192 in high salinity brine. A more rapid increase is observed for B192. The viscosity development due to increasing polymer concentration is still relative low for D118 in high salinity brine. A change in the dominance of the intramolecular hydrophobic associations in untangled solutions to intermolecular hydrophobic associations in entangled solutions is expected at the end of this concentration range (Wever et al., 2011). So the observations of viscosity increase in C319 and B192 corresponds well with these expectations of typical associating behavior as concentration increases.

In the concentrated range (above the second dotted line), the macromolecules are expected to physically interact due to overlapping chains and intermolecular hydrophobic associations (McCormic and Johnson, 1988, Regalado et al., 1999). Comparing the steepness in the curves at polymer concentration of 5000ppm solutions in low salinity brine where a formation of network of associating polymers seems to most likely have occurred, the steepest curve is observed for B192. The steepness in low salinity brine increased with increasing degree of hydrophobicity in this concentration range (HPAM<C319<D118<B192). At a given polymer concentration at the end of semi- diluted concentration range or at the beginning of the concentrated range, a change in the hydrophobic interactions occurred. It seems like the critical aggregation concentration (CAC) most likely is between 600ppm to 2000ppm, since the rapid viscosity build up starts in this region.

Increasing the salinity of the brine the steepest curves of the polymer solutions are even steeper than in low salinity brine. At the end of the concentrated range at polymer

concentration of 5000ppm, which most likely seems to above CAC, the same trend as in low salinity brine is observed regarding thickening ability and degree of hydrophobicity (HPAM<C319<D118<B192). The viscosities are now significantly higher for associating polymers in high salinity brine, compared to the viscosities in low salinity brine.

Conclusions:

A graphic approach to estimate C^* and CAC was difficult due to irregularities in viscosities. Estimation attempts in the low and the high salinity brines are illustrated in *appendix section A.4.*

At low polymer concentrations, the viscosities of polymer solutions decrease with increasing hydrophobicity (HPAM>C319>D118>B192). The viscosity of the associating solutions decreases even more as the salinity of the brine increases. This range is defined as the diluted concentration range.

In the semi- diluted concentration range, between the two dotted lines a transition from untangled to entangled solutions is observed. Entangled solutions are observed at high concentrations where the steepness of the curve (thickening ability) increases. In low salinity brine, this transition effect from dominating intramolecular to intermolecular hydrophobic association is observed for D118 and B192. Whereas in high salinity brine, the viscosities seem to be still lower than in low salinity brine, the transition is observed for B192 and C319.

Above the highest dotted line at 5000ppm concentration, the rapid gel formation is compared for the polymer solutions in low and high salinity brine. The thickening ability is greatly improved in at these polymer concentrations, which indicates that the given association concentration, CAC is reached. Above the critical associating concentration (CAC) a network of polymers are formed due to physical chain overlap in addition to intermolecular hydrophobic interactions. The steepness of the curves seems to represents the thickening ability, and the steepness increases with decreasing degree of hydrophobicity in low salinity brine (HPAM<C319<D118<B192). In high salinity brine the trend is the same, but the thickening ability is observed to be even more pronounced than in low salinity brine.

The thickening ability above CAC and the low salinity effect on the hydrodynamic volume makes the associating polymers very interesting to polymer flood, and injectivity and/or production modifications. Form these observations, a small amount of hydrophobic groups incorporated onto the polyacrylamide backbone of HPAM seems to stabilize the macromolecule when increasing the salinity of the brine. Instead of precipitation and viscosity loss as observed for HPAM dissolved in high salinity brines, a small hydrophobicity increase is observed to greatly improve the thickening ability at lower polymer concentrations (HPAM<C319<D118<B192).

Above the critical aggregation concentration (CAC), gel- like solutions is formed. Increase of salinity of in the brine, seems to increase the viscosities even further for associating polymers. The rapid thickening ability due to formation of associating network that creates gel- like solutions, may be quite favorable as a near well diversion technique. Since a lower polymer concentration is observed to be needed to reach a given gel- like solution.

4.2 Viscoelastic measurements

In this study the *linear viscoelastic Maxwell model* (Sochi, 2010) was chosen to estimate the viscoelastic behavior of the polymer solutions above critical overlap concentration (C^*) at 22 ± 0.1^oC.

From the background of viscoelasticity given in section 2.2.4, the dominance of the storage and loss modulus is evaluated from amplitude sweep. The dominant modulus of polymeric gels (highly viscous polymer solutions) is the storage modulus, and hence the linear viscoelastic (LVE) range is detected. The characteristic relaxation time, known as the *yield point* of the polymer solution is estimated at the end of the LVE- range.

After the linear viscoelastic region of polymeric gels is defined, a frequency sweep is carried out for these solutions. In the frequency sweep the crossover point of the storage and loss moduli is estimated, and this point is known as the *gel- point* of polymeric gels. From the frequency sweep the phase shift angle between the loss modulus and the complex shear modulus are recorded to illustrate the elastic and viscous dominated behavior of the solution under different deformations.

4.2.1 Yield point

The yield point of a polymer solution with dominating intermolecular hydrophobic interactions is defined as the maximum deformation stress before the structure of the solution starts to deform and split up to several units.

Through an amplitude sweep where the storage (G') and loss (G'') moduli is given as a function of shear stress (τ), the yield point are estimated at the end of linear viscoelastic (LVE) range on the dominating modulus. Since the yield point is defined for entangled polymer solutions, due to the dominance of intermolecular hydrophobic interactions, the dominating modulus of such polymeric gels are storage modulus (damping factor tan $\delta < 1$) (Anton Paar, 2008). A graphic approach illustrated in *figure 4.4*, is utilized to estimate the yield point of polymeric solutions.

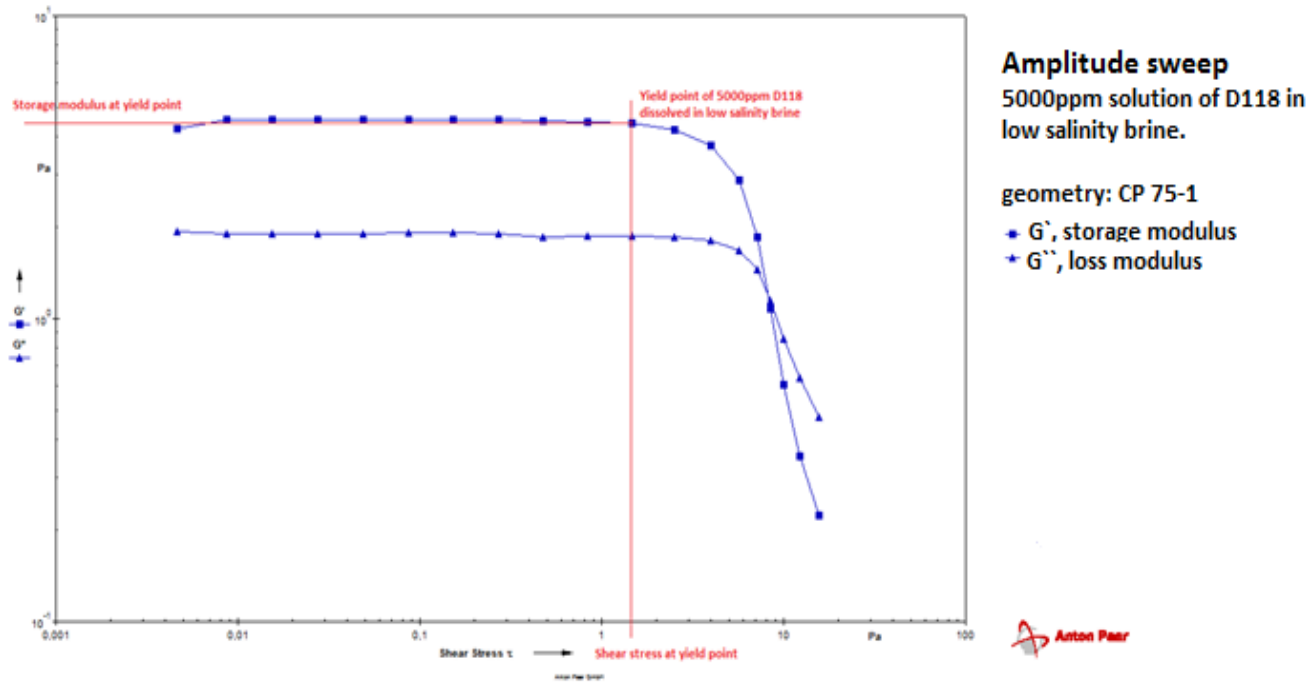

Figure 4.4 Illustration of the graphic approach to estimate yield point of a polymer solution through amplitude sweep.

The yield point of a gel- like polymer solution presented with a given shear stress and storage modulus value, as shown in *figure 4.4.* The shear stress at yield point (τ_y,) of a polymer solution is the maximum deformation stress that can be exposed to polymer molecules before the network of associating polymers starts to deform and split up. The storage modulus at the yield point ($G_y^{'}$.), represent the strength of the intermolecular interactions holding the network structure for polymers together in the entangled solution. Below the critical shear stress at yield point, the concentrated polymer solutions act as solids since the storage modulus dominates over the loss modulus. The gel- like solution absorbs the deformation energy, without flowing (TA Instruments, 2004). Once the deformation stress becomes stronger than the interactions holding the associating network together, the associating bond starts to break. Above this threshold stress, the polymer solution will initiate flow.

For typical Maxwellian fluids, an increase in the shear stress above the yield point value, a declining response on the storage modulus curve is shown. This deformation is due to the transition from gel- like polymer behavior to a more liquid- like flow behavior above threshold shear stress.

In this study, the amplitude sweep was only carried out for polymer concentrations from 600ppm to 5000ppm. Due to limitations on the rheometer regarding viscoelasticity in diluted solutions, polymer concentrations below 600ppm was not performed.

The amplitude sweeps of C319 in low and high salinity brine are presented in *figure 4.5* and *figure 4.6*, and the rest of the amplitude sweeps are presented in *appendix section A.5.* All the amplitude sweeps were carried out at room temperature of 22 ± 0,05^{o}C.

Observations:

The amplitude sweep, storage and loss moduli as a function of shear stress of C319 in low salinity brine is presented in *figure 4*.5.

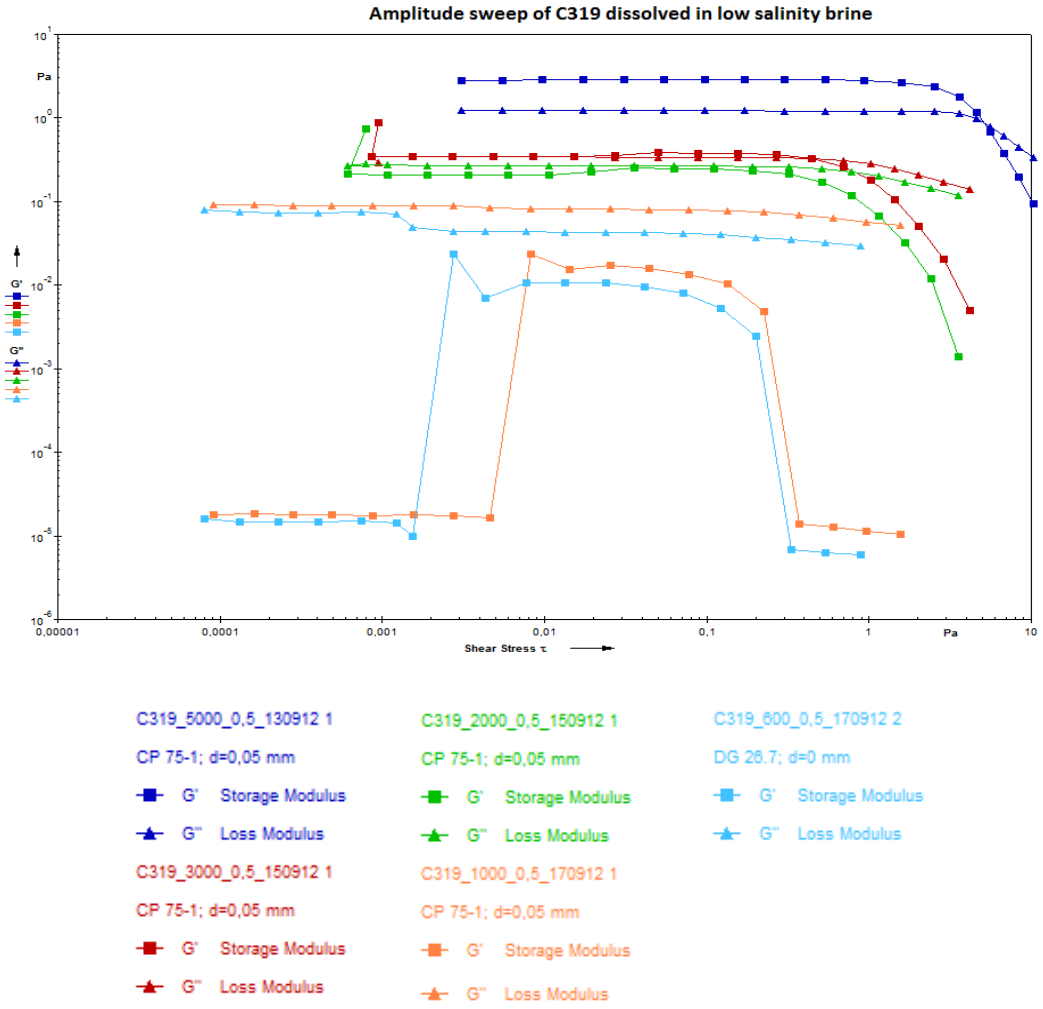

Figure 4.5 Amplitude sweep of C319 dissolved in low salinity brine at different polymer concentrations at 22 ± 0.1^{o}C.

In *figure 4.5* where the storage and loss moduli are given as functions of shear stress for C319 solutions in low salinity brine. It is observed for 3000ppm and 5000ppm solutions of C319 that storage modulus is dominating over loss modulus, before these two moduli cross. Polymer concentrations below 3000ppm are viscous dominated over the defined shear stress interval, which indicates that this associating polymer is able to form physical gels at high enough concentrations. The estimated yield point of the gel solutions of C319 with concentrations 3000ppm and 5000ppm is observed to move to higher shear stress value as the concentration increases. This indicates that the intermolecular forces holding the formed network structure together in these entangled solutions, becomes strengthen as the polymer concentration increases. This observation corresponds well with expected entangled solutions of modified HPAM.

The amplitude sweep, storage and loss moduli as a function of shear stress of C319 in high salinity brine is presented in *figure 4.*6.

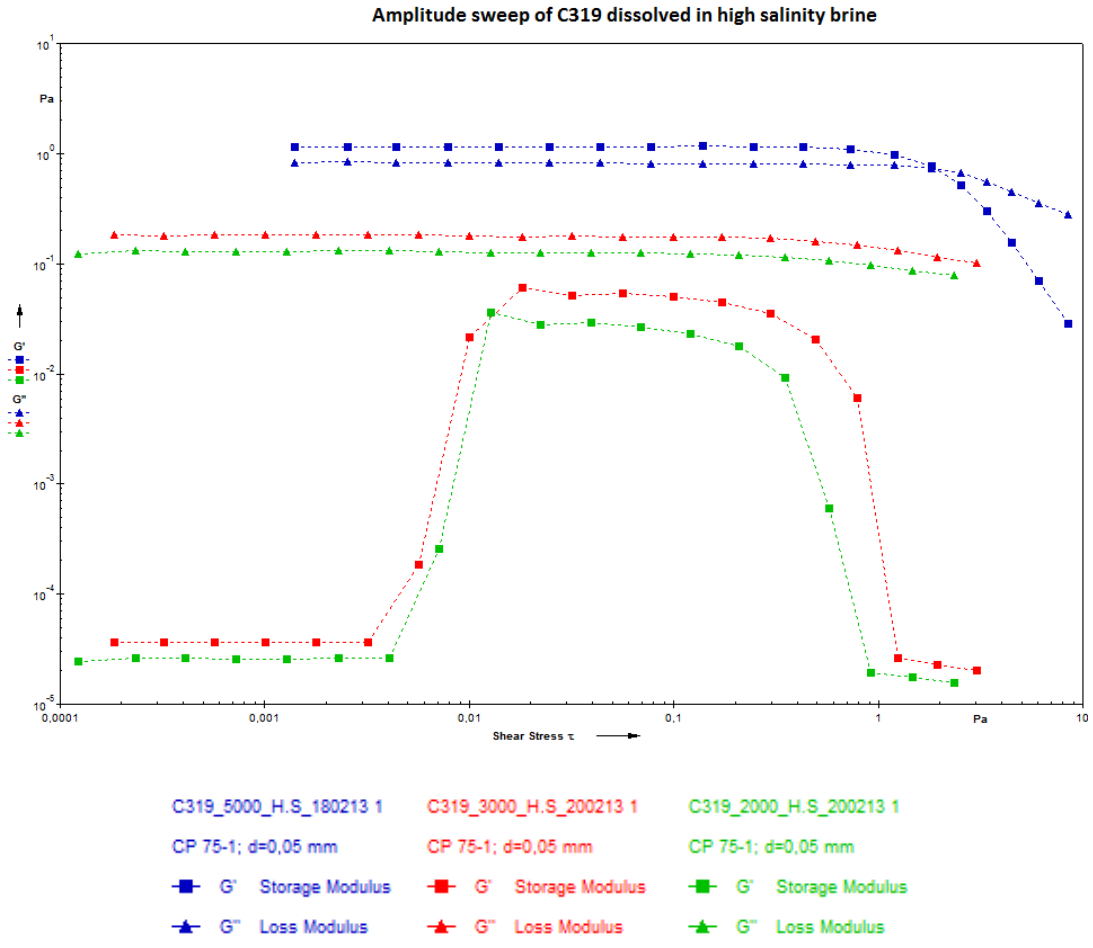

Figure 4.6 Amplitude sweep of C319 dissolved in high salinity brine at different polymer concentrations at 22 ± 0.1^{o}C.

In *figure 4.6* where the storage and loss moduli are given as functions of shear stress for C319 solutions in high salinity brine. A gel solution behavior is only observed for 5000ppm solution of C319 in this high salinity brine. The storage modulus dominates over loss moduli until a given shear stress, where these two moduli cross. All solutions below 5000ppm show viscous dominating behavior over the whole shear stress interval. Increase of the ionic strength of the solution, seems to reduce the strength of the intermolecular interactions. Below the concentration of 5000ppm where the macromolecules most likely are jammed, increasing ionic components seems to prevent the macromolecules to form network. In these solutions the macromolecules may associate to clusters or isolated macromolecules. Comparing this effect on C319 in high salinity brine to HPAM, the viscosity effect and this gel- like behavior of 5000ppm solution are still efficient even with low degree of hydrophobicity.

A summarization plot of the polymer solutions with dominating storage modulus as a function of shear stress is presented in *figure 4.7*.

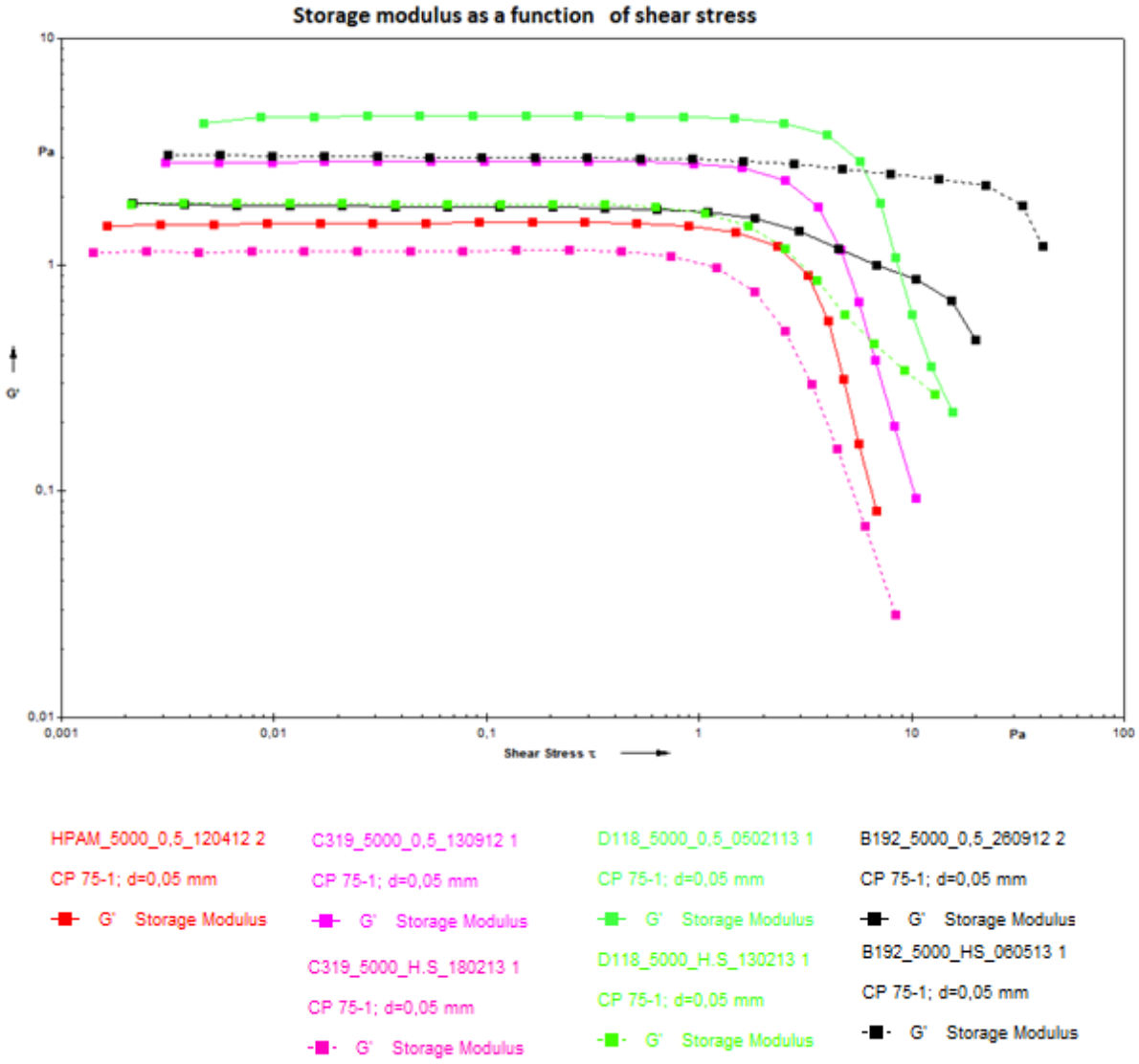

Figure 4.7 Storage moduli as functions of shear stress of different gel- like polymer solutions at 22 ± 0.1°C. Polymers dissolved in low salinity brine are shown with solid line, whereas dissolutions in high salinity brines are shown as dotted line.

The 3000ppm solution of C319 dissolved in low salinity brine, the storage modulus was dominating over loss modulus. The storage modulus of 3000ppm was not presented in summarizing *figure 4.*7, since the yield point value was so small compared to the other solutions. The estimated yield point value is not presented in *table 4.3,* neither. The measured shear stress at yield point of 3000ppm C319 dissolved in low salinity brine was 0.16 Pa, and the measured storage modulus at yield point was 0.38.

Table 4.3 Estimated yield points of gel- like polymer solutions at 22 ± 0.1^{o}C.

Polymer concentration [ppm]	***Polymer***	***Salinity***	***Yield point at 22 ± 0.1^{o}C***	
			Shear stress, τ_y [Pa]	***Storage modulus, $G_y^{'}$ [Pa]***
5000	***HPAM***	Low	0.89	1.49
		-	-	-
	C319	Low	0.94	2.81
		High	0.43	1.14
	D118	Low	1.47	4.41
		High	0.63	1.80
	B192	Low	0.63	1.80
		High	4.71	2.65

The yield point indicates the strength of the intermolecular interactions holding the gel network together in entangled polymer solutions, and how the deformation process of this gel structure degenerate with increasing shear stress above this threshold value.

Comparing the yield point of HPAM, the shear stability and strength of the intermolecular interactions are observed to be increase with increasing amount of associating groups in low salinity brine (HPAM<C319<D118). The intermolecular hydrophobic interactions seem to reinforce the strength with increasing degree of hydrophobicity. These observations correspond well with earlier viscoelasticity studies carried out on associating polymers (Kujawa et al., 2006). A higher deformation stress is needed to initiate flow of these associating polymer solutions compared to the gel solution of HPAM without any hydrophobic group.

The yield point in low salinity brine of B192 compared to the HPAM based polymers, a lower shear stress is observed. This may be due a different composition of the gel structure. From the observed loss of shear stress at yield point of B192, in spite of the relative strong interactions that is observed; it seems like the solution of B192 consist of associating clusters that hydrophobically interact with each other and form a network. This network seems to be easier to deform than the network in HPAM based polymers, where isolated macromolecules or smaller clusters are associated together to form the gel structure.

The shear stress at yield point of D118 is observed to be higher than for C319 dissolved in high salinity brine. This seems to indicate that the higher amount of hydrophobic groups in D118 reinforces the intermolecular hydrophobic interactions in the gel structure. Comparing this salinity effect to the viscoelastic study of multisticker associating polymers carried out in

2006 by Kujawa et. al (Kujawa et al., 2006), they found that increasing salinity of the solution give a less pronounced effect on the yield point. These observations do not correspond with the observed salinity effect in this study. The increasing salinity of the brine has a pronounced effect in the strength of interactions in these associating solutions. The strength of the interactions in the gel structure becomes lower due to increasing amount of ionic components in the solvent.

The salinity effect seems to have a dramatic effect on the yield point for B192. The interactions in this gel solution are observed to be much stronger at high salinity, and the shear stability is also much higher compared to dissolution in the low salinity brine. This may be related to the relative high degree of hydrophobicity and low degree of hydrolysis. The hydrophobic groups reinforces the strength of the network of macromolecules for B192, and so does the relatively lower electrostatic repulsion of B192 compared to D118 and C319. The electrostatic repulsion of B192 becomes lower with increasing salinity of the solvent. This seems to induce a lower salinity sensitivity of B192, compared to C319 and D118 with higher degree of hydrolysis.

From *figure 4.7* the storage modulus curves start to deform after yield point. The decreasing deformation curve represents the decomposition of the intermolecular interactions holding the associating network together. The slope on the deformation curve is observed to be less steep for D118 and B192 in high salinity brine. The reason may be that during deformation of these gel structures, where the intermolecular hydrophobic interactions starts to break, the outcome of the deformed gel network are different from the others. Deformation of D118 and B192 seems to results in associating clusters instead of isolated macromolecules or smaller clusters in the solutions. These clusters will have higher viscosity and elasticity in the solution, compared to a deformed polymer solutions into isolated macromolecules molecules (Kujawa et al., 2006).

Conclusions:

In low salinity brine the strength of the gel network and the shear stress at yield point increased by increasing degree of hydrophobicity for the polymers HPAM < C319 < D118. A lower shear stress at yield point was found for B192 in low salinity brine compared to HPAM.

The low yield point may be due to a different gel structure that is easier to deform compared to HPAM in the low salinity brine.

In high salinity brine, the strength of the gel structure seems to increase with increasing amount of associating groups (C319< D118). For B192 in high salinity brine the strength of the interactions observed to be increased. It seems like the relative high degree of hydrophobicity strengthens the interactions in the network and low degree of hydrolysis makes B192 less affected to increasing salinity of the brine.

From the shear viscosity measurements an increase of the degree of hydrophobicity seems induce higher shear stress stability, due to reinforcement of the intermolecular associations between the hydrophobic groups in the gel network of polymers. Relating the shear viscosity measurement of gel solution of D118 (5000ppm) to the viscoelasticity measurements in low and high salinity brines, some interesting observations was observed. The shear viscosity and the effect on shear stress stability of D118 in low and high salinity brine was observed to be similar. From the viscoelastic measurements the strength of the gel structure of D118 in the high salinity brine seems to be higher than in the low salinity brine. This seems to result in a different deformation behavior above yield point. In high salinity the network seems to deform to associating clusters with high elasticity and viscosity, compared to the deformation process in low salinity brine where the network seems to deform to isolated macromolecules.

4.2.2 Gel point

After defining the polymers linear viscoelastic region by amplitude sweep, the molecular structure of the polymer can be further characterized using a frequency sweep. In a frequency sweep of polymer solutions the storage modulus, the loss modulus and the complex shear viscosity are given as functions of the angular frequency at constant amplitude. This amplitude or strain must be below the critical amplitude at yield point. The critical amplitude (γ_c) was set to 10% to insure that the gel- like structure due to associating network is still intact.

From a frequency sweep more information about the interactions occurring between the molecules in the entangled network can be found. The most important characterizing parameter from the frequency sweep is the *crossover point* of storage and loss moduli at a given angular frequency.

The crossover point at a given angular frequency (ω_c) where $G''(\omega_c) = G'(\omega_c)$, is a characteristic time of the polymer gels. The crossover point is referred to as the *gel point* of a given polymer solution, and is characterized with an equal balance of viscous and elastic portion. This point indicates the strength of the interactions holding the gel structure (network) together in the entangled polymer solution.

The gel- point of the polymer solutions in this study is estimated through a graphic approach from the frequency sweep, as illustrated in *figure 4.8.*

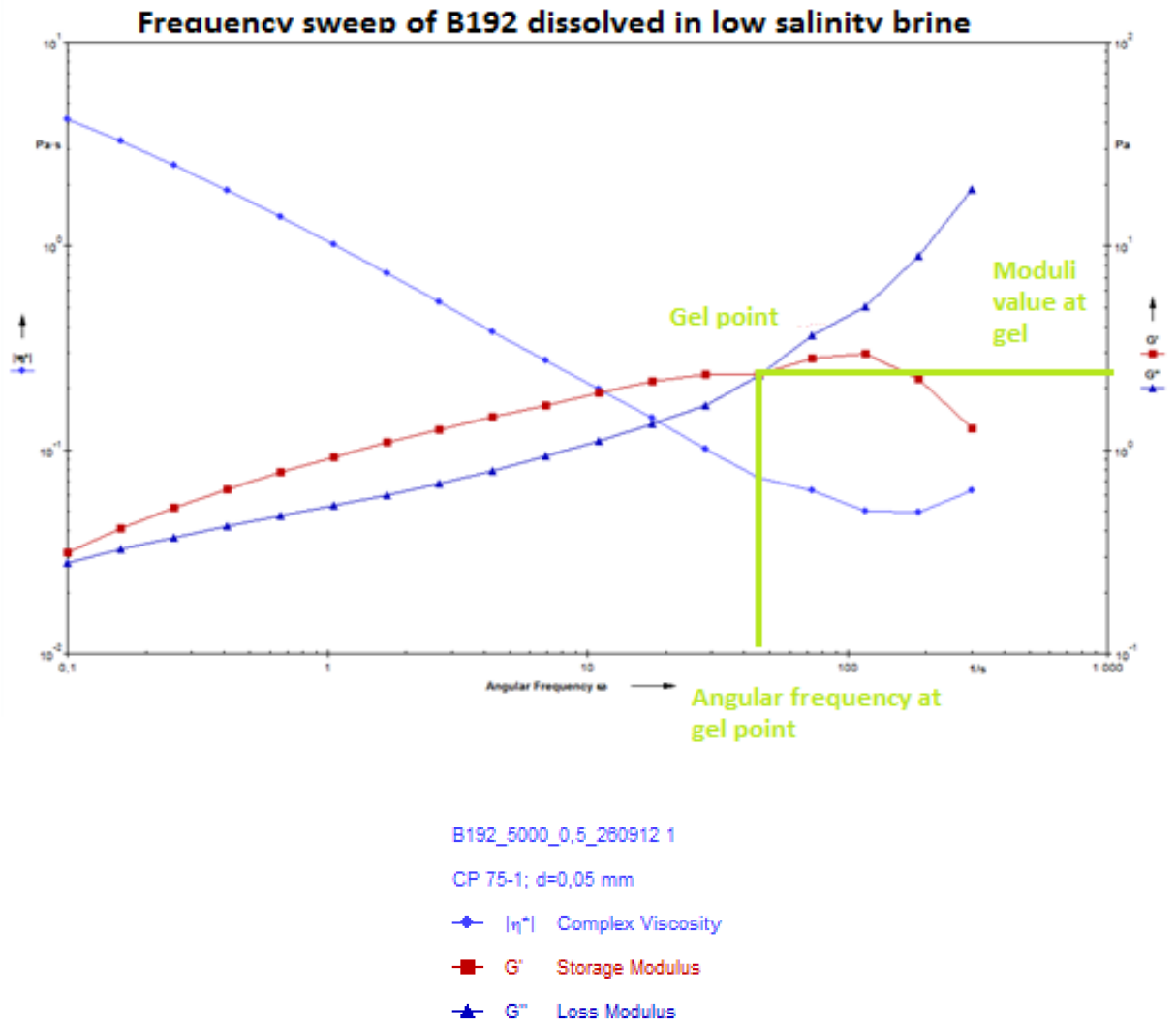

Figure 4.8 Illustration of the graphic approach to estimate gel point of a polymer solution through frequency sweep.

The value of the angular frequency at the gel- point (ω_c) indicates the external stress applied on the polymer solution. The value of the crossover point ($G''(\omega_c) = G'(\omega_c)$), indicates the strength of the interactions holding the gel structure together.

In this study, the frequency sweep was only carried out for the polymer solutions which had a dominance of storage modulus in amplitude sweep. The actual polymer solutions are listed in *table 4.3* in section 4.2.1, in addition to 3000ppm solution of C319 dissolved in low salinity brine. The frequency sweep of 5000ppm solution of C319 dissolved in low and high salinity brines are presented in *figure 4.9* and *figure 4.10*, and the rest of the frequency sweeps are presented in *appendix section A.5.* All frequency sweeps were carried out at room temperature of 22 ± 0.1^{o}C.

From the linear plateau of the complex viscosity curves in the frequency sweep, the zero-shear viscosity (μ_o) can be extrapolate to zero angular frequency according to **Eq. 2.23** in section 2.2.4. It was not possible to extrapolate down to zero angular frequencies due to measurement limitations of the rheometer at low angular frequencies. The linear plateau of the complex viscosity curves are presented in *appendix section A.6.*

Observations:

The frequency sweep where the storage modulus, loss modulus and complex shear viscosity given as functions of angular frequency of 5000ppm solution of C319 the in low salinity brine, is presented in *figure 4.9.*

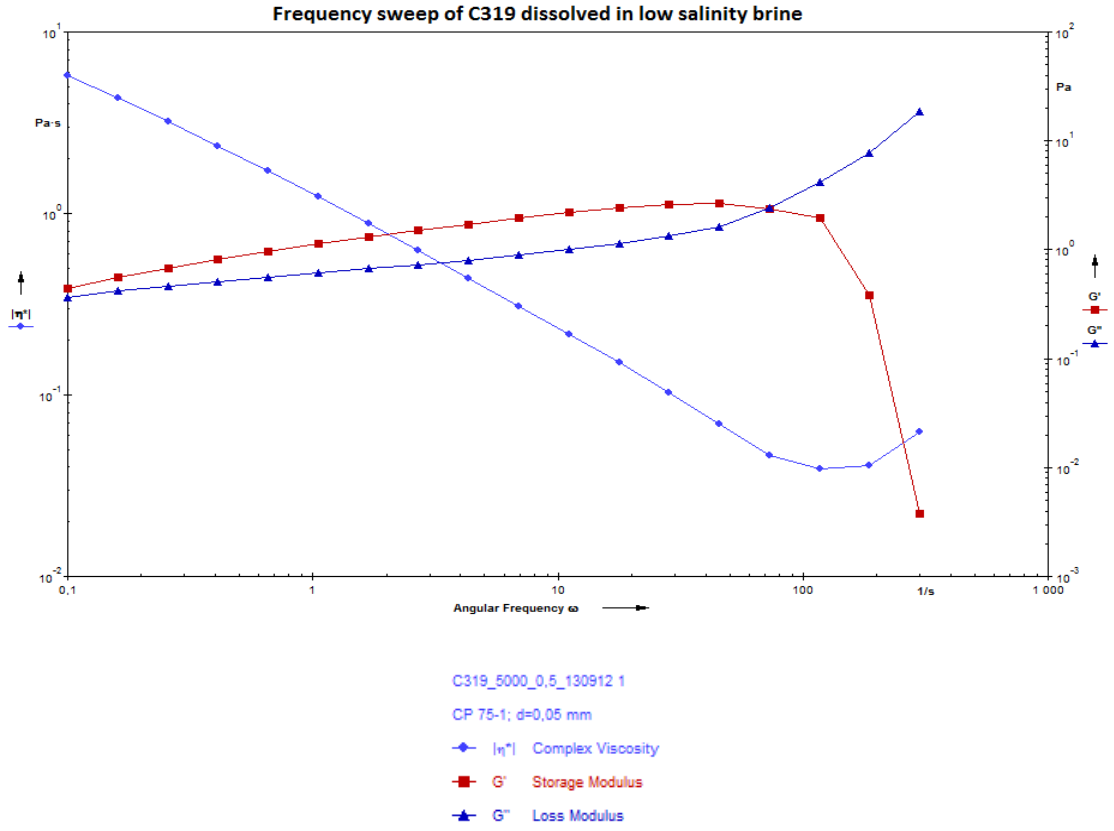

Figure 4.9 Frequency sweep of 5000ppm solution of C319 the in low (solid line) salinity brine measured at 22 ± 0.1^{o}C.

The frequency sweep where the storage modulus, loss modulus and complex shear viscosity given as functions of angular frequency of 5000ppm solution of C319 in high salinity brine, is presented in *figure 4.10.*

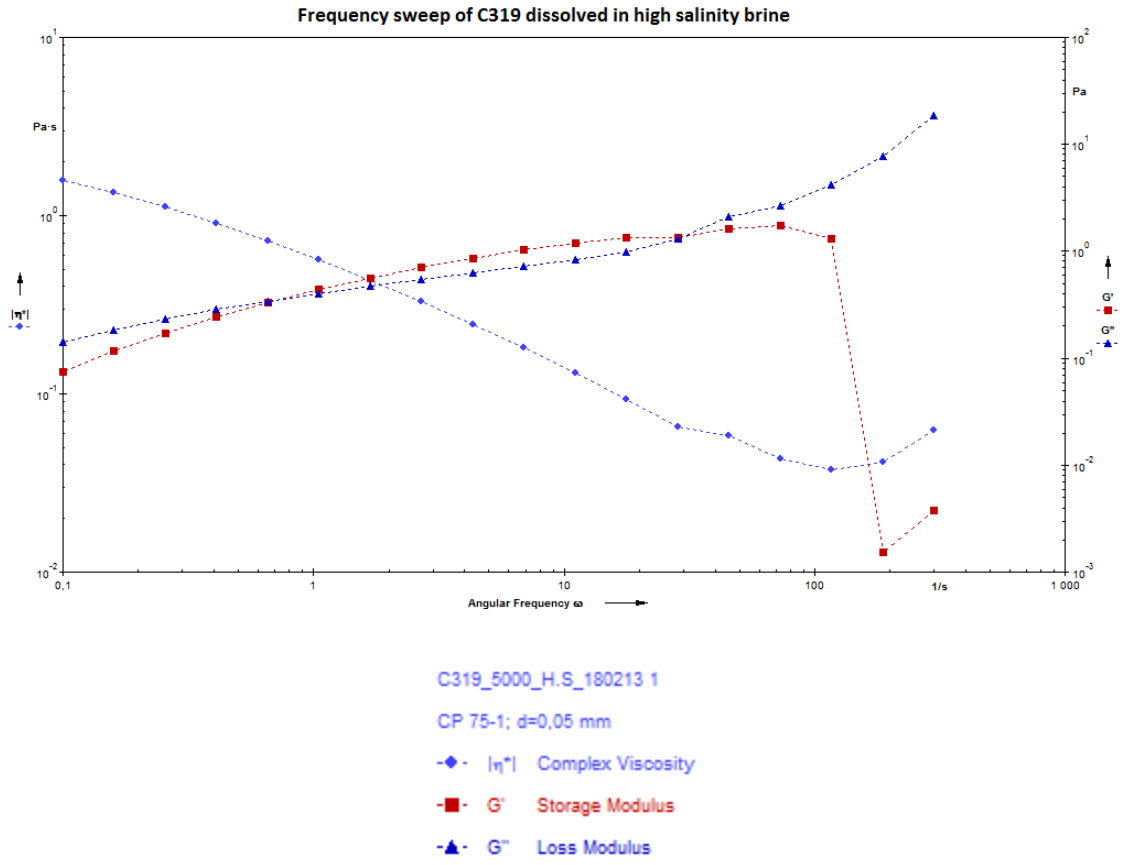

Figure 4.10 Frequency sweep of 5000ppm solution of C319 the in high (dotted line) salinity brine measured at 22 ± 0.1°C.

The estimated gel point value of the 5000ppm solution is presented in *table 4.4.* The estimated gel point of 3000ppm solution of C319 is too low to be presented in *table 4.4.* The measured angular frequency at gel point of 3000ppm C319 dissolved in the low salinity brine was 16 (1/s), and the measured moduli value at gel point was 0.45 Pa.

The gel point of the entangled polymer solution can also be found through the damping factor (tan δ) as a function of angular frequency. As described in section 2.2.4, the damping factor at gel point ($G''(\omega_c) = G'(\omega_c)$ is equal to unity (tan δ= 1). This plot is presented in *appendix section A.5.*

Table 4.4 The gel- point estimated for the different polymer solutions in both brines at 22 ± 0.1°C.

Polymer concentration [ppm]	***Polymer***	***Salinity***	***Gel point at*** *22 ± 0.1°C*	
			Angular frequency, ω_c [1/s]	***Crossover value of moduli, $G''(\omega_c) = G'(\omega_c)$ [Pa]***
5000	***HPAM***	Low	140	1.90
		-	-	-
	C319	Low	73.0	2.38
		High	32.0	1.50
	D118	Low	94.0	5.40
		High	54.0	2.20
	B192	Low	49.0	2.40
		High	81.0	2.80

The gel point of a polymer solution indicates the strength of the interactions holding the network together. The strength of the gel structure seems to be increasing with increasing amount of associating groups (HPAM<C319<D118) in low salinity brine. It seems like the intermolecular strength in the gel network is reinforced with increasing degree of hydrophobicity.

The strength in the gel structure of B192 is observed to be stronger than HPAM, but a lower frequency is observed for B192 in the low salinity brine. It seems like B192 has a different character of the gel structure, which is highly viscous and highly elastic, and will easier deform compared to the structure of HPAM. The strength in the gel structure of B192 is due to strong hydrophobic intermolecular interactions within the associating clusters.

The salinity effect on C319 and D118 seems to reduce the strength of the interactions in the gel structure, due to electrostatic repulsion of the charged segments. Increase in ionic strength effect the B192 solution different then C319 and D118. The intermolecular hydrophobic interactions seem the increase to some extend with increasing salinity of the brine. From the observations of yield point in section 4.2.1, this may be related to the relative high degree of hydrophobicity and the low degree of hydrolysis. C319 and D118 have the same polymer base as HPAM, they only differs in degree of hydrophobicity. Whereas B192, has a lower molecular weight compared to HPAM, and a much higher degree of hydrophobicity. The large amount of associating groups strengthen the gel structure, and the low degree of

hydrolysis makes B192 less effected to electrostatic screening of the charged segments compared to the others.

Conclusions:

In the low salinity brine the gel strength seems to increase with increasing amount of associating groups (HPAM<C319< D118). The interactions become stronger due to reinforcement of the intermolecular hydrophobic interactions. The interactions holding the gel structure together seems to be reduced due to electrostatic repulsion, when the salinity of the brine increases.

In low salinity brine the gel structure of B192 is observed to be stronger than HPAM, even though a low frequency is observed for B192. This may indicate that B192 has different gel structure that is more viscos and elastic, and has stronger hydrophobic intermolecular interactions than HPAM. It seems like it is easier to deform the interactions in the network of associating clusters (B192), than interactions in the network of isolated macromolecules (HPAM). Increasing ionic strength of the brine seems to strengthen the interactions in B192. This may be related to the high degree of hydrophobic groups in addition to low degree of hydrolysis which make B192 less sensitive to electrostatic screening.

5. Overall conclusions

The thickening ability of HPAM was observed to be significantly improved above CAC by incorporation of a small amount of associating groups. The viscosifying power seems to be the formation of associating gel structure in entangled chain solutions, where the intermolecular hydrophobic interactions is observed to be strengthen with increasing degree of hydrophobicity (HPAM<C319<D118<B192). Increasing ionic strength of the brine seems to improve the viscous properties of HPAM dramatically in entangled solutions, due to reinforcement of the intermolecular interactions. These observations correspond well with earlier observations.

The shear viscosity response to shear stress is observed to be similar for the entangled solution of D118 dissolved in the low and the high salinity brine. The strength of the gel structure and the elastic deformation response seems to differ, due to different gel structures.

Below C^*, the thickening ability is observed to alter from the trend observed above CAC. This observation corresponds well with earlier viscosity studies carried out for associating polymer solutions. The observed viscosity of the untangled solutions seems to be reduced with increasing degree of hydrophobicity (HPAM>C319>D118>B192). This seems to be due to the dominance of intramolecular hydrophobic interaction between the associating groups within macromolecules. Increasing ionic strength of the brine seems to enhance the intramolecular associations further.

The strength of the associating gel structure above CAC was detected from the yield- and the gel point for viscoelastic solutions. The observed trend is that the strength of the intermolecular hydrophobic interactions increases with increasing amount of associating groups in low salinity brine (HPAM<C319<D118). For B192 the strength of the structure was observed to be higher than HPAM, but the shear stability was lower. It seems like the gel structure of B192 may be different and easier to deform due to different configurations. Increasing ionic strength is observed to reduce the strength of the hydrophobic interactions in C319 and D118, due to electrostatic screening. For B192, a salinity increase is observed to increase the intermolecular hydrophobic interactions in the gel structure. This may be related to the relative high degree of hydrophobicity and low degree of hydrolysis, which makes B192 less affected by electrostatic effects.

6. Further work

A continuation of this experimental study is to see the thickening ability, shear stress stability and elastic deformation response of a hydrophobic modified HPAM in high salinity brine, when increasing the relative amount of hydrophobic groups on the hydrophilic chain more than twice as much (D118). The intention of this work is to observe the thickening and stability limitations of associating polymers, since the solubility in the brine decreases with increasing degree of hydrophobicity.

Dissolve the studied associating polymers in synthetic sea water (SSW) and increasing the environmental temperature up to a reservoir temperature may also be interesting. The purpose of this study is to see how much thickening ability, shear stress stability and elastic deformation response are affected. Dissolution of the associating polymers in this brine and at this temperature provides a more realistic effect when considering a future offshore application, like on the Norwegian continental shelf (NCS).

Detecting the critical overlap concentration (C^*) and the critical association concentration (CAC) of the associating polymer solutions in SSW, is important to predict the characteristic flow behavior of a given polymer solution. To estimate the C^*, several polymer solutions in the concentration range from 200ppm to 600ppm has to be made. In the case of estimating CAC, several polymer solutions have to be made between 600ppm to 2000ppm. Through a graphic approach carried out during this study, these broad concentration ranges were found.

Another approach to interpret these experimental data is to improve the knowledge about the chemical composition and structure of the macromolecule. These findings may provide necessary information to understand the physical and chemical interactions occurring in associating polymer solutions. This might help to understand the formation of foam during filtration and precipitation of polymers during pH adjustments in high salinity brine.

A further investigation of the adsorption ability of associating polymer solution can be interesting when considering polymer floods and injectivity and/ or production modifications. This can be carried out by core flood under reservoir conditions.

A change in the preparation method of associating polymers in high salinity brines to a more gradual salinity increase in the polymer solution. A change in the preparation procedure is the

most uncertain parameter during this study, and a different salinity increase of the solution may provide a better solubility.

References:

ANTON PAAR 2008. eLearning course. *Basics of Rheometry (rotation and oscillation) and Basics of viscometry*.

ARGILLIER, J. F., AUDIBERT, A., LECOURTIER, J., MOAN, M. & ROUSSEAU, L. 1996. Solution and adsorption properties of hydrophobically associating water-soluble polyacrylamides. *Elsevier Colloids and Surfaces,* Physicochemical and Engineeering Aspects 113 (1996)**,** 247- 257.

BARNES, H. A., HUTTON, J. F. & WALTERS, K. 1989. An introduction to Rheology. *Elsevier*.

BERG, J. C. 2010. An Introduction to Interfaces and Colloids - The Bridge to Nanoscience. *World Scientific Publishing Co. Pte. Ltd*.

BOLTON, P. 2013. Oil prices. *Social & General Statistics, UK*.

BUCHGRABER, M., CLEMENS, T., CASTANIER, L. M., KOVSCEK, A. R. & STANFORD UNIVERSITY 2009. The Displacement of Viscous Oil by Associative Polymer Solutions. *Society of Petroleum Engineers, SPE,* SPE 122400.

CAPUTO, M. R., SELB, J. & CANDAU, F. 2004. Effect of temperature on the viscoelastic behavior of entangeled solutions of multisticker associating polyacrylamides. *Elsevier,* Polymer 231- 240.

CHASSENIEUX, C., NICOLAI, T. & BENYAHIA, L. 2010. Rheology of associative polymer solutions. *Current Opinion in Colloid & Interface Science,* 16**,** 18-26.

CHAUVETEAU, G. 1986. Fundamental Criteria in Polymer Flow Through Porous Media. *American Chemical Society***,** 228-267.

DUPUIS, G., RIGOLINI, J., CLISSON, G., ROUSSEAU, D., TABARY, R. & GRASSI, B. 2009. Determination of the macromolecular dimensions of hydrophobically modified polymers by micellar size exclusion chromatography coupled with multiangle light scattering. *Analytical Chemistry,* 81**,** 8993- 9001.

DUPUIS, G., ROUSSEAU, D. & GRASSL, B. 2010. How to Get the Best Out of Hydrophobically Associative Polymers for IOR? New experimental Insights. *Society of Petroleum Engineers, SPE,* SPE 129884.

DUPUIS, G., ROUSSEAU, D., TABARY, R. & GRASSI, B. 2011a. Flow of Hydrophobically Modified Water-Soluble-Polymer Solutions in Porous Media: New Experimental Insights in the Diluted Regime. *Society of Petroleum Engineers Journal, SPE Journal,* SPE 129884.

DUPUIS, G., ROUSSEAU, D., TABARY, R. & GRASSL, B. 2011b. Injectivity of Hydrophobically Modified Water Soluble Polymers for IOR: Controlled Resistance Factors vs. Flow- Induced Gelation. *Society of Petroleum Engineers Journal, SPE Journal*.

GOUVEIA, L. M., PAILLET, S., KHOUKH, A., GRASSL, B. & MÜLLER, A. J. 2008. The effect of the ionic strength on the rheological behavior of hydrophobically modified polyacrylamide aqueous solutions mixed with sodium dodecyl sulfate (SDS) or cetyltrimethylammonium p-toluenesulfonate (CTAT). *Colloids and Surfaces A: Physicochemical and Engineering Aspects,* 322**,** 211-218.

INTERNATIONAL ENERGY AGENCY, I. 2013. Oil Market Report.

JIMÉNEZ-REGALADO, E. J., CADENAS-PLIEGO, G., PÉREZ-ÁLVAREZ, M. & HERNÁNDEZ-VALDEZ, Y. 2004. Study of three different families of water-soluble copolymers: synthesis, characterization and viscoelastic behavior of semidilute solutions of polymers prepared by solution polymerization. *Polymer,* 45**,** 1993-2000.

KUJAWA, P., AUDIBERT- HAYET, A., JOSEPH, S. & CANDAU, F. 2004. Rheological Properties of Multisticker Associative Polyelectrolytes in semidilute aqueous solutions. *Journal of Polymer Science* 42**,** 1640-1655.

KUJAWA, P., AUDIBERT- HAYET, A., SELB, J. & CANDAU, F. 2006. Effect of Ionic Strength on the Rheological Properties of Multisticker Associative Polyelectrolytes. *Macromolecules,* 39**,** 318-392.

LEE, S., KIM, D. H., HUH, C. & POPE, G. A. 2009. Development of a Comprehensive Rheological Property Database for EOR polymers. *Society of Petroleum Engineers Journal, SPE Journal,* SPE 124798.

LIEN, J. R. 2009. PTEK 212- Reservoarteknikk I. *University of Bergen*.
LIN, Y., KAIFU, L. & RONGHUA, H. 2000. A study on P(AM-DMDA) hydrophobically associating water-soluble copolymer. *European Polymer Journal, Elsevier,* 36**,** 1711- 1715.
LU, H., HUANG, Z. & FENG, Y. 2010. Solution Association Characterization of Hydrophobically Associating Polyacrylamide Obtained from Produced Fluids. *Journal of Macromolecular Science, Part A,* 47**,** 423-428.
LUNESTAD, S. F. 2011. Characterisation of Linked Polymer Solution (LPS)- Influence of salinity and divalent ions". *MS Thesis, Department of chemistry, University of Bergen, Bergen, Norway*.
MA, S. X. & COOPER, S. L. 2001. Macromolecules: Shear Thickening in Aqueous Solutions of Hydrocarbon End-Capped Poly(ethylene oxide). *American Chemical Society,* 34**,** 3294- 3301.
MAIA, A. M. S., BORSALI, R. & BALABAN, R. C. 2009. Comparison between a polyacrylamide and a hydrophobically modified polyacrylamide flood in a sandstone core. *Materials Science and Engineering: C,* 29**,** 505-509.
MAIA, A. M. S., COSTA, M., BORSALI, R. & GARCIA, R. B. 2005. Rheological Behavior and Scattering Studies of Acrylamide-Based Copolymer Solutions. *Macromolecular Symposia,* 229**,** 217-227.
MAIA, A. M. S., VILLETTI, M. A., VIDAL, R. R. L., BORSALI, R. & BALABAN, R. C. 2011. Solution Properties of a Hydrophobically Associating Polyacrylamide and its polyelectrolyte derivates. *J. Braz. Chem. Soc.,* 22**,** 489- 500.
MCCORMIC, C. L. & JOHNSON, C. B. 1988. Structurally Tailored Macromolecules for Mobility Control in Enhanced Oil Recovery. *Water-Soluble Polymers for Petroleum Recovery***,** 161 - 180.
MOREL, D., VERT, M., JOUENNE, S., GAUCHET, R. & BOUGER, Y. 2012. First Polymer Injection in Deep Offshore Field Angola: Recent Advances in the Dalia/Camelia Field Case. *Society of Petroleum Engineers, SPE,* SPE 135735.
MOREL, D., VERT, M., JOUENNE, S. & NAHAS, E. 2008. Polymer Injection in Deep Offshore Field: The Dalia Angola Case. *Society of Petroleum Engineers, SPE,* SPE 116672.
NORDLI, M. 2010. Kryssbundet polymerløsning (LPS) for andvendelse i saltholdige reservoarer. *MS Thesis, Department of chemistry, University of Bergen, Bergen, Norway*.
ODELL, J. A., MÜLLER, A. J. & KELLER, A. 1987. Non-Newtonian behaviour of hydrolysed polyacrylamide in strong elongational flows: a transient network approach. *Polymer,* 29**,** 1179-1190.
OLJE OG ENERGIDEPARTEMENT 2011. En næring for framtida- om petroleumsvirksomheten. *Stortingsmelding 28*.
PANCHAROEN, M. 2009. Physical Properties of Associative Polymer Solutions. *MS Thesis, Department of Energy Resources and Engineering, Stanford University, California, USA*.
POPE, G. A. 2007. Overview of Chemical EOR. *Power point presentation from Casper EOR, workshop*.
RAI, K., MCCOMB, T., RODRIGUEZ, E., WITHERS, R. & COMPANY, C. E. T. 2012. Development of a Tool to Predict Technical Success of Polymer Flooding Applications. *Society of Petroleum Engineers, SPE,* SPE 153878.
RANEY, K., AYIRALA, S., CHIN, R. & VERBEEK, P. 2011. Surface and Subsurface Requirements for Successful Implementation of Offshore Chemical Enhanced Oil Recovery. *Offshore Technology Conference, OTC, Society of Petroleum Engineers, SPE,* OTC 21188, SPE 155116.
REGALADO, E. J., SELB, J. & CANDAU, F. 1999. Viscoelastic Behavior of Semidilute Solutions of Multisticker Polymer Chains. *Macromolecules,* 32**,** 8580- 8588.
REICHENBACH-KLINKE, R. B. C. P. G. T., LANGLOTZ, B. G. P. R., BASF CONSTRUCTION CHEMICALS GMBH, TROSTBERG, WENZKE, B. W. H. G., BARNSTORF & SPINDLER, C. B. S., LUDWIGSHAFEN, GREGOR BRODT, BASF SE, LUDWIGSHAFEN 2011. Hydrophobic Associative Copolymer with Favorable Properties for the Application in Polymer Flooding. *Society of Petroleum Engineers, SPE,* SPE 141107.
SCHRAMM, G. 1998. A Practical Approach to Rheology and Rheometry. *HAAKE, Karlsruhe, Germany,* 2. Edition.
SERIGHT, R. S., FAN, T., WAVRIK, K., WAN, H., GAILLARD, N. & FAVÉRO, C. 2011. Rheology of a New Sulfonic Associative Polymer in Porous Media. *Society of Petroleum Engineers, SPE*.

SINGHAL, A. 2011. Preliminary Review of IETP Projects Using Polymers.
SKARESTAD, M. & SKAUGE, A. 2009. PTEK 213- Reservarteknikk II. *University of Bergen*.
SOCHI, T. 2010. Flow of non-newtonian fluids in porous media. *Journal of Polymer Science Part B: Polymer Physics,* 48**,** 2437-2767.
SORBIE, K. S. 1991. Polymer- Improved Oil Recovery. *Blackie, Glascow- London*.
TA INSTRUMENTS 2004. Understanding Rheology of Structured Fluids. *Paper revised by Franck, A.J in TA Instruments*.
TAYLOR, K. C. 2003. Rheology of Hydrophobically Associating Polymers for Oilfield Applications. *Annual Transaction of the Nordic Rheology Society,* 11.
TAYLOR, K. C. & NASR- EL- DIN, H. A. 1995. Water- Soluble Hydrophobically Associating Polymers for Improved Oil Recovery: A literature Review. *Society of Petroleum Engineers, SPE,* SPE 29008.
TAYLOR, K. C. & NASR- EL- DIN, H. A. 2007. Hydrophobically Associating Polymers for Oil Field Applications. *Petroleum Society*.
TOTAL E&P 2008. EOR Maximazing Recovery Factors. *The know- how SERIES*.
UTVINNINGSUTVALGET 2010. Rapport: Økt utvinning på norsk kontinentalsokkel. *Rapport fra Olje og Energidepartementet*.
VOLPERT, E., SELB, J. & CANDAU, F. 1998. Adsorption of Hydrophobically Associating Polyacrylamides on Clay. *American Chemical Society, Languir,* 14**,** 1870- 1879.
WEVER, D. A. Z., PICCHIONI, F. & BROEKHUIS, A. A. 2011. Polymers for enhanced oil recovery: A paradigm for structure–property relationship in aqueous solution. *Progress in Polymer Science,* 36**,** 1558-1628.
WU, Y., MAHMOUDKHANI, A., WATSON, P., FENDERSON, T., NAIR, M. & KEMIRA 2012. Development of New Polymers with Better Performance under conditions of High Temperature and High Salinity. *Society of Petroleum Engineers, SPE,* SPE 155653.
ZHAO, Q., SUN, J., LIN, Y. & ZHOU, Q. 2010. Study of the properties of hydrolyzed polyacrylamide hydrogels with various pore structures and rapid pH-sensitivities. *Elsevier,* 70**,** 602- 609.
ZOLOTUKHIN, A. B. & URSIN, J.-R. 2000. Introduction to Petroleum Reservoir Engineering. *Høyskoleforlaget AS*.

Appendix

A.1 Uncertainties

In following tables uncertainties are considered during preparation of polymer solution and salty brines, and during rheology measurements on the rheometer. The frequency of the uncertainty, the importance and preventive actions are considered.

Table A.1.2 Uncertainties considered during preparation of solutions.

Area of interest	***Type***	***Uncertainty***	***Frequency***	***Importance***	***Preventive actions***
Weighing scales	*AB 204-S,* fine	± 0.0001g	Always	Low	
	PB 3002S, medium	± 0.01g	Always	Low	
	SG 16001g, coarse	± 0.1g	Always	Low	
pH meters	*Hach-Lange* and *twinpH B-212*	±0.1pH	Always	Low	
Equipment	All	Pollution	Rare	Low-medium	Cleansing with distilled water
Degradation	-	Temperature	Rare	Low	Storage in temperature regulated room
		Mechanical	Medium	Low	Regulated stirring speed after type of polymer and concentration
		Air	Rare	Low	All solution was stored with sealing parafilm around the cork
Chemicals	-	Section 3.1	Always	Low	

Table A.1.2 Uncertainties during measurements shear viscosity and viscoelastic measurements.

Area of interest	*Uncertainty*	*Frequency*	*Importance*	*Preventive actions*
Solutions	Inhomogeneous	Medium	Low	
	Pollution	Rare	Low	Control of equipment and minimal exposure to air
Sampled volume (utilizing different pipettes)	± 2% (Averaging systematic error of volume by Eppendorf model 1-10mL with standard ep.T.I.P.S)	Always	Medium	Difficult to sample gel- like polymer solutions (high viscosity)
MCR300 rheometer	± 2.5% (Instrumental error by Anton Paar)	Always	Low	
Equipment	Pollution	Rare	Low	Washing procedure (soap, water, distilled water, acetone and pressurized air)
	Stability	Rare	Low	Air check tests and PDMS tests
Shear viscosity (experimental uncertainties)	100 (1/s): ± 0.01 mPa·s 10 (1/s): ± 6.1 mPa·s	Always	Low	
Storage moduli (experimental uncertainties)	± 0.007Pa	Always	Low	
Loss moduli	± 0.0001Pa	Always	Low	

(experimental uncertainties)				
Damping factor (experimental uncertainties)	±0.003	Always	Low	
Complex viscosity (experimental uncertainties)	0.0001 Pa·s	Always	Low	

The greatest uncertainty regarding reproducibility is the preparation procedure and sampling volume. The measurement uncertainties on the rheometer are relative low compare to inhomogeneous solutions.

A.2 Flow curves (shear viscosity as a function of shear rate)

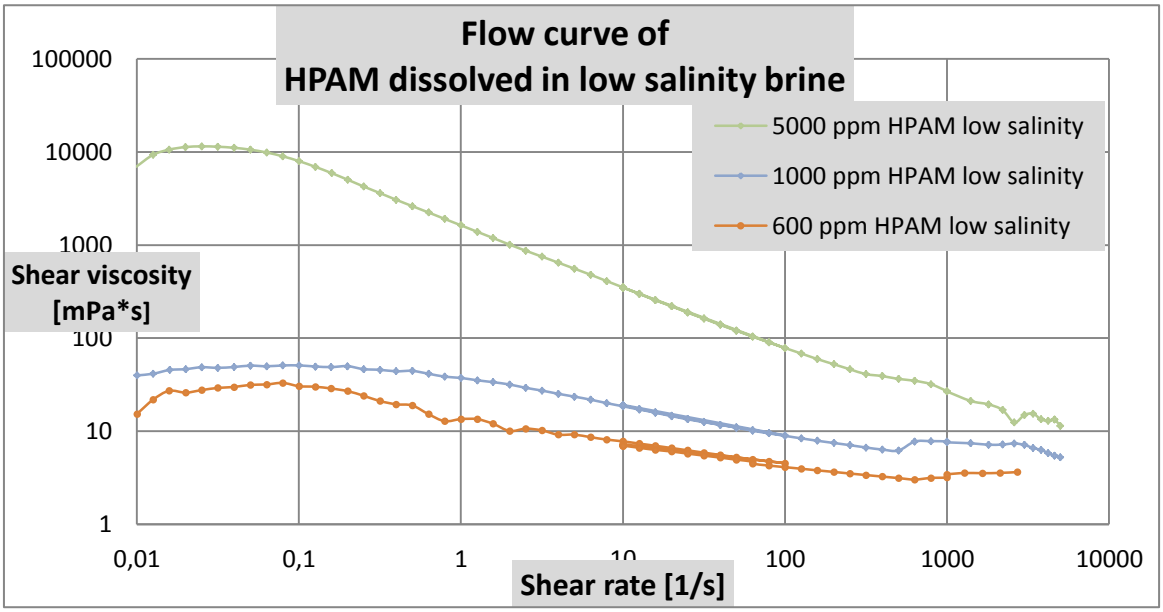

Figure A.2.1 Shear viscosity as a function of shear rate for different polymer concentrations (different colors) of HPAM dissolved in low salinity brine at 22 ± 0.1°C.

Table A.2.1 Shear viscosity of HPAM solutions in low and high salinity brines at 22 ± 0.1°C. Measured at reference shear rate of 10 (1/s).

Polymer concentration of HPAM [ppm]	*Shear viscosity [mPa·s]*	
	Low salinity brine	*High salinity brine*
5000	360	-
2000	-	-
1000	18.3	-
600	7.88	-

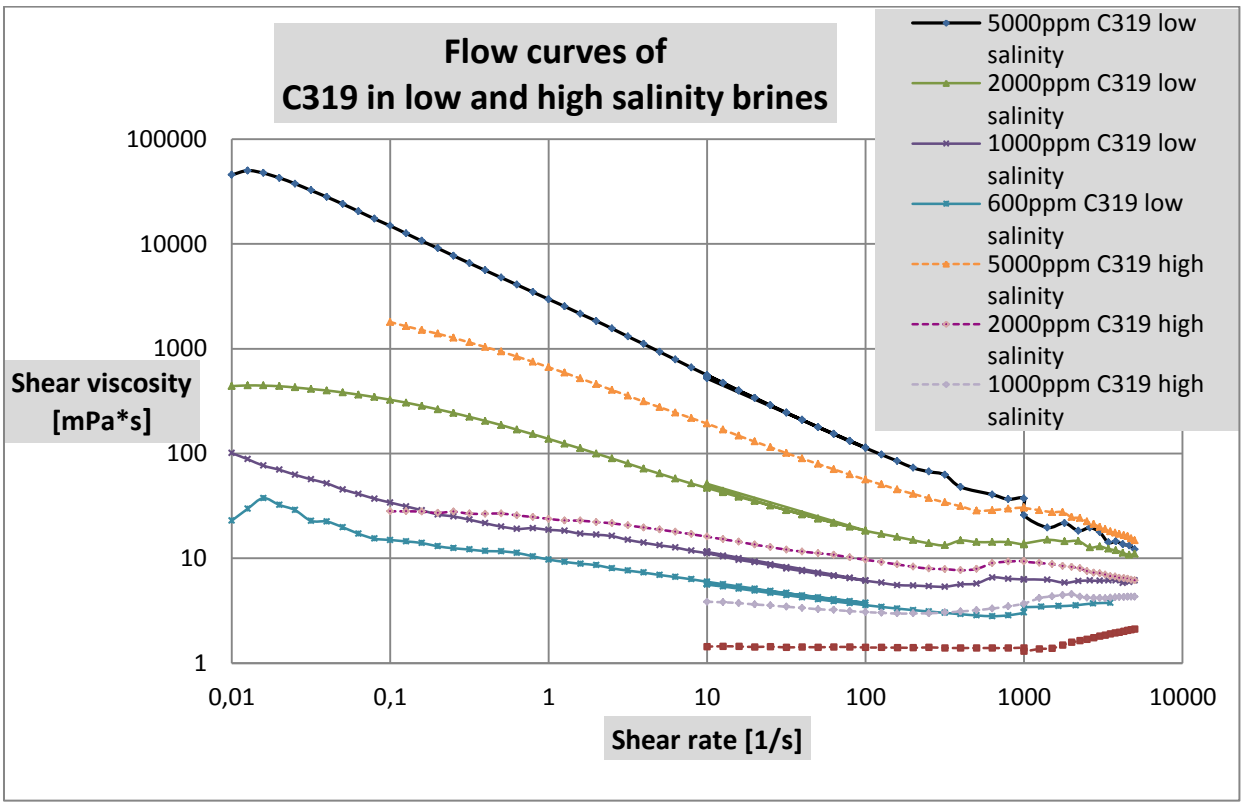

Figure A.2.2 Shear viscosity as a function of shear rate at different concentrations (different colors) of C319 dissolved in low (solid) and high (dotted) salinity brines at 22 ± 0.1°C.

Due to limitations of the rheometer, the measured values below 10 (1/s) was eliminated for 600ppm and 1000ppm solutions (section 3.3.2).

Table A.2.2 Shear viscosity of C319 solutions in low and high salinity brines at 22 ± 0.1°C. Measured at reference shear rate of 10 (1/s).

Polymer concentration of C319 [ppm]	*Shear viscosity [mPa·s]*	
	Low salinity brine	*High salinity brine*
5000	573	192
2000	46.6	16.1
1000	10.9	3.86
600	6.16	2.19

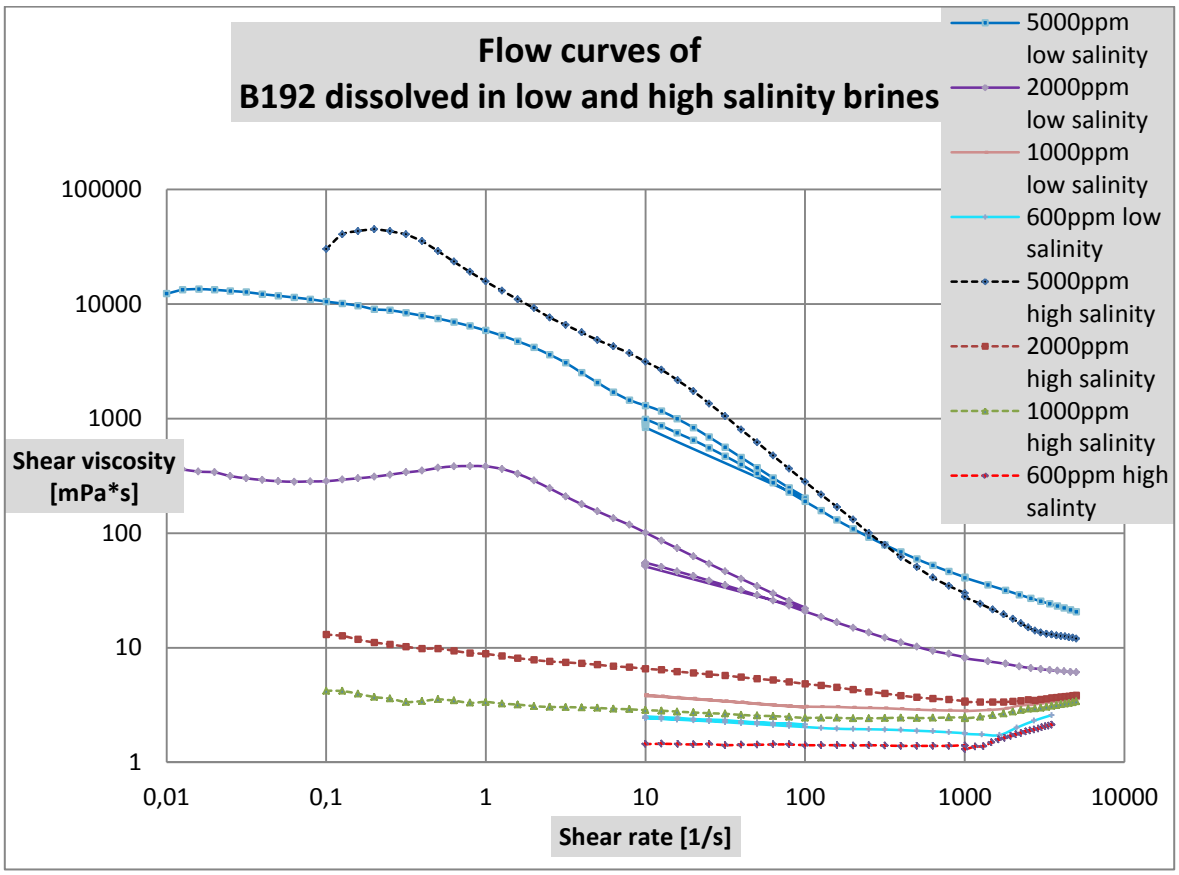

Figure A.2.3 Shear viscosity as a function of shear rate at different concentrations (different colors) of B192 dissolved in low (solid) and high (dotted) salinity brines at 22 ± 0.1°C.

Due to limitations of the rheometer, the measured values below 10 (1/s) was eliminated for 600ppm solutions in both brines, and 1000ppm solution in low salinity brine (section 3.3.2).

Table A.2.3 Shear viscosity of C319 solutions in low and high salinity brines at 22 ± 0.1°C. Measured at reference shear rate of 10 (1/s).

Polymer concentration of B192 [ppm]	***Shear viscosity [mPa·s]***	
	Low salinity brine	***High salinity brine***
5000	1310	3140
2000	103	6.57
1000	3.78	2.85
600	2.52	1.42

Table A.2.4 Shear viscosity of D118 solutions in low and high salinity brines at 22 ± 0.1°C. Measured at reference shear rate of 10 (1/s).

Polymer concentration of D118 [ppm]	***Shear viscosity [mPa·s]***	
	Low salinity brine	***High salinity brine***
5000	690	837
2000	84.7	2.52
1000	10.9	1.53
600	3.13	1.29

A.3 Reduced viscosity as a function of polymer concentration

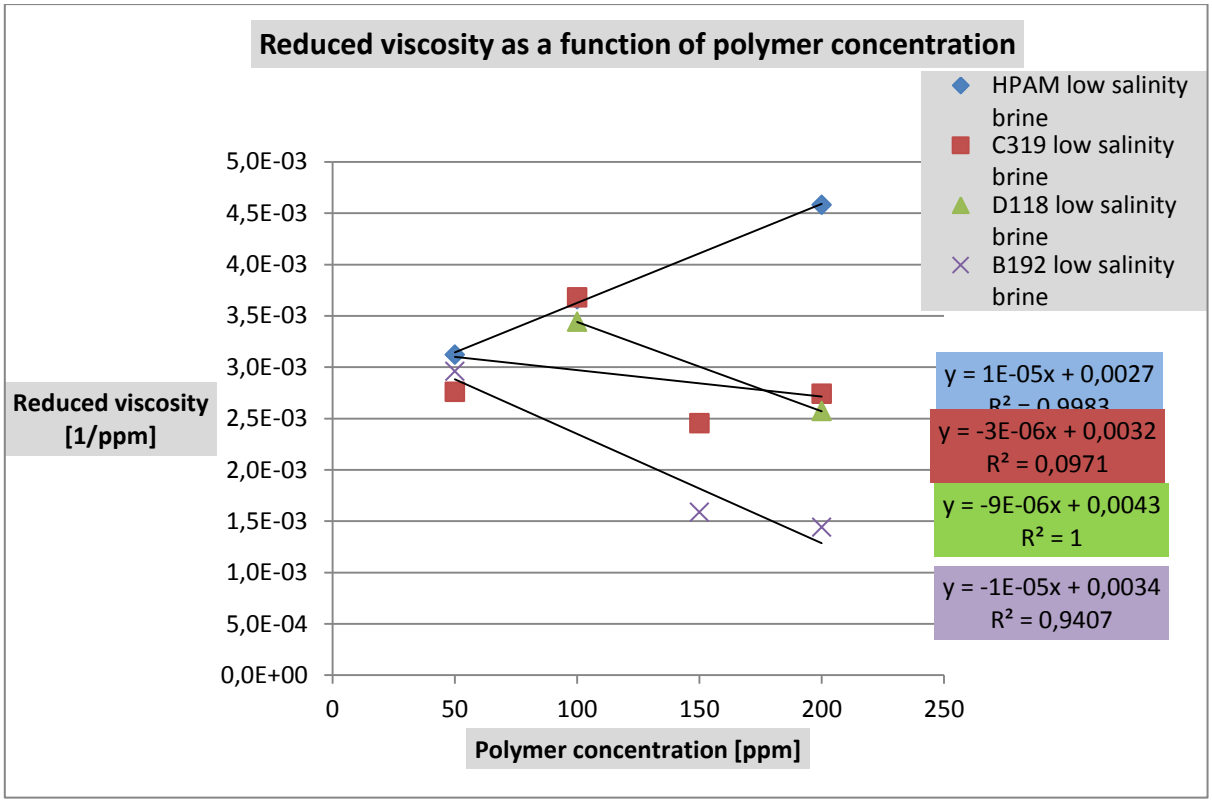

Figure A.3.1 Reduced viscosity as a function of polymer concentration of all polymers dissolved in low salinity brine at 22 ± 0.1°C.

A.4 Shear viscosity as a function of polymer concentration

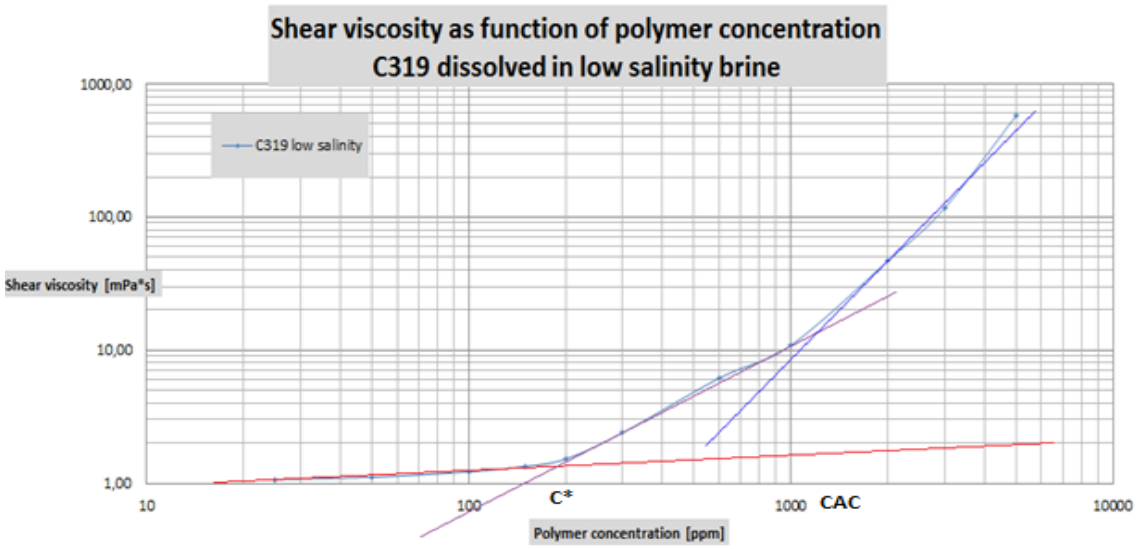

Figure A.4.1. Shear viscosity as a function of polymer concentration of C319 in the low salinity brine at 22 ± 0.1°C.

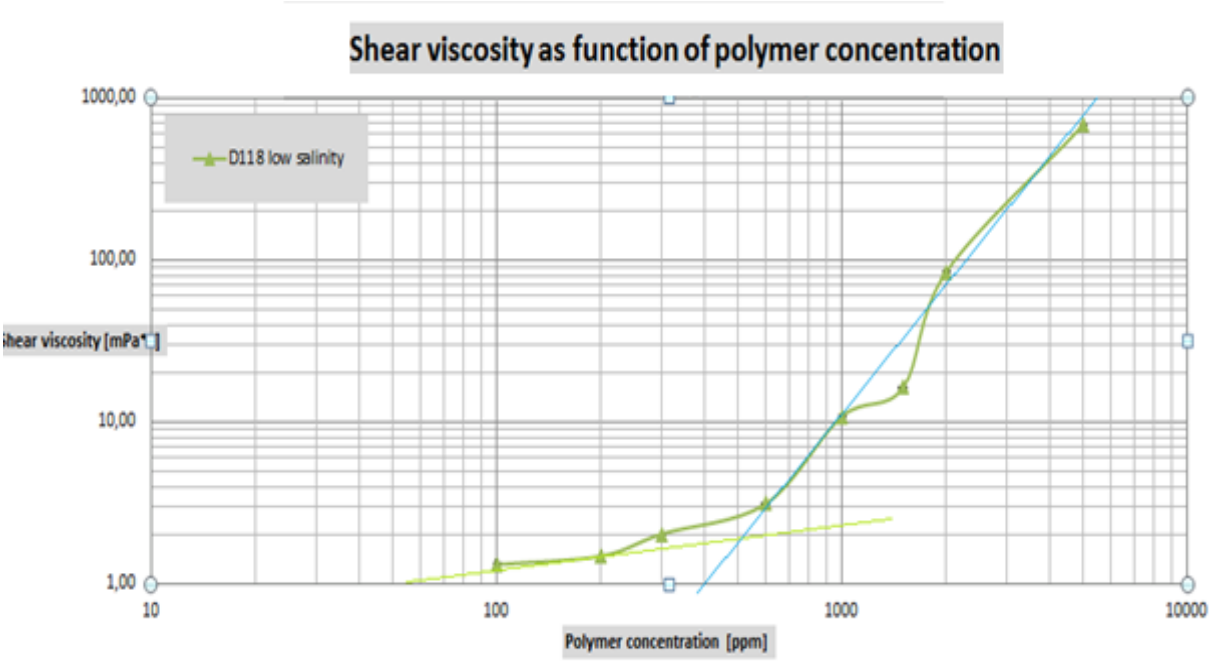

Figure A.4.2 Shear viscosity as a function of polymer concentration of D118 dissolved the in low salinity brine at 22 ±0.1°C.

Table A.4.1 Estimated critical overlap concentration (C^*) and critical aggregation concentration (CAC) of all polymer solutions in low and high salinity brines.

Polymer solution	*Salinity of brine*	*C^* range [ppm]*	*CAC range [ppm]*
C319	*Low*	*200-300*	*1000-2000*
	High	*100-600*	*600-2000*
D118	*Low*	*200-300*	*600-1000*
	High	*C*=CMC*	*1000-2000*
B192	*Low*	*200-300*	*600-1000*
	High	*100-600*	*1000-2000*

A.5 Amplitude sweep (storage- and loss moduli as functions of shear stress)

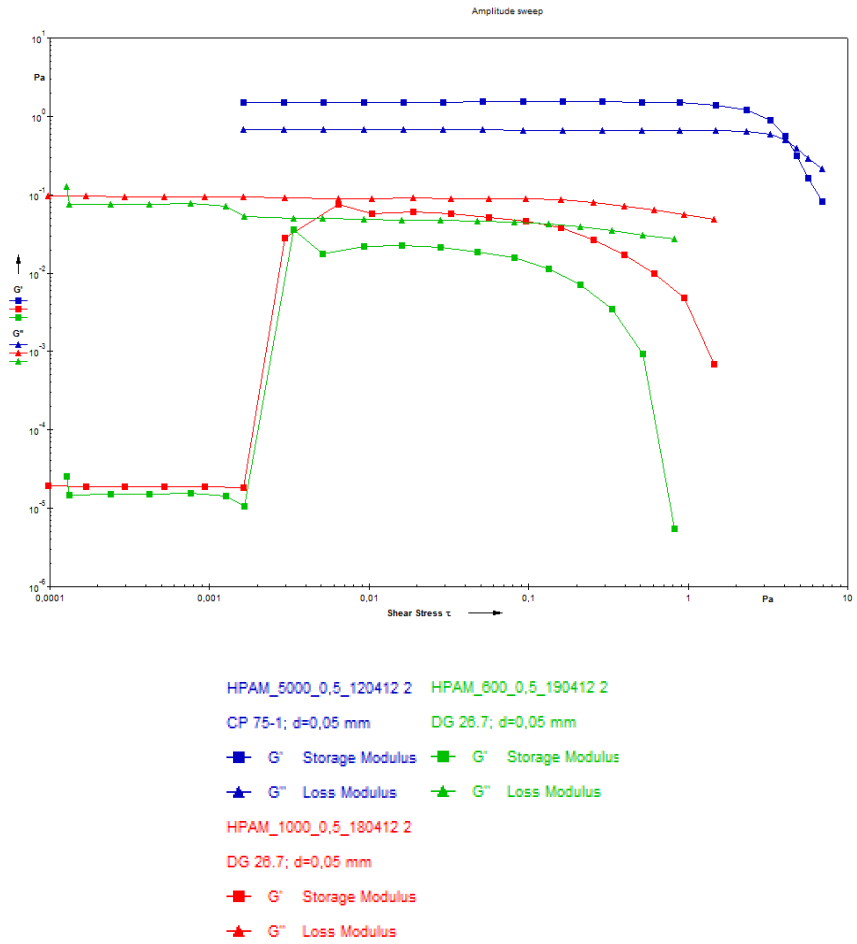

Figure A.5.1 Amplitude sweep for 600, 1000 and 5000ppm solutions of HPAM in low salinity brine at 22 ±0.1^{o}C.

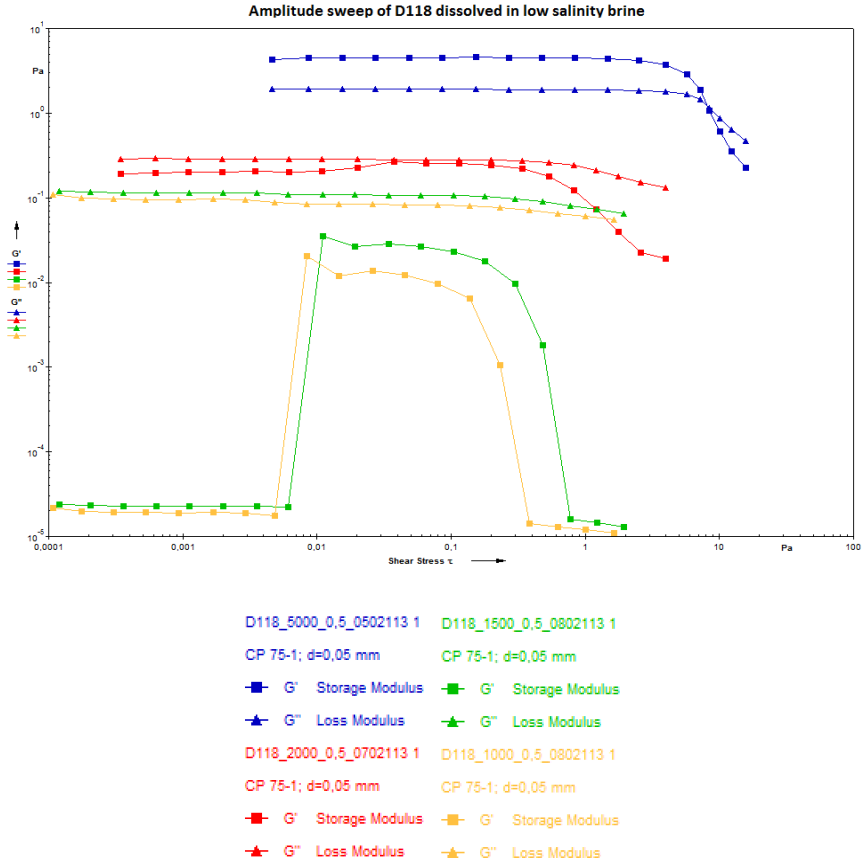

Figure A.5.2 Amplitude sweep for 1000, 1500, 2000 and 5000ppm solutions of D118 in low salinity brine at 22 ±0.1^{o}C.

During amplitude sweep of D118 dissolved in the low salinity brine, measured values at low and high shear stress was not valid. Due to limitations of the rheometer no valid measurements was detected for 600ppm solution of D118.

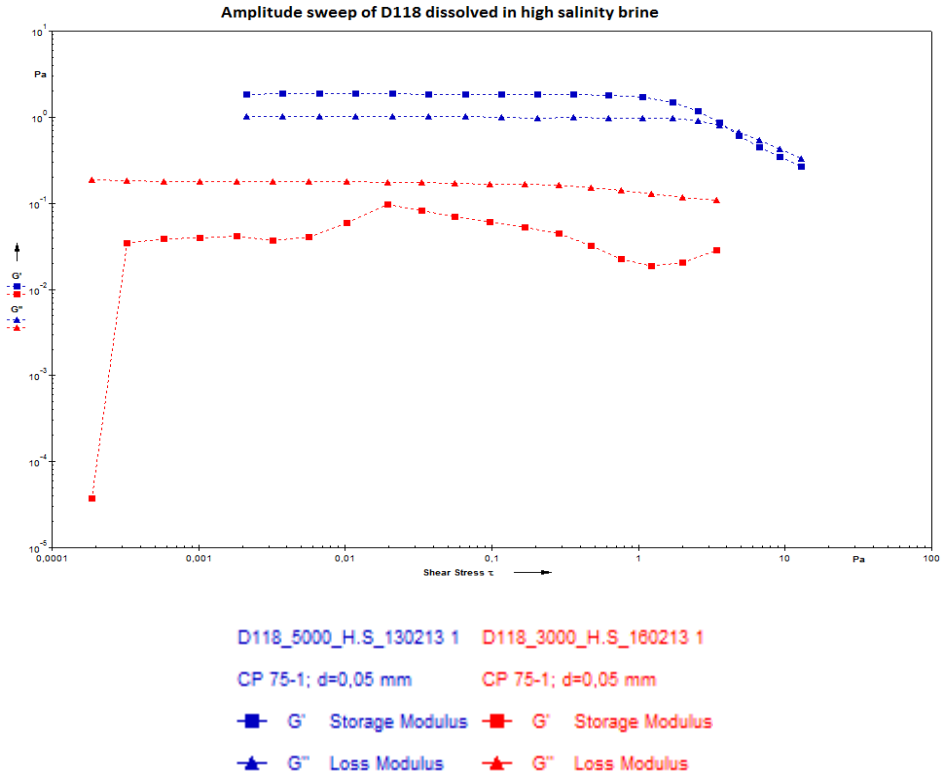

Figure A.5.3 Amplitude sweep for 3000ppm and 5000ppm solution of D118 in high salinity brine at 22 ±0.1^{o}C.

During amplitude sweep of D118 dissolved in the high salinity brine, measured values at low and high shear stress was not valid. Due to limitations of the rheometer no valid measurements was detected for 600, 1000, 1500 and 2000ppm solution of D118.

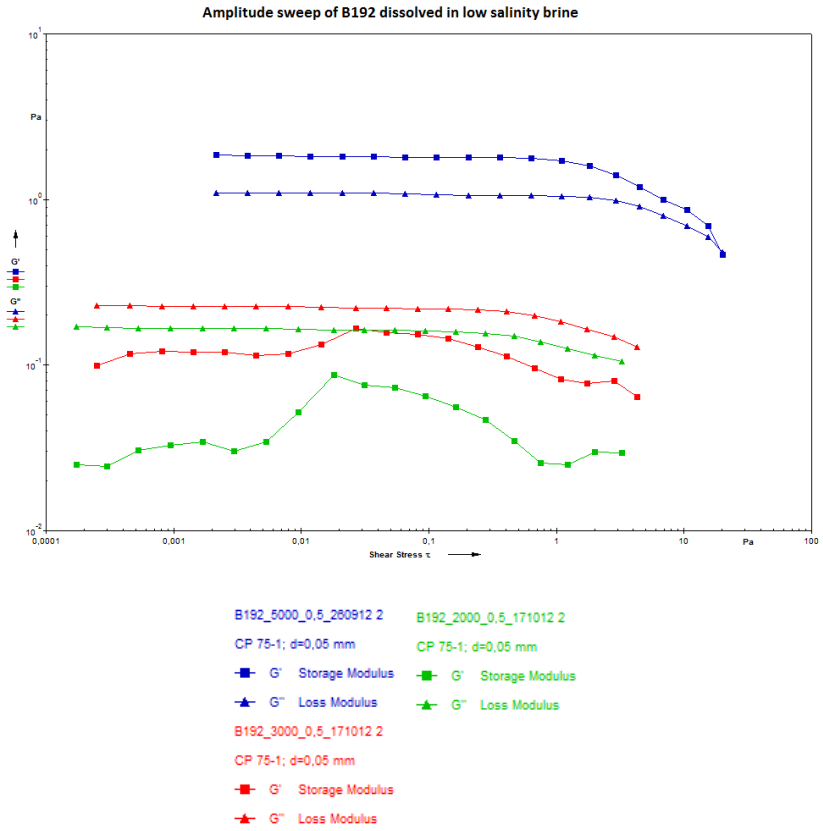

Figure A.5.4 Amplitude sweep for 5000ppm solution of B192 in low salinity brine at 22 ±0.1^{o}C.

No valid measurements of 600ppm and 1000ppm solutions of B912 dissolved in the low salinity brine were detected during amplitude sweep, due to limitations.

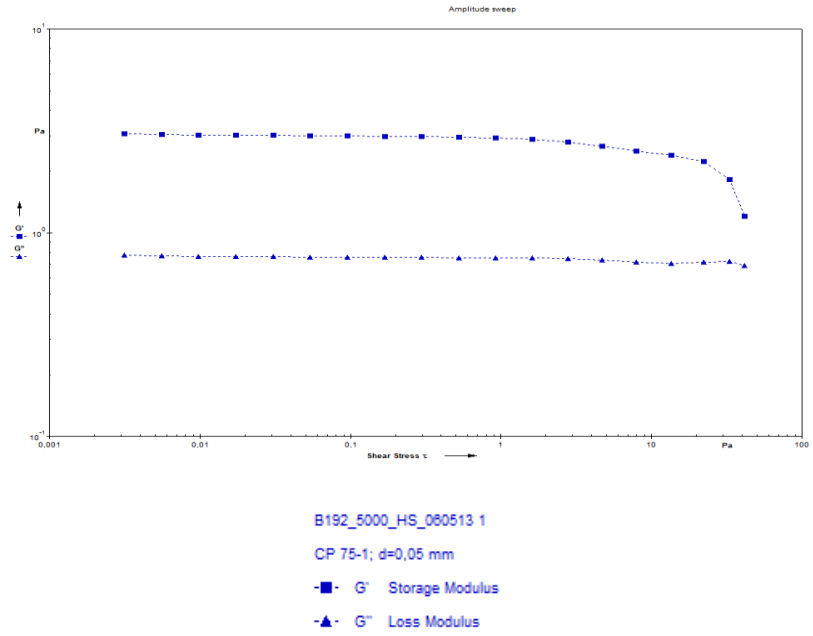

Figure A.5.5 Amplitude sweep for 5000ppm solution of B192 in high salinity brine at 22 ±0.1°C.

No valid measurements of 600, 1000 and 2000ppm solutions of B912 dissolved in the high salinity brine were detected during amplitude sweep, due to limitations.

A.6 Frequency sweep (storage- and loss moduli and complex viscosity as functions of angular frequency)

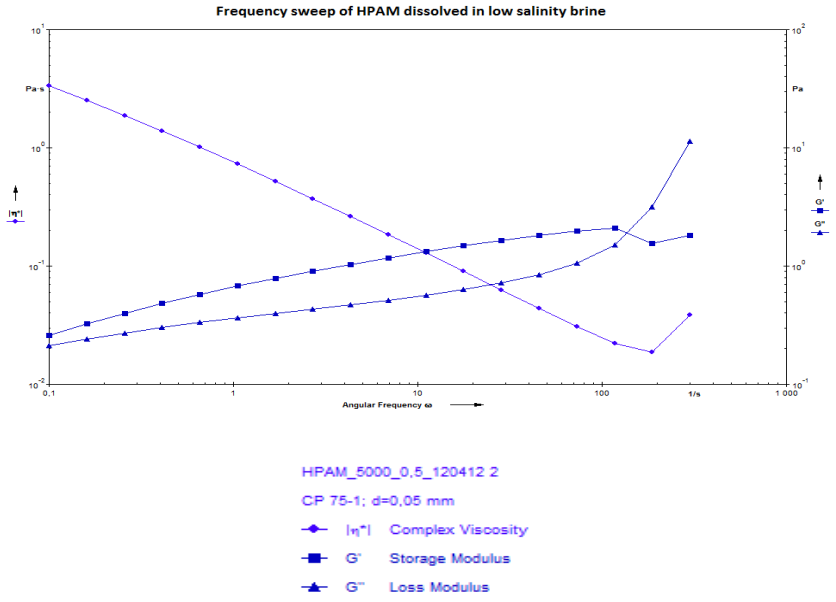

Figure A.6.1 Frequency sweep for 5000ppm solution of HPAM in low salinity brine at 22 ±0.1°C.

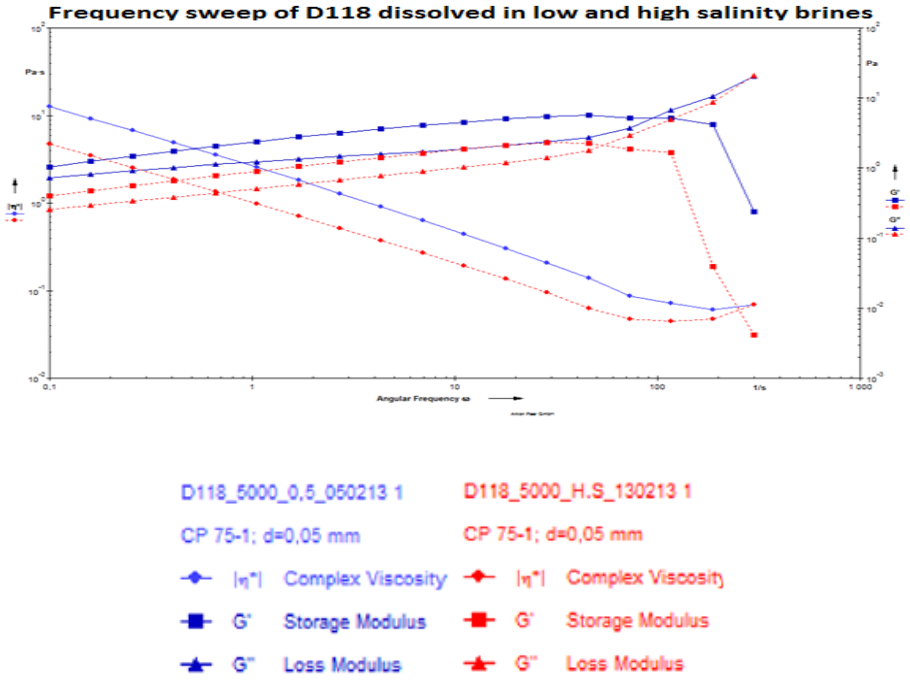

Figure A.6.2 Frequency sweep for 5000ppm solution of D118 dissolved in low (solid line) and high (dotted line) salinity brines at 22 ±0.1^{o}C.

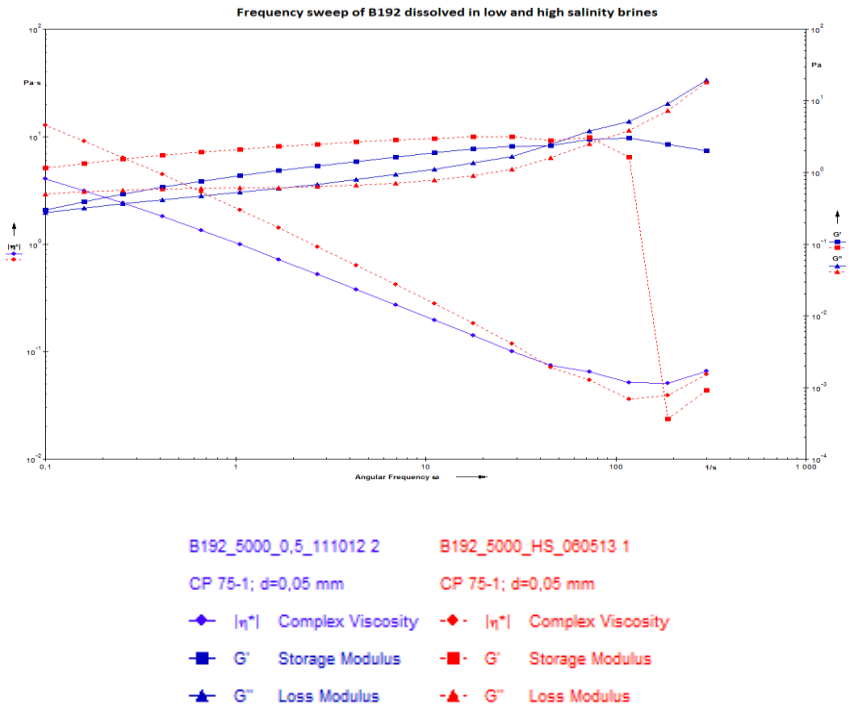

Figure A.6.3 Frequency sweep for 5000ppm solution of B192 dissolved in low (solid line) and high (dotted line) salinity brines at 22 ±0.1^{o}C.

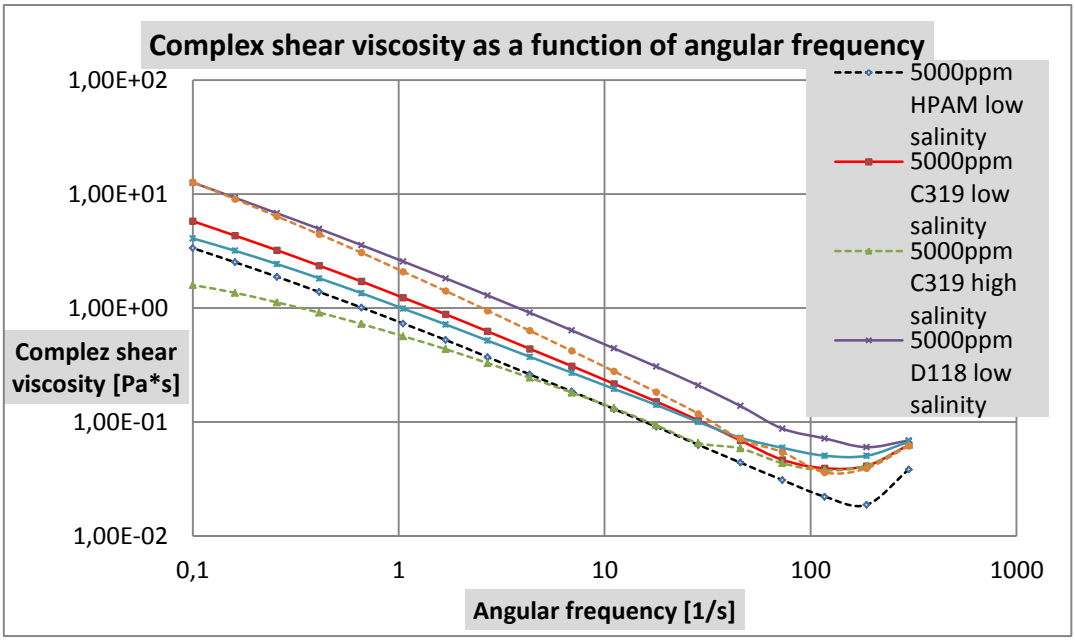

Figure A.6.4 Complex viscosity as a function of angular frequency for all polymers at 22 ±0.1°C. Low (solid line) and high (dotted line) salinity brine.

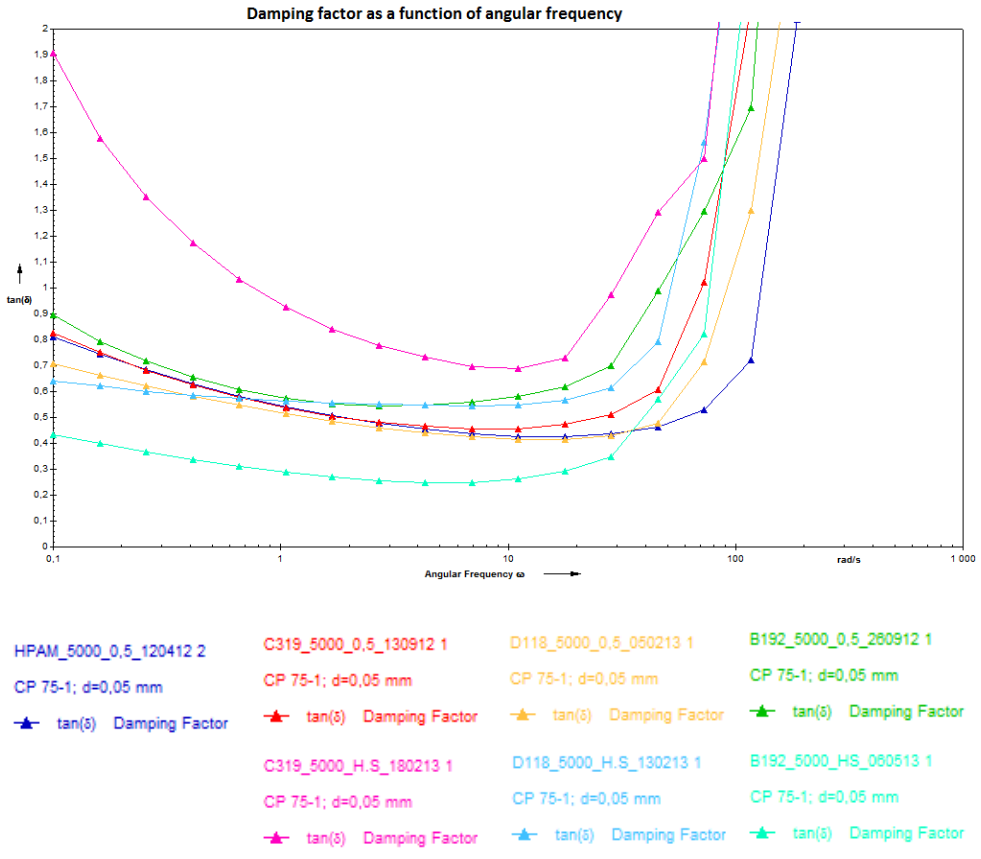

Figure A.6.5 Damping factor as a function of angular frequency for all polymers at 22 ±0.1°C. Low (solid line) and high (dotted line) salinity brine.